SEP 1957 18

REGISTERED No. M. 3121

UNIVERSITY OF MICHIGAN
SEP 16 1957
PHYSICS LIBRARY

PROCEEDINGS
OF THE
INDIAN ACADEMY
OF SCIENCES

VOL. XLVI] SECTION A [No. 1

JULY 1957

Price Rs. 2 or 3 Sh. *Annual Subscription Rs. 18*

PRINTED AT THE BANGALORE PRESS, BANGALORE (CITY), BY G. VASUDEVA RAO, SUPERINTENDENT AND PUBLISHED BY THE INDIAN ACADEMY OF SCIENCES, BANGALORE.

GENERALISED THEORY OF INTERFERENCE AND ITS APPLICATIONS

Part IV. Interference Figures in Absorbing Biaxial Crystals

BY S. PANCHARATNAM

(*Memoir No. 98 of the Raman Research Institute, Bangalore-6*)

Received April 22, 1957

(Communicated by Sir C. V. Raman)

§ 1. INTRODUCTION

THE interference figures displayed by absorbing biaxial crystals are of some general interest—quite apart from the light they throw on the optics of such media (Voigt, 1902 *a*; Boguslowski, 1914; Pancharatnam, 1955 *b*). The appearance of idiophanic interference rings with no analyser, or with no polariser, or with neither polariser nor analyser, finds no parallel in the field of transparent crystals; these peculiarities arise mainly from the fact that the two waves propagated along any particular direction are in *non-orthogonal* states of elliptic polarisation. Attention has already been directed in the introductions to Parts I and II (Pancharatnam, 1956 *a*, *b*) to some of of these phenomena and their broad explanation. It is sufficient therefore to remark that here we meet with practical instances of some of the most general cases of dissolution, composition, etc., which were theoretically envisaged in those papers on completely and partially coherent pencils. The physical concepts developed there enable us to give a comparatively intelligible explanation to otherwise complex phenomena, and the fruitfulness of these ideas is evidenced by the discovery of certain new phenomena in this field, *e.g.*, the formation of spiral interference figures even with optically inactive crystals (§ 8 *b*).

The general theoretical approach is outlined in Sections 2 and 6 which deal respectively with the two classes of interference phenomena into which the subject may be broadly divided, *viz.*, those exhibited respectively *without* and *with* the aid of an analyser behind the plate—the incident light being either completely polarised, partially polarised or even unpolarised. The concept of partially coherent beams discussed in Part II, apart from giving physical insight into the interference phenomena exhibited when the incident light is unpolarised (§§ 4 and 7), also explains certain new phenomena observed when the incident light is partially polarised (§§ 5 and 8 *b*).

§ 2. General Discussion of Interference Phenomena Observed Without any Analyser

In the succeeding sections we shall discuss the interference phenomena exhibited by a plate of an absorbing biaxial crystal without the use of an analyser, when the incident light is either completely polarised (§ 3), unpolarised (§ 4) or partially polarised (§ 5). When a *parallel* beam of unit intensity falls on such a plate it is split into two elliptically polarised streams in the states of polarisation A and B that are propagated without change of form in that direction. Let I_1 and I_2 be the intensities of the component beams, ϕ_1 their initial 'phase difference' at the point of entry into the medium, and γ their mutual degree of coherence (which will be equal to unity only in the case when the incident light is completely polarised). The streams travel through the crystal with different velocities and coefficients of absorption. Emerging from the crystal plate, we therefore have two beams (in states of polarisation A and B) whose intensities are now I_1' and I_2', the 'phase advance' of the first beam over the second being now $\triangle'$, where

$$\left.\begin{aligned} &I_1' = I_1 e_a^2; \quad I_2' = I_2 e_b^2 \\ &\triangle' = \delta + \phi_1 \end{aligned}\right\} \tag{1}$$

the phase retardation introduced by the plate being denoted by δ. These beams can directly interfere with one another, since in general they are in non-orthogonal states of polarisation and are not incoherent. The intensity I obtained on compounding the pencils is given by the general interference formula for beams in different states of polarisation (Part II, eq. 13).

$$I = I_1' + I_2' + 2\gamma \sqrt{I_1' I_2'} \cos \tfrac{1}{2} c \cos \triangle' \tag{2}$$

where c is the angular separation of the states A and B when represented on the Poincaré sphere.

The variation of I with the direction of propagation may be observed in *convergent* light, using a plate cut normal to an optic axis, each *point* P in the convergent light figure corresponding to a definite *direction* of propagation. For a plate of moderate thickness the retardation δ introduced by the plate increases rapidly as we proceed outwards along directions normal to the curves of constant retardation. The rate of variation of I as we proceed outwards from regions near the optic axis can therefore be taken to be predominantly due to the change in $\triangle'$ (for most regions of the convergent light figure). Hence we should in general expect the appearance of idiophanic interference rings. From what has been said above the curves

of minimum intensity occur along directions where the emerging beams destructively interfere, that is, along the curves

$$\triangle' = (2n + 1)\pi$$

or

$$\delta = (2n + 1)\pi - \phi_1 \tag{3}$$

and a measure of the 'visibility' of the fringes (in the sense defined by Michelson) at any point in the convergent light figure is given by

$$V = \gamma \cos \tfrac{1}{2} c \frac{2\sqrt{I_1' I_2'}}{I_1' + I_2'} \tag{4}$$

From (3) we see that the curves of minimum intensity do not occur at the same position as those obtained between crossed polaroids (which occur at $\delta = 2n\pi$); in fact they do not even follow the curves of constant retardation $\delta = \text{const.}$, because the initial phase difference ϕ_1 itself varies with direction (since the states A and B vary with direction). In the case of non-active crystals, as we shall see the idiophanic rings in plane polarised light exhibit clearly the first effect but not the second—which may, however, be strikingly seen with the use of circularly polarised light.

Since all the factors in (4) vary *along* a curve $\triangle' = \text{const.}$, we should expect the visibility of the rings to be maximum along some particular zone in the field of view—the determination of which is in general very complex since it depends not only on the state of polarisation of the incident light, but also on the thickness of the plate.

The explanation of the appearance of idiophanic rings (in completely polarised, unpolarised or partially polarised light), and of some of their broad characteristics is thus immediately obvious in the present treatment and applies equally well to absorbing biaxial crystals possessing *optical activity*—where the non-orthogonal elliptic vibrations A and B bear no simple relation to one another (Pancharatnam, to be published).

§ 3. Phenomena in Absorbing Biaxial Crystals Using a Polariser Alone

(*a*) *General discussion.*—If completely polarised light be incident on the plate, the component beams into which it is split will be completely coherent. Their intensities I_1 and I_2, and their initial phase difference ϕ_1, may be expressed (see Part I, eqns. 3 and 5 *b*) in terms of the sides of the spherical triangle ABC_1 on the Poincaré sphere—where C_1 represents the state of polarisation of the incident elliptic vibration, and A and B the states of the beams into which it is split.

$$\left.\begin{aligned} I_1 &= \frac{\sin^2 \frac{1}{2} a_1}{\sin^2 \frac{1}{2} c}\ ; \quad I_2 = \frac{\sin^2 \frac{1}{2} b_1}{\sin^2 \frac{1}{2} c} \\ \phi_1 &= \pi - \tfrac{1}{2} E' \end{aligned}\right\} \tag{5}$$

Here E′ is the area of the triangle $C_1'BA$ (measured with the usual sign convention) C_1' being the point opposite to the incident state C_1 (see Fig. 1, text).

The intensity I at the corresponding point in the field of view is obtained by substituting in (2):

$$I = \operatorname{cosec}^2 \tfrac{1}{2} c \{e_a^2 \sin^2 \tfrac{1}{2} a_1 + e_b^2 \sin^2 \tfrac{1}{2} b_1 - 2e_a e_b \sin \tfrac{1}{2} a_1 \sin \tfrac{1}{2} b_1 \cos \tfrac{1}{2} c \cos (\delta - \tfrac{1}{2} E')\} \tag{6}$$

(*b*) *Phenomena in non-active crystals.*—In order to illustrate that our general method of analysis is capable of handling specific cases we shall briefly consider some of the phenomena exhibited by a plate (cut normal to an optic axis) of the optically inactive orthorhombic mineral iolite. We shall refer to the photographs of the different phenomena exhibited by this mineral published in this paper and in a previous paper (Pancharatnam, 1955 *b*, hereafter referred to as P. 2). The idiophanic rings are always absent along the directions where the waves are orthogonally polarised ($\cos \frac{1}{2} c = 0$)—*i.e.*, along the trace of the axial plane. (The axial plane is kept horizontal in all the photographs).

Voigt (*loc. cit.*) has shown that in non-active absorbing biaxial crystals the two elliptically polarised waves A and B propagated along any one direction, have their major axes crossed and have the same ellipticity ϵ (which, according to the usual sign convention, means that they are also described in the *same* sense). Hence on the Poincaré sphere the longitudes of the points A and B differ by π, but their latitudes are both equal to 2ϵ, as drawn in Fig. 2. [See also Pancharatnam, 1955 *a*.] Accordingly we have to substitute $\frac{1}{2} c = \frac{1}{2} \pi - |2\epsilon|$ in (6), for all the cases discussed below.

If the incident light is, say, *left-circularly polarised*, so that the point C_1 now coincides with the upper pole C_l, then we have to substitute in (6): $a_1 = b_1 = \frac{1}{2} \pi - 2\epsilon$; and $\frac{1}{2} E'$ equal to π or zero, according as ϵ is positive or negative. Hence the intensity at any point in the field of view is,

$$I = \frac{1}{2(1 + \sin 2\epsilon)} (e_a^2 + e_b^2 + 2e_a e_b \sin 2\epsilon \cos \delta). \tag{7}$$

The *asymmetry* of the idiophanic rings with respect to the axial plane, which is observable in Fig. 3, Plate I (taken with left-circularly polarised light)

is now readily explicable. In the upper half of the figure where the sense of rotation of the ellipses propagated is opposite to that of the incident circularly polarised light, ϵ is negative and hence the minima occur at $\delta = 2\pi$, 4π, etc. (This is verified from the fact that they occur in the same position as in Fig. 1, Plate I, which is obtained when a circular analyser which can cross out the incident light is also introduced.) In the lower half of the figure where ϵ is positive, the minima occur at $\delta = \pi$, 3π, etc. (which is verified from the fact that the fringes are shifted down by half a fringe width relative to those appearing in the upper half of the figure). The expression for I becomes indeterminate at $\epsilon = -\pi/4$, *i.e.*, at the singular axis where *only* a right circular vibration can be propagated *unchanged*. That the emergent intensity is larger than at the other singular axis where the incident light is propagated unchanged, is clearly shown by referring to Fig. 3. This remarkable phenomenon has been theoretically discussed elsewhere (Pancharatnam, 1955 *a*, *b*). When right circularly polarised light is used, the sign of the third term in (7) has to be changed, and the asymmetry about the axial plane will be reversed (see P. 2, Figs. 13 and 14).

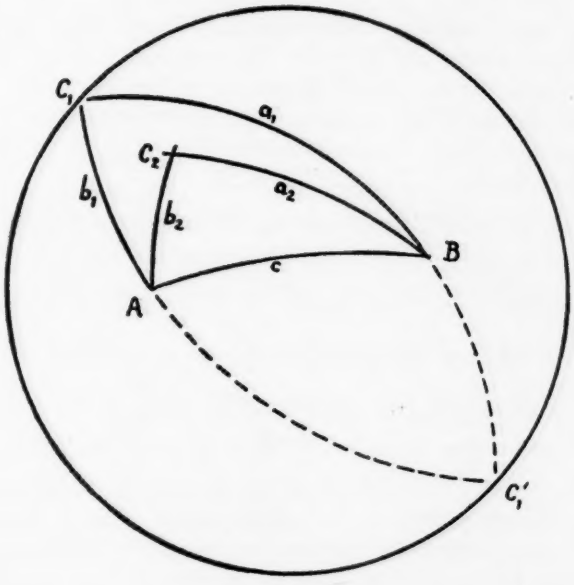

FIG. 1

If the incident light is *plane polarised*, the point C_1 lies on the equator as is drawn in Fig. 2, text. From the figure we see that $b_1 = (\pi - a_1)$ and $E' = -\angle AC_1B$ (since the area E′ of the triangle $C_1'BA$ is numerically half the area of the lune of $\angle AC_1B = \hat{C}_1$). Substituting these values in (4), we have

$$I = \operatorname{cosec}^2 \tfrac{1}{2} c \{e_a^2 \sin^2 \tfrac{1}{2} a_1 + e_b^2 \cos^2 \tfrac{1}{2} a_1 - 2e_a e_b \sin \tfrac{1}{2} a_1 \cos \tfrac{1}{2} a_1 \cdot \cos \tfrac{1}{2} c \cos (\delta + \tfrac{1}{2} \hat{C_1})\} \quad (8)$$

Let $-\nu$ be the azimuth of the major axis of the faster elliptic vibration with respect to the vibration-direction of the incident light. In directions where the ellipticity is small (so that the points A and B lie near the equator), an approximate formula may be obtained by substitutions $\sin^2 \tfrac{1}{2} a_1 \simeq \cos^2 \nu$; $\cos^2 \tfrac{1}{2} a_1 \simeq \sin^2 \nu$; $\sin^2 \tfrac{1}{2} c \simeq 1$; $\cos \tfrac{1}{2} c \simeq |2\epsilon|$; and $|\hat{C}_1| = \pi$. We then obtain the approximate formula that is customarily used (Pockels, 1906, p. 423, eq. 9).

$$I = e_a^2 \cos^2 \nu + e_b^2 \sin^2 \nu + 2\epsilon \sin 2\nu \, e_a e_b \sin \delta \quad (9)$$

Figure 2 of the text shows qualitatively that the last substitution $|\hat{C}_1| = \pi$ will be justified except for directions of propagation where $\nu \simeq 0$, where in any case the interference effects [depending on the last term in (9)], vanish by virtue of the first substitutions. The maxima and minima are thus shifted by *quarter* of a fringe width compared to those obtained between crossed polaroids (see P. 2, Figs. 2 and 9).

To obtain the exact formula for the intensity at any point in the field, we have to use in (8) the exact values of a_1, c and $\hat{C}_1$ which are obtained by spherical trigonometry, from the right-angled triangle AXC_1:

$$\tan \tfrac{1}{2} \hat{C}_1 = \sin 2\nu / \tan 2\epsilon; \quad \cos a_1 = -\cos 2\epsilon \cos 2\nu;$$

$$\sin a_1 \cos \tfrac{1}{2} c = \frac{\cos 2\epsilon \sin 2\nu}{\sin \tfrac{1}{2} \hat{C}_1} \cdot \sin 2\epsilon.$$

It can thus be shown that the approximate formula (9) neglects only the squares and higher powers of the ellipticity ϵ. [Strictly speaking, the idiophanic rings on each side of the axial plane will take the form of the arcs of a spiral (see § 8 *b*) when the polariser is inclined to the axial plane.] It can also be shown that the exact formula deduced by Voigt can be put in the same form as that obtained by the above substitutions.

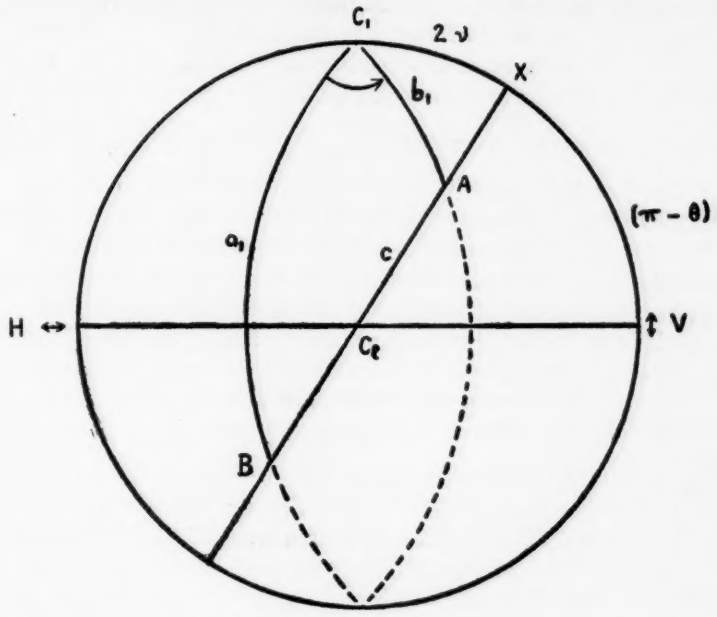

FIG. 2

§ 4. INTERFERENCE PHENOMENA IN ABSORBING BIAXIAL CRYSTALS IN UNPOLARISED LIGHT

It was shown in Part II, § 7, that when unpolarised light is split into two non-orthogonally polarised beams (in the states of polarisation A and B), the component beams are *partially* coherent with one another. The intensities I_1 and I_2 of the component beams, their initial phase difference ϕ_1, and their mutual degree of coherence γ are given by

$$I_1 = I_2 = \tfrac{1}{2}\operatorname{cosec}^2 \tfrac{1}{2}c; \quad \gamma = \cos \tfrac{1}{2}c; \quad \phi_1 = \pi. \tag{10}$$

The intensity I at any point in the field of view, is given by substituting in (2)

$$I = \tfrac{1}{2}\operatorname{cosec}^2 \tfrac{1}{2}\, c\, \{e_a{}^2 + e_b{}^2 - 2e_a e_b \cos^2 \tfrac{1}{2}\, c \cos \delta\} \tag{11}$$

The interference effects observed (Fig. 5, Plate I) are extremely feeble since they depend on the *square* of the factor $\cos \frac{1}{2}c$, which becomes appreciable only in immediate neighbourhood of the singular axes. What is actually seen—both in the optically active crystal amethyst and in the inactive crystal iolite—is the occurrence of the first minimum on either side of the optic axis as two dark spots at the terminii of the Brewster's brushes. These

minima should occur at $\delta = 2\pi$; and in the case of iolite (Fig. 5, Plate I), this is confirmed by the fact that they occur at the same position as the first minima obtained between crossed polaroids (Fig. 6, Plate I)—as may be verified by measurement (see also § 5 *b*).

§ 5. INTERFERENCE PHENOMENA IN PARTIALLY POLARISED LIGHT

(*a*) *Incident light partially circularly polarised.*—Just as the addition of two incoherent *non-orthogonally* polarised beams results in a partially polarised beam, so also when a partially polarised beam is split into two non-orthogonally polarised beams it is possible under certain circumstances for the component beams to be completely incoherent with one another. Hence with partially polarised light incident on a plate of an absorbing biaxial crystal, it should be possible under certain conditions for the interference fringes to completely vanish near some particular regions in the convergent light figure (observed with or without an analyser).

Fig. 7, Plate II of this paper shows a photograph of this curious phenomenon as exhibited by a plate of iolite when the incident light is partially circularly polarised. An analysing polaroid was set behind the plate with its vibration direction perpendicular to the axial plane. The partially left-circularly polarised light was obtained by passing partially plane polarised light—emerging from a pile of plates—through a quarter-wave plate.

For analysing the phenomenon we shall use the representation discussed in Part II whereby any beam (completely or partially polarised) is characterised by its total intensity and by a ' Stokes vector ' drawn from the centre of the Poincaré sphere; the length of the vector and its orientation (*i.e.*, point of intersection with the sphere) give respectively the intensity and state of polarisation, of the ' polarised fraction ' of the beam. Let us denote by $\mathbf{S}$ the vector representing the incident partially left-circularly polarised light (of unit intensity and degree of polarisation p); and let $\mathbf{S}_1$ and $\mathbf{S}_2$ be the Stokes vectors representing the component beams—completely polarised in states A and B—into which the incident light is split. Then obviously

$$\mathbf{S} = p\mathbf{C}_l;\ \mathbf{S}_1 = \mathrm{I}_1\mathbf{A};\ \mathbf{S}_2 = \mathrm{I}_2\mathbf{B} \tag{12}$$

where $\mathbf{C}_l$, $\mathbf{A}$, $\mathbf{B}$ are unit vectors directed towards the points C_l, A and B respectively (see Fig. 3, text). The intensities I_1 and I_2 of the component beams must be equal to one another, since the states A and B are symmetrically situated with respect to the pole C_l, for a non-active crystal; they are given by eq. 21 of Part II,

$$\mathbf{I}_2 = \mathbf{I}_1 = \tfrac{1}{2}(1 - \mathbf{S} \cdot \mathbf{B}) \operatorname{cosec}^2 \tfrac{1}{2}c$$
$$= \tfrac{1}{2}(1 - p \sin 2\epsilon)/\cos^2 2\epsilon \qquad (13)$$

It was shown in Part II, § 6, that when two completely polarised beams $\mathbf{S}_1$ and $\mathbf{S}_2$ are combined to give a resultant beam $\mathbf{S}$, then

$$\mathbf{S} = \mathbf{S}_1 + \mathbf{S}_2 + \mathbf{S}_{12}$$

where $\mathbf{S}_{12}$ is a vector arising from the interference of the component beams, and by determining which we can in the present case calculate the degree of coherence γ and the effective phase difference ϕ_1 between the component beams. Substituting from (12) and referring to Fig. 3, text, we have

$$\mathbf{S}_{12} = (p - 2\mathbf{I}_1 \sin 2\epsilon)\, \mathbf{C}_l$$

or from (13)

$$\mathbf{S}_{12} = 2\mathbf{I}_1 \cdot \frac{p - \sin 2\epsilon}{1 - p \sin 2\epsilon} \mathbf{C}_l \qquad (14)$$

Since $\mathbf{S}_{12}$ is coplanar with $\mathbf{S}_1$ and $\mathbf{S}_2$ it follows from the geometric construction for $\mathbf{S}_{12}$ given in Part II, Fig. 2, that (*a*) the length of the vector $\mathbf{S}_{12}$ is equal to $2\gamma \sqrt{\mathbf{I}_1 \mathbf{I}_2}$, and (*b*) the effective phase difference between the component beams is zero or π according as $\mathbf{S}_{12}$ bisects the interior or exterior angle between $\mathbf{S}_1$ and $\mathbf{S}_2$.

The appearance of the figure presented (either without any analyser or with an analyser set along or perpendicular to the axial plane) may now be understood in terms of the variation of the ellipticity of the waves over the region covered by the convergent light figure. (See Voigt, 1902 *a*; also P. 2, Fig. 1.)

In the lower half of the figure where ϵ is negative (because of the manner in which the plate was set), we see from (14) that the degree of coherence never vanishes and the initial phase difference is π. On the other hand, in the region above the trace of the axial plane the degree of coherence vanishes where $\mathbf{S}_{12} = 0$, *i.e.*, where $\sin 2\epsilon$ is equal to the degree of polarisation p. Towards the interior of this region the ellipticity ϵ becomes greater and the initial phase difference ϕ_1 between the component beams is π; while towards the exterior of this region $\sin 2\epsilon < p$ and accordingly the initial phase difference jumps to zero. Thus in Fig. 7, Plate II, as we proceed upwards from the optic axis, the first ring is clearly seen (appearing at the same distance as that in the lower half of the figure); further on *the rings disappear* and then reappear with *a shift of half a fringe width* compared ot those in the lower half of the figure—thus confirming our theoretical

deductions. The use of an analyser behind the crystal plate increases the clarity of the interference phenomena by resolving the beams into the same state of polarisation before making them interfere. This does not affect the main conclusions of our discussion.

(*b*) *Incident light partially plane polarised.*—When a partially polarised beam is decomposed into two non-orthogonally polarised beams, it may be shown that the effective phase difference between the component beams is *not* independant of the degree of polarisation. Let us suppose that the incident light of degree of polarisation p is partially *plane* polarised in any state C_1 (Fig. 2, text). It would then be represented by a vector **S** of length p directed towards C_1. The initial phase difference ϕ_1 between the component beams in the states of polarisation A and B is given by Part II, eqns. 22 *a* and 23 *a*:

$$\tan \phi_1 = V'/U', \ (\tfrac{1}{2}\pi \leq \phi_1 \leq 3\pi/2)$$

where

$$V' = S_z \operatorname{cosec} \tfrac{1}{2} c; \quad U' = -\cos \tfrac{1}{2} c \operatorname{cosec}^2 \tfrac{1}{2} c$$

and where the positive z direction is in the direction of the vector $\mathbf{A} \times \mathbf{B}$. Considering the case when the beam is incident on an optically inactive absorbing crystal (*e.g.*, iolite) we will have (see Fig. 2, text)

$$\tan \phi_1 = p \sin 2\nu / \tan 2\epsilon = p \tan \tfrac{1}{2} \hat{C}_1 \qquad (15)$$

where the symbols have the same meaning as previously (§ 3 *b*). Thus as the degree of polarisation is increased from zero the initial phase difference ϕ_1 alters continuously from π to $(\pi + \frac{1}{2}\hat{C}_1)$.

This was experimentally demonstrated by partially polarising the incident light with its vibration parallel to the axial plane of iolite by the use of a pile of plates, and observing the convergent light figure without the use of an analyser. Starting with the light more or less completely polarised (P. 2, Fig. 6), the degree of polarisation was gradually decreased to zero (by turning the pile of plates about an axis perpendicular to the axial plane). It was then observed that not only did the rings become less distinct at the border of the figure, but at the same time they moved slightly *outwards*, till finally when the light was unpolarised what was left were the minima in the Brewster's brushes.

Incidentally the above experiment demonstrates clearly a fact which follows from the theoretical discussion of §§ 3 and 4, namely, that the minima in the Brewster's brushes do not exactly coincide with those observed when

the light is polarised parallel to the axial plane. This fact was not realized in a previous paper (P. 2), though a measurement on the photographs (Figs. 5 and 6) published in that very paper confirms the above result.

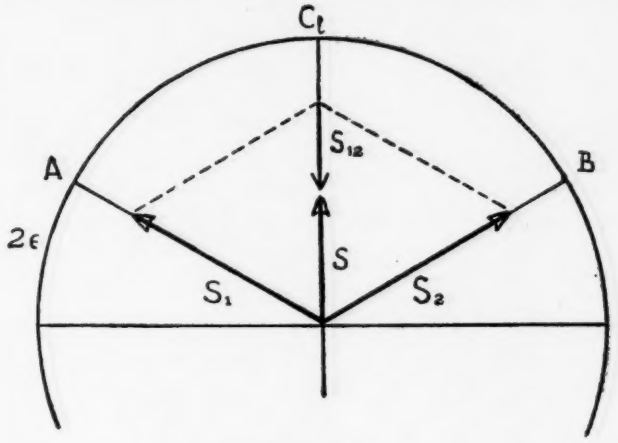

FIG. 3

§ 6. GENERAL DISCUSSION OF INTERFERENCE PHENOMENA INVOLVING USE OF AN ANALYSER

In the succeeding sections we shall discuss the interference phenomena exhibited in convergent light by a crystal plate when an analyser C_2 (which transmits light of elliptic polarisation C_2) is used behind the crystal plate—the incident light being either unpolarised (§ 7), or completely or partially polarised (§§ 8, 9). As before let I_1' and I_2' be the intensities of the two pencils (in the states of polarisation A and B respectively) which emerge from the crystal plate along any particular direction, their degree of coherence being γ, and the effective phase advance of the first beam over the second being Δ'. The analyser transmits the resolved components of these beams in the state of polarisation C_2, and these components can interfere with one another. Let the intensities of the resolved components be I_1'' and I_2'', their effective phase difference being Δ''. These may be written down in terms of the spherical triangle ABC_2 (Fig. 1, text) using the results of Part I, § 8, and Part II, § 4.

Writing $\Delta'' = \Delta' + \phi_2$, we have

$$\left.\begin{aligned} &I_1'' = I_1' \cos^2 \tfrac{1}{2} b_2; \quad I_2'' = I_2' \cos^2 \tfrac{1}{2} a_2; \\ &\phi_2 = -\tfrac{1}{2} E_2 \end{aligned}\right\} \qquad (16)$$

where E_2 is the area of the triangle ABC_2. The phase diffrence Δ'' between the two finally interfering beams is thus the sum of three terms:

$$\Delta'' = \phi_1 + \delta + \phi_2 \tag{17}$$

where ϕ_1 is the initial phase difference—'introduced in the process of decomposition'—between the pencils at the first surface of the plate, δ is the phase retardation introduced by the plate, and ϕ_2 may be called the phase difference introduced in the process of analysation.

The resultant intensity I transmitted by the analyser is given by the formula for the interference of two beams in the same state of polarisation, having a degree of coherence γ.

$$I = I_1'' + I_2'' + 2\gamma \sqrt{I_1'' I_2''} \cos \Delta'' \tag{18}$$

The general arguments following eq. 2 may be applied *mutatis mutandis* in the present case. The appearance of interference figures with an analyser is therefore to be expected whether the incident light is unpolarised or completely or partially polarised. The curves of minimal intensity follow the curves where $\Delta'' = (2n + 1)\pi$. Since Δ'' is given by (17) these curves will not in general follow the curves of constant retardation $\delta = \text{const.}$; this is because *the sum of the phase differences ϕ_1 and ϕ_2* (which are introduced by the processes of resolution and analysation respectively) *is not constant, but is itself a function of the direction of propagation.* This is the true physical reason why the interference figures in quartz, and, as we shall see, also in iolite, can under suitable conditions even take the form of spirals.

§ 7. IDIOPHANIC RINGS WITH AN ANALYSER ALONE

The idiophanic rings in the present case (with the incident light unpolarised) are of the same clarity as those obtained with a polariser *alone* in front of the plate. In the present case, however, the intensity I at any point in the field of view is obtained by substituting the values given by (10) in (18):

$$\begin{aligned} I = \tfrac{1}{2} \operatorname{cosec}^2 \tfrac{1}{2} c \{ & e_a^2 \cos^2 \tfrac{1}{2} b_2 + e_b^2 \cos^2 \tfrac{1}{2} a_2 \\ & - 2 e_a e_b \cos \tfrac{1}{2} a_2 \cos \tfrac{1}{2} b_2 \cos \tfrac{1}{2} c \cos (\delta - \tfrac{1}{2} E_2) \} \end{aligned} \tag{19}$$

In view of the fact that this expression differs from (6), an explanation is required as to why the idiophanic rings seen with the polaroid set either before or after the plate do *not* differ in the case of non-active absorbing crystals like iolite (compare Figs. 8 and 10 of P. 2). This equivalence is not a general result but a consequence of the peculiar fact that in non-active

crystals the two ellipses propagated along any direction have their major axes crossed and their ellipticities equal. In such a case (see Fig. 2, text) we have $a = (\pi - b)$ and $E = E'$, so that the expressions (6) and (19) become equal. However in the case of optically active absorbing crystals it can be shown that the states A and B do not bear this simple relation to one another (work to be published), and in such a case the idiophanous figure presented with a polaroid set in front of the crystal should not be the same as that obtained with the polaroid set behind the plate in the same position. This difference has been observed in the case of amethyst.

That the effects presented with a polariser C alone are *in general* not the same as those obtained with an analyser C alone, may be confirmed even in the case of inactive absorbing biaxial crystals if C represents a state of elliptic polarisation. Thus the idiophanic rings with a left-circular analyser (Fig. 4, Plate I) are not the same as with a left-circular polariser (Fig. 3, Plate I), but should be the same as the figure seen with a *right*-circular polariser (as may be shown by comparing eqns. 6 and 19]). This latter proposition has also been confirmed experimentally in iolite.

§ 8. Interference Figures in Absorbing Biaxial Crystals Between Polariser and Analyser

(*a*) *General discussion.*—When *completely* polarised light of unit intensity in the state of polarisation C_1 is incident on a plate of an absorbing biaxial plate, and an analyser C_2 is used behind the plate, the intensities I_1'' and I_2'' and the difference in phase Δ'' of the two pencils transmitted by the analyser along any particular direction are given by substituting in (16) from (5) and (1):

$$I_1'' = \frac{\sin^2 \tfrac{1}{2} a_1 \cos^2 \tfrac{1}{2} b_2}{\sin^2 \tfrac{1}{2} c} \cdot e_a^2; \quad I_2'' = \frac{\sin^2 \tfrac{1}{2} b_2 \cos^2 \tfrac{1}{2} a_2}{\sin^2 \tfrac{1}{2} c} e_b^2$$

$$\Delta'' = \delta + \pi - \tfrac{1}{2}(E_1' + E_2)$$

where, it may be noted, $(E_1' + E_2)$ is the area of the spherical quadrilateral $C_1'BC_2A$ (see Fig. 1, text).

The resultant intensity I_2 transmitted by the analyser is given by the formula (18) for the interference of two completely coherent pencils in the same state of polarisation. Hence

$$I = \operatorname{cosec}^2 \tfrac{1}{2} c \,[e_a^2 \sin^2 \tfrac{1}{2} a_1 \cos^2 \tfrac{1}{2} b_2 + e_b^2 \sin^2 \tfrac{1}{2} b_1 \cos^2 \tfrac{1}{2} a_2 - 2 e_a e_b \sin \tfrac{1}{2} a_1 \sin \tfrac{1}{2} b_1 \cos \tfrac{1}{2} a_2 \cos \tfrac{1}{2} b_2 \cos \{\delta - \tfrac{1}{2}(E_1' + E_2)\}] \quad (20)$$

The equation for the case of transparent crystals (Part III), is obviously a particular case of the above.

For the particular case when polariser and analyser are crossed we have $a_1 = \pi - a_2$; $b_1 = \pi - b_2$ and $(E_1' + E_2) = 0$. Hence

$$I = \frac{\sin^2 \frac{1}{2} a_1 \sin^2 \frac{1}{2} b_1}{\sin^2 \frac{1}{2} c} (e_a^2 + e_b^2 - 2e_a e_b \cos \delta) \qquad (21)$$

We see therefore that—independant of the orientation of the crossed states C_1 and C_1'—the minima of the ring system occur at $\delta = 2\pi, 4\pi$, etc., and that the rings are seen most clearly along the zone where the absorption coefficients of the two waves are equal, or $e_a = e_b$ (see Figs. 1, 2 and 6, Plate I).

We can now easily show that the interference figures exhibited between crossed nicols by a plate of an absorbing biaxial crystal *not* possessing optical activity, will be unaltered if the polariser and analyser are interchanged. In such a medium (as we have seen at the end of § 3 *b*) the states of polarisation A and B of the waves propagated in any direction are such that when the incident light is *linearly* polarised we will have $a_1 = \pi - b_1$ (see Fig. 2, text). The effect of interchanging analyser and polariser is then got by changing a_1 to $\pi - a_1$ and b_1 to $\pi - b_1$ and such a change will leave the expression (21) for the emergent intensity unaltered.

It is to be noted however that such an interchange of the crossed nicols could alter the expression for the emergent intensity, if the points A and B are any two general points on the sphere—a situation which occurs in optically active absorbing crystals; the alteration of the observed interference figure on interchanging the crossed nicols has been observed in the case of amethyst (work to be published). That the interchange of the crossed polariser and analyser will in general alter the interference figure may be observed even in the *non*-active crystal iolite provided the incident light is not linearly polarised. This may be seen from the photographs (1) and (2) in which one has been taken between a left-circular polariser and a right-circular analyser, while the other has been taken between a right-circular polariser and a left-circular analyser; the difference between the two figures is small but striking and is mainly in the shift in the position of the eccentric spot from the upper to the lower singular axis.

(*b*) *Spiral figures in inactive absorbing crystals.*—It was observed that when the incident light is plane polarised at an angle of, say, 45° to the axial plane, and a circular analyser is used behind the crystal plate, the interference figure takes a spiral form in the centre of the field of view (Figs. 10 and 11, Plate II). If the incident light is only *partially* plane polarised, the kinks occurring along the vertical line of the field of view

become less marked, and several convolutions of the spiral can be clearly traced (Figs. 8 and 9, Plate II).

On the Poincaré sphere (Fig. 2, text) let the horizontal direction (which is also the trace of the axial plane) be represented by H. We shall first treat the case when the analyser is a left-circular analyser C_l, and the state of maximum polarisation of the incident partially plane polarised light is inclined at an angle of $-45°$ to the axial plane and hence represented by the point C_1 on the Poincaré sphere. Any point P in the field of view may be specified by its polar co-ordinates (r, θ) with respect to a horizontal line, and corresponds to a particular direction of propagation in the crystal. Except for points very close to the optic axis, we may take $\frac{1}{2}\theta$ and $(\frac{1}{2}\pi - \frac{1}{2}\theta)$ as the aximuths with respect to the axial plane of the major axes of the faster and slower elliptic vibrations (A and B) propagated in the direction P, their common ellipticity ϵ being given by

$$\epsilon = (K/2\delta) \sin \theta \tag{22}$$

where K is proportional to the dichroism along the optic axis (see Pockels, *loc. cit.*, p. 425, eq. 13). On the Poincaré sphere, A and B will then have the common latitude 2ϵ and longitudes θ and $(\pi - \theta)$ respectively as indicated in Fig. 2, text. According to (17), the phase difference Δ'' between the resolved components transmitted by the analyser in the direction $P(r, \theta)$ exceeds the retardation δ introduced by the plate by an angle ϕ,

$$\Delta'' = \delta + \phi, \tag{23}$$

and we have to show that the locus of the direction for which these beams destructively interfere $[\Delta'' = (2n + 1)\pi]$, forms a spiral. The retardation δ of the plate is proportional to the radius vector r, $(\delta = \beta r)$, for regions not too close to the optic axis, and it remains to express ϕ as a function of the direction of propagation. From (16) we have,

$$\phi = \phi_1 - \tfrac{1}{2} E_2 \tag{24}$$

Since E_2 is the area of the triangle ABC_l we have $\frac{1}{2} E_2 = \pi$ for points above the axial plane, and $\frac{1}{2} E_2 = 0$ for points below. The value of the initial phase difference ϕ_1 is given by (15):

$$\tan \phi_1 = - p \cos \theta / \tan 2\epsilon; \qquad (\pi/2 \leq \phi_1 \leq 3\pi/2) \tag{25}$$

Substituting from (22), we have, on neglecting the squares and higher powers of ϵ,

$$\tan \phi_1 = (p/K)\, \delta \cot \theta \tag{26}$$

From a consideration of equations 26, 23 and 24 we easily obtain the following result. As we proceed along the circle $\delta = (2n + \frac{1}{2})\pi$ described about the optic axis, the phase retardation Δ'' between the interfering pencils (transmitted by the analyser) falls short of the value $(2n + 1)\pi$ by an angle which *increases continually* with the aximuth θ, and which in fact becomes equal to θ at $\theta = m\pi/2$. In order therefore to plot the curve $\Delta'' = (2n + 1)\pi$ (condition for destructive interference), we have to increase the radii vectors of the circular curve $\delta = (2n + \frac{1}{2})\pi$ by amounts which increase continuously with the polar angle θ, the radius vector of this curve at the plolar angles $\theta = m\pi/2$ taking the values corresponding to $\delta = (2n + \frac{1}{2})\pi + \frac{1}{2}m\pi$. The curves of minimum intensity thus obtained form a continuous spiral which is described in an anticlockwise or left-handed sense (Fig. 8, Plate II). It may be easily shown that the curve of minimum intensity is wrapped round the curve of maximum intensity, the one being obtained from the other by a rotation of 180° about an axis normal to the plane of the figure.

Fig. 10, Plate II, illustrates that a left-handed spiral is still obtained even when a *right*-circular analyser is used, the plane of maximum polarisation of the incident light being the same as in Fig. 8 (though the incident light is now completely polarised). This is not really surprising, because when a right-circular analyser is used, the only difference is that the value of $(-\frac{1}{2}E_2)$—the phase retardation introduced by the process of analysation—differs by π from the corresponding value when a left-circular analyser is used; so that what was a curve of maximum intensity with a left-circular analyser becomes now a curve of minimum intensity.

If, however, the incident light has its plane of maximum polarisation turned through 90°, so that it is inclined at + 45° to the axial plane, it may be shown, by going through the theoretical explanation of the spiral figure, that the sense of description of the spirals will be reversed (being obtained by reflection about a plane perpendicular to the axial plane). Figs. 9 and 11 show the right-handed spirals thus obtained with the incident light respectively partially and completely polarised—the former figure being obtained with a left-circular analyser and the latter with a right-circular analyser.

Along the spiral we have $d\Delta'' = 0$, so that the spiral will be given by

$$\frac{dr}{d\theta} = -\frac{\partial\Delta''}{\partial\theta}\Big/\frac{\partial\Delta''}{\partial r}$$

Writing $\delta = \beta r$ and $(p/K) = a$, it may be shown by using (23), (24) and (26) that

$$\frac{dr}{d\theta} = \frac{ar}{\sin^2\theta + a^2\beta^2r^2\cos^2\theta + a\sin\theta\cos\theta}$$

so that at $\theta = 0$,

$$\left(\frac{dr}{d\theta}\right)_1 = \frac{K}{p\beta^2 r}$$

and at $\theta = \frac{1}{2}\pi$,

$$\left(\frac{dr}{d\theta}\right)_2 = \frac{pr}{K}.$$

Thus as the arm of the spiral turns from a horizontal to a vertical position the increase in its length from $r = (2n + \frac{1}{2})\pi/\beta$ to $r = (2n + 1)\pi/\beta$ does not take place uniformly. Along the horizontal diameter of the figure the increase in the arm of the spiral per unit increase of the polar angle is inversely proportional to the radius of the spiral and *to the degree of polarisation*, while along the vertical diameter it is directly proportional to the same factors. We have thus explained the fact that as the degree of polarisation is raised, the successive arcs of the spiral approximate more and more towards circular arcs along the horizontal diameter while they become more and more kinked along the vertical zone.

The author owes a debt of gratitude to Prof. Sir C. V. Raman, F.R.S., N.L,, but for whose encouragement the present work could not have been undertaken.

§ 9. Summary

Phenomena—involving the interference of polarised light—displayed by crystalline plates (in parallel or convergent light) may be given a general method of analysis, using the physical concepts developed in Parts I and II. The subject is discussed under two main heads: the interference phenomena exhibited *without* and *with* the aid of an elliptic analyser behind the crystal plate—the former involving the interference of beams in different non-orthogonal states of elliptic polarisation. The cases when the incident light is either unpolarised, partially polarised, or completely polarised are all discussed—the concept of partially coherent beams finding fruitful applications in the first two cases.

Illustrative photographs of the interference figures in convergent light shown by the optically inactive mineral iolite accompany the paper. Parti-

cular mention may be made of the interference figure with the incident light partially circularly polarised—showing the fading away of the ring system (due to incoherence) at a particular region in the figure; also of the *spiral* interference figures which are observed between a plane polariser and a circular analyser—even though the crystal is optically inactive.

REFERENCES

Boguslowski, S. .. *Ann. der Physik.*, 1914, **44**, 1084.

Pancharatnam, S. .. *Proc. Ind. Acad. Sci.*, 1955 *a*, *b*, **42 A**, 86, 235.

———— .. *Ibid.*, 1956 *a*, *b*, **54 A**, 247, 398.

Pockels .. *Lehrbuch der Kristalloptik*, Teubner, 1906.

Voigt .. *Ann. Phys.*, 1902 *a*, **9**, 367.

———— .. *Phil. Mag.*, 1902 *b*, **4**, 90.

DESCRIPTION OF PLATES

All the photographs show the optic axial interference figures exhibited in convergent light by the absorbing biaxial mineral, iolite, the axial plane being horizontal. Figures 5, 6 and 7 were taken with a much denser specimen than that used for the other photographs.

FIG. 1. Left-circular polariser and right-circular analyser: lower singular axis extinguished.

FIG. 2. Right-circular polariser and left-circular analyser: upper singular axis extinguished.

FIG. 3. Left-circular polariser *alone*: dark rings in lower half of the figure correspond to bright rings in upper half, and the lower singular axis appears darker than the other.

FIG. 4. Left-circular analyser *alone*: asymmetry with respect to the axial plane is reversed, compared to Fig. 3.

FIG. 5. Brewster's brushes with neither polariser nor analyser: minima at tip of brushes are at the same distance as first dark ring in Fig. 6.

FIG. 6. Crossed polaroids: vibration directions along and perpendicular to axial plane.

FIG. 7. Incident light partially left-circularly polarised, and linear analyser with vibration-direction vertical: in the upper half of the figure, the ring system fades away near second and third rings, and reappears further out with a shift of half a fringe width.

FIGS. 8–9. Left-circular analyser, incident light *partially* plane polarised with vibration at $-45°$ and $+45°$ respectively, with respect to axial plane: note the difference in the handedness of the spiral in the two cases.

FIGS. 10–11. Right-circular analyser, incident light *completely* plane polarised, with vibration at $-45°$ and $+45°$ respectively, with respect to axial plane: kinks along the vertical diameter are conspicuous compared to Figs. 8 and 9.

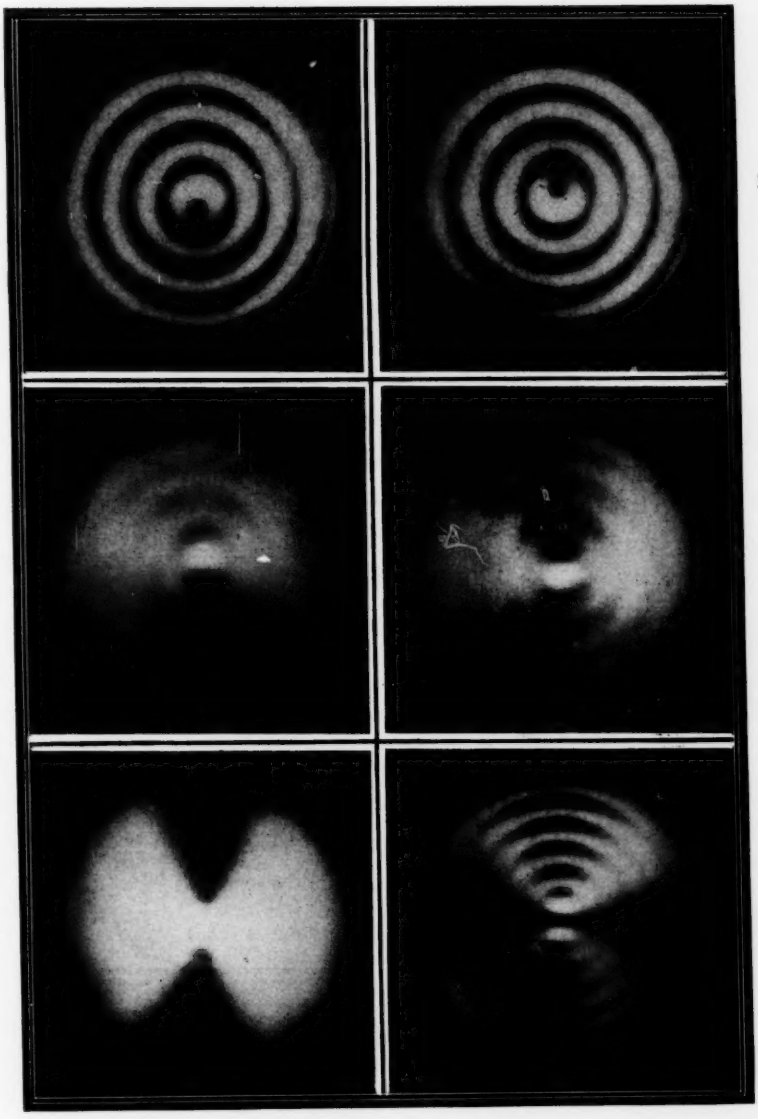

FIG. 1

FIG. 2

FIG. 3

FIG. 4

FIG. 5

FIG. 6

FIG. 7

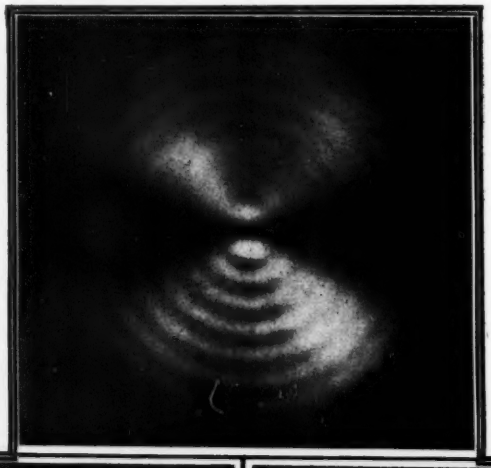

FIG. 8

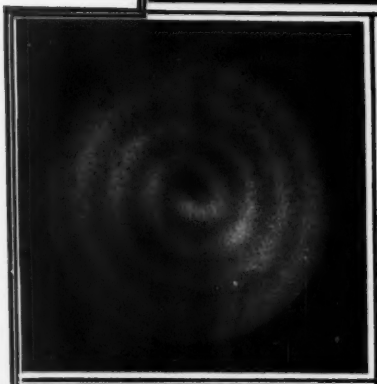

FIG. 9

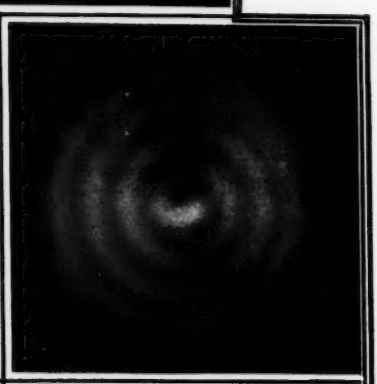

FIG. 10

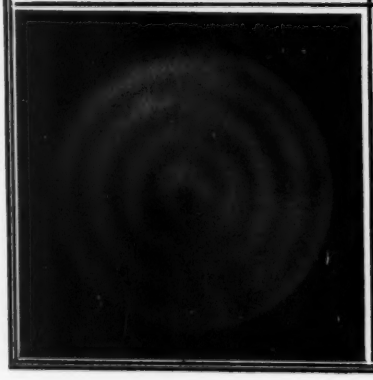

FIG. 11

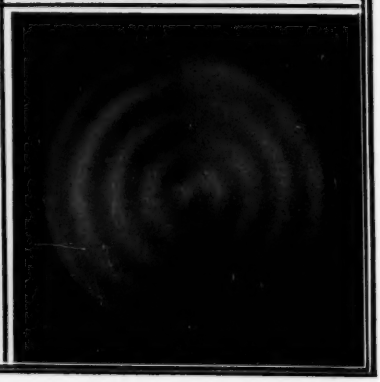

SYNTHETIC EXPERIMENTS IN THE BENZO-PYRONE SERIES

Part LXV. Synthesis of α-Methyl Karanjin and Related Compounds

By S. S. Chibber, A. K. Ganguli, S. K. Mukerjee and T. R. Seshadri, F.A.Sc.

Received May 4, 1957

In earlier work[1-4] on the synthesis of furanochromones in which the furan ring was built on an existing chromone, flavone or isoflavone system, it was noticed that, when there was no substitution in the furan ring, the yield of the final product was very poor, mainly due to large losses in the last stage of decarboxylation. On the other hand if a methyl group was present in the β-position, comparatively good yields were obtained.[4] It could be expected that the substituents may affect also the physiological properties of the furano compounds concerned. Rotenone, a powerful insecticide, has substitution in the α-position of the furan ring. In order to study the potency of compounds with methyl substituents in the α-position, α-methyl karanjin and its analogues have now been prepared.

The method adopted has already been mentioned in a previous publication.[5] 3-Methoxy-7-hydroxy flavone and its derivatives with substituents in the side phenyl nucleus have been allylated and subjected to Claisen migration. Addition of hydrogen bromide to the allylic double bond and subsequent elimination of it with pyridine effected the dihydro-furan ring closure. The final stage of dehydrogenations was brought about by N-bromo-succinimide.

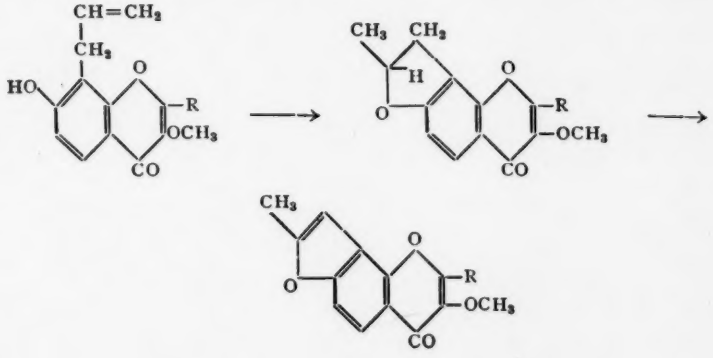

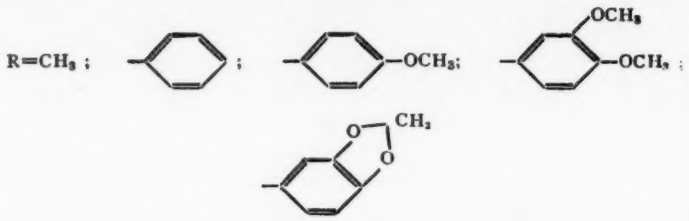

The yields of the dihydrofuran derivatives were uniformly good in all the cases. Particular mention should be made of the use of N-bromo-succinimide as a dehydrogenating agent in this series of compounds. The difficulties reported by Pavanaram and Row[6] in the preparation of certain linear furanoflavones were not experienced. Pyridine was adequate for dehydrobromination and no demethylation took place. The bromination proceeded with increasing slowness as the bulk of the substituent in the 2-position was increased and this is markedly exhibited by experiments carried out with closely related 2-methyl chromones. The study of the chromones is given at the end of the paper.

The results obtained by testing 6 selected compounds as fish poisons are presented in Table I.

TABLE I

Toxicity of α-methyl karanjin and related compounds

(6 Fish were employed in each test)

	Compound	P.P.M. (Concentration)	Turning time
1.	α-Methyl karanjin	8	38
		19	14
2.	α-Methyl-4′-methoxy karanjin ..	15	30
3.	α-Methyl-3′ : 4′-Dimethoxy karanjin ..	32	No effect
4.	α-Methyl-3′ : 4′-methylenedioxy karanjin (α-Methyl pongapin)..	25	18
		37	10
5.	Dihydro derivative of (1)	8	15
		17	5
6.	Dihydro derivative of (2)	17	5
		21	4

The following broad conclusions seem to be justified. The dihydro compounds are definitely more toxic than the corresponding furan derivatives and substitution in the α-position of the furan seems to diminish toxicity. It was earlier reported[7] that 12 p.p.m. of karanjin yields a turning time of 5·5 minutes; the α-methyl compound in a concentration of 18·9 p.p.m. gives a turning time of 14 minutes.

Experimental

3-Methoxy-7-hydroxy-8-(β-bromopropyl)-flavone.—An ice-cold suspension of 3-methoxy-7-hydroxy-8-allyl flavone[8] (2 g.) in dioxan (250 c.c.) containing a little anhydrous ferric chloride was saturated with dry hydrogen bromide gas, kept for 24 hours at room temperature and then poured into ice-water. The solid (2·9 g.) that separated, crystallised from chloroform as colourless needles, m.p. 219–20° (Found: C, 58·6; H, 4·2; $C_{19}H_{17}O_4Br$ requires C, 58·6; H, 4·8%).

3-Methoxy-α-methyl dihydrofurano-(2′: 3′: 7: 8)-flavone.—The above bromoflavone (2 g.) smoothly cyclised when heated with pyridine (5 c.c.) for 1 hour. The product was purified by percolating a benzene solution of it through a column of alumina (30 g.). The percolate together with benzene washings furnished the dihydrofurano flavone (0·7 g.) which came out of alcohol as colourless needles, m.p. 142–43° (Found: C, 74·0; H, 4·7; $C_{19}H_{15}O_4$ requires C, 74·0; H, 5·2%).

3-Methoxy-α-methyl furano-(2′: 3′: 7: 8)-flavone (α-methyl karanjin).—A solution of the dihydrofuranoflavone (0·5 g.) and benzoyl peroxide (trace) in dry carbon tetrachloride (25 c.c.) was refluxed for 20 minutes with N-bromosuccinimide (0·3 g.). The cooled mixure was filtered from the precipitated succinimide and the filtrate evaporated to dryness. The yellow residue was dissolved in pyridine (6 c.c.), kept at 100° for 20 minutes and then poured into dilute acid when the furanoflavone (0·4 g.) separated as an oil which solidified on cooling and stirring. It crystallised from dilute alcohol as colourless rectangular plates, m.p. 121–22° (Found: C, 73·9; H, 5·1; $C_{19}H_{14}O_4$ requires C, 74·5; H, 4·6%).

3: 4′-Dimethoxy-7-allyloxy flavone.—Obtained by the allylation of 3: 4′-dimethoxy-7-hydroxy flavone,[9] this allyl ether came out as colourless rectangular prisms from dilute acetone, m.p. 102–3° (Found: C, 71·5; H, 5·1; $C_{20}H_{18}O_5$ requires C, 71·0; H, 5·3%).

3: 4′-Dimethoxy-7-hydroxy-8-allyl flavone.—Claisen migration of the allyl ether (2 g.) at 200° for 2·5 hrs. under reduced pressure and working up in the usual manner yielded the hydroxy allyl flavone (1·3 g.) as colourless

needles from acetone. It melted at 238–9° and gave a sparingly soluble sodium salt with sodium hydroxide solution (Found: C, 71·0; H, 5·6; $C_{20}H_{18}O_5$ requires C, 71·0; H, 5·3%).

3: 4′-*Dimethoxy-7-hydroxy-8-(β-bromopropyl)-flavone*.—Crystallised from chloroform as colourless rectangular plates, m.p. 212–13° (Found: C, 57·6; H, 4·8; $C_{20}H_{19}O_5$ Br requires C, 57·3; H, 4·5%).

3: 4′-*Dimethoxy-α-methyl dihydrofurano*-(2′: 3–7: 8)-*flavone*.—Cyclisation of the bromoflavone (1·7 g.) and purification of the pale yellow product as in a previous case gave the dihydro furanoflavone (0·6 g.). It came out of alcohol as colourless prisms, m.p. 147–48° (Found: C, 71·1; H, 5·2; $C_{20}H_{18}O_5$ requires C, 71·0; H, 5·3%).

3: 4′-*Dimethoxy-α-methyl furano*-(2′: 3′-7: 8)-*flavone*.—Dehydrogenation of the above with N-bromosuccinimide in the usual manner yielded the furano-flavone in 60% yield. It formed colourless needles from alcohol, m.p. 159–60° (Found: C, 71·2; H, 4·7; $C_{20}H_{16}O_5$ requires C, 71·4; H, 4·8%).

3: 3′: 4′-*Trimethoxy-7-allyloxy flavone*.—Obtained by the allylation of 3: 3′: 4′-trimethoxy-7-hydroxy flavone,[10] the allyl ether crystallised from a mixture of chloroform and alcohol as colourless silky needles, m.p. 152–53° (Found: C, 68·7; H, 5·7; $C_{21}H_{20}O_6$ requires C, 68·5; H, 5·4%).

3:3′: 4′-*Trimethoxy-7-hydroxy-8-allyl flavone*.—It formed colourless plates from alcohol, m.p. 228–30° (Found: C, 68·5; H, 5·4; $C_{21}H_{20}O_6$ requires C, 68·5, H, 5·4%).

3: 3′: 4′-*Trimethoxy-7-hydroxy-8-(β-bromopropyl)-flavone*.—It crystallised from ethyl acetate as colourless needles, m.p. 202–04°, yield 90% (Found: C, 56·1; H, 4·9; $C_{21}H_{21}O_6$ Br requires C, 56·1; H, 4·7%).

3: 3′: 4′-*Trimethoxy-α-methyl dihydrofurano*-(2′: 3′: 7: 8)-*flavone*.—Obtained by the cyclisation of the bromoflavone and purified in the manner mentioned already, the dihydrofurano-flavone came out of alcohol as colourless long rectangular plates, m.p. 144–45° (Found: C, 68·1; H, 5·7; $C_{21}H_{20}O_6$ requires C, 68·5; H, 5·4%).

3: 3′: 4′-*Trimethoxy-α-methyl furano*-(2′: 3′-7: 8)-*flavone*.—The reaction between the dihydro compound (0·5 g.) and N-bromosuccinimide (·25 g.) under the usual conditions was slow and appeared to be complete after 2·5 hours. Subsequent dehydro-bromination with hot pyridine (2 c.c.) yielded the furano-flavone (0·3 g.) which formed pale yellow needles from alcohol, m.p. 152–53° (Found: C, 68·8; H, 5·1; $C_{21}H_{19}O_6$ requires C, 68·9; H, 4·9%).

3-*Methoxy*-7-*allyloxy*-3′: 4′-*methylenedioxy flavone*.—Allylation of 3-methoxy-7-hydroxy-3′: 4′-methylenedioxy flavone[11] (4·5 g.) yielded the allyl ether which formed colourless plates from alcohol, m.p. 128–29° (Found: C, 67·8; H, 4·5; $C_{20}H_{16}O_6$ requires C, 68·2; H, 4·6%).

3-*Methoxy*-7-*hydroxy*-8-*allyl*-3: 4′-*methylenedioxy flavone*.—This hydroxy allyl flavone (0·8 g.), obtained by the Claisen migration of the allyl ether (1·2 g.), crystallised from alcohol as colourless needles, m.p. 271–73° (Found: C, 68·0; H, 4·3; $C_{20}H_{16}O_6$ requires C, 68·2; H, 4·6%).

3-*Methoxy*-3′: 4′-*methylenedioxy*-7-*hydroxy*-8-(*β-bromopropyl*) *flavone*.—Obtained from the hydroxy allyl flavone (1·2 g.) this bromoflavone (1 g.) formed pale yellow prisms from a mixture of chloroform and methanol, m.p. 218–19° (Found: C, 55·2; H, 3·8; $C_{20}H_{17}O_6Br$ requires C, 55·4; H, 3·9%).

3-*Methoxy*-3′: 4′-*methylenedioxy*-α-*methyl dihydrofurano*-(2′: 3′-7: 8)-*flavone*.—The above bromoflavone (0·9 g.) cyclised smoothly with pyridine and the product (0·6 g.) came out of alcohol as colourless prisms melting at 145–46° (Found: C, 68·5; H, 4·7; $C_{20}H_{16}O_6$ requires C, 68·2; H, 4·6%).

3-*Methoxy*-3′: 4′-*methylenedioxy*-α-*methyl furano*-(2′: 3′-7: 8)-*flavone* (α-*methyl pongapin*).—The dihydrofurano-flavone (0·5 g.) was dehydrogenated in the usual manner by the N-bromosuccinimide-pyridine method. The furano-flavone (0·2 g.) formed colourless plates from alcohol and melted at 190-91° (Found: C, 68·1; H, 3·8; $C_{20}H_{14}O_6$ requires C, 68·6; H, 4·0%).

2-*Methyl*-3-*methoxy*-7-*hydroxy*-8-(*β-bromopropyl*)-*chromone*.—Formed from 2-methyl-3-methoxy-7-hydroxy-8-allyl chromone[8] (2·3 g.) by the usual method, this bromochromone (3 g.) crystallised from ethyl acetate as colourless rectangular tablets, m.p. 210–11° (Found: C, 51·5; H, 4·5; $C_{14}H_{15}O_4Br$ requires C, 51·4; H, 4·6%).

α: 2-*Dimethyl*-3-*methoxy*-*dihydrofurano*-(2′: 3′-7: 8)-*chromone*.—Obtained by the cyclisation of the above bromo compound, the dihydrofurano-chromone came out of alcohol as colourless plates melting at 151–52° (Found: C, 68·0; H, 5·6; $C_{14}H_{14}O_4$ requires C, 68·4; H, 5·7%).

α: 2-*Dimethyl*-3-*methoxy furano*-(2′: 3′-7: 8)-*chromone*.—Dehydrogenation of the dihydro compound (6 mt.) yielded the furano-chromone, which formed colourless needles melting at 151–52°, from alcohol. Its yellow solution in concentrated sulphuric acid changed to deep crimson on warming (Found: C, 68·4; H, 4·6; $C_{14}H_{12}O_4$ requires C, 68·9; H, 4·9%).

2-*Methyl*-5-*hydroxy*-7-*allyloxy chromone*.—Partial allylation of 2-methyl-5: 7-dihydroxy chromone[12] during 5 hours yielded this allyl ether. It crystallised from alcohol as colourless prisms melting at 111–12° and gave a violet

ferric reaction (Found: C, 67·3; H, 4·7; $C_{13}H_{12}O_4$ requires C, 67·2; H, 5·2%).

2-*Methyl*-5 : 7-*dihydroxy*-8-*allyl chromone*—was obtained as pale yellow plates from dilute alcohol and melted at 190–91° (Found: C, 67·2; H, 5·4; $C_{13}H_{12}O_4$ requires C, 67·2; H, 5·2%).

2-*Methyl*-5: 7-*dihydroxy*-8-(*β-bromopropyl*)-*chromone*.—Prepared in the usual manner, this bromo derivative came out of ethyl acetate as colourless needles melting at 199–200° (Found: C, 49·3; H, 4·3; $C_{13}H_{13}O_4$ Br requires C, 49·8; H, 4·2%).

α-2-*Dimethyl*-5-*hydroxy*-*dihydrofurano*-(2′: 3′-7: 8)-*chromone*.—Cyclisation of the bromo derivative yielded the dihydrofurano-chromone which formed colourless plates melting at 156–57° from alcohol and gave a violet ferric reaction (Found: C, 66·7; H, 5·1; $C_{13}H_{12}O_4$ requires C, 67·2; H, 5·2%). The acetate crystallised from alcohol as rectangular prisms melting at 170–71°.

SUMMARY

A number of α-methyl-furano-flavones and their dihydro derivatives have been prepared using 7-hydroxy-8-allyl flavone derivatives. Ring closure is effected with anhydrous hydrogen bromide followed by pyridine and dehydrogenation with N-bromosuccinimide. 2-Methyl cromone derivatives have also been made. Tests with fish of select compounds indicate that dihydrofurano compounds are better poisons and an α-methyl group reduces toxicity in the furano compounds.

Our thanks are conveyed to Prof. S. Rangaswami, F.A.SC., Head of the Department of Pharmacy, Andhra University, Waltair, for carrying out the toxicity tests on fish.

REFERENCES

1. Rangaswamy and Seshadri — *Proc. Ind. Acad. Sci.*, 1939, **9 A**, 259.
2. Row and Seshadri .. *Ibid.*, 1951, **33 A**, 168.
3. Murty and Seshadri .. *Ibid.*, 1949, **30 A**, 107.
4. Row and Seshadri .. *Ibid.*, 1951, **34 A**, 187.
5. Ahluwalia, Mukerjee and Seshadri — *J. Sci. Ind. Res.*, 1953, **12 B**, 283.
6. Pavanaram and Row .. *Ibid.*, 1955, **14 B**, 157.
7. Krishnaswamy and Seshadri — *Proc. Ind. Acad. Sci.*, 1942, **13 A**, 231.
8. Rangaswami and Seshadri — *Ibid.*, 1937, **9 A**, 4.
9. Rao and Seshadri .. *Ibid.*, 1948, **24 A**, 96.
10. Allan and Robinson .. *J.C.S.*, 1926, 2334.
11. Rao and Seshadri .. *Proc. Ind. Acad. Sci.*, 1946, **43 A**, 148.
12. Gulati, Seth and Venkataraman — *J.C.S.*, 1934, 1766.

A CONVENIENT METHOD OF PREPARATION OF CYANIDIN CHLORIDE FROM (+) CATECHIN AND (−) EPICATECHIN

By A. K. Ganguli, T. R. Seshadri, F.A.Sc. and P. Subramanian
(*Department of Chemistry, Delhi University, Delhi*)

Received April 18, 1957

The conversion of cyanidin (IV) to (+) epicatechin (I) by reduction[1] played an important part in establishing the constitution of catechins. The reverse change of (+) catechin (I) to cyanidin chloride (IV) was effected by Appel and Robinson.[2] They employed (+) catechin tetramethyl ether and treated it with excess of bromine in technical dioxan solution. The crude bromocyanidin tetramethyl ether bromide which contained bromine in the 8-position also, was subjected to treatment with hydriodic acid in presence of red phosphorus. The resulting cyanidin iodide was converted into the chloride through the colour base as intermediate. We have repeated this process using pure samples of the naturally occurring stereoisomer (−) epicatechin (I) prepared from the heartwood of *Acacia catechu*. The same results are obtained, the yield being almost the same as from (+) catechin. When the penta-acetates of the catechins are used instead, only a trace of cyanidin is produced, the major product appearing to be a red-coloured polymer.

Though the method involving the bromination of the methyl ether works, it is rather time-consuming and gives poor yields. The conversion becomes far more convenient when N-bromosuccinimide and the acetate of (−) epicatechin (II) are used in carbon tetrachloride solution. A monobromo compound (III) is produced and it can be readily converted into cyanidin chloride (IV) by boiling with excess of alcoholic hydrochloric acid; the yield was poor in this method (18%). In her preparation of cyanidin chloride from butea gum Lady Robinson[3] used an ingenious method employing an aqueous solution of sodium acetate, zinc chloride and picric acid for extraction and simultaneous conversion of leucoanthocyanidin into cyanidin picrate. This method has also been employed in the present case on the assumption that the bromo compound (III) is similar to leucoanthocyanidin, and thereby a considerably enhanced yield of cyanidin picrate has been obtained and this could be converted into the chloride (IV). There is some loss involved in the conversion of picrate into the chloride. In later experiments it was found that purification through the picrate is not necessary in the present case and the chloride (IV) can be obtained directly in higher

yield (25%). Using (+) catechin (I) the yield of the bromo compound was the same though somewhat better yields of cyanidin (30%) have been obtained in repeated experiments. The difference however may not be significant for the stereochemistry of the 2 and 3 positions of the catechins.

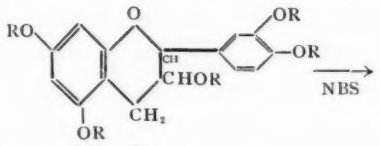

I R = H
II R = CH_3COO

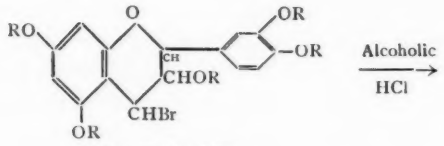

III R = CH_3COO

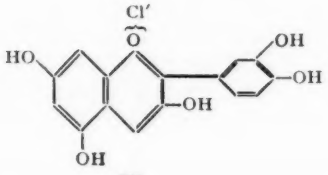

IV

The mechanism of the conversion of the catechins into cyanidin could be visualised as follows:

(*a*) The first stage is the entry of a bromine atom in the 4-position of the catechin penta-acetate (II) to form the monobromo derivative (III). In support of this may be mentioned the following points. The presence of acetoxy groups has been known to diminish the possibility of substitution in the benzene ring. Of the other possible positions for the substitution by N-bromosuccinimide the 2 and 4 positions should be considered because they are activated by the neighbouring benzene rings. Since the hydrogen atoms of a CH_2 group are known to be far more reactive as compared with the tertiary hydrogen atom the above conclusion seems to be valid.

(*b*) When the monobromo compound (III) is boiled with alcoholic hydrochloric acid, the deacetylated compound behaves like a leucoantho-cyanidin of the flavan-diol type undergoing dismutation and yielding the flavylium salt along with the simultaneous production of phlobaphenes.

The product, after purification, is found to be pure flavylium chloride having practically no bromide in it. This should be attributed to the predominantly large excess of chloride ions present in the acid solution.

Experimental

Bromination

To a solution of (−) epicatechin penta-acetate (1 gm.) in dry carbon tetrachloride (130 c.c.) were added N-bromosuccinimide (0·35 g.) and benzoyl peroxide (0·02 g.) and the mixture refluxed on a water-bath for seven hours. Initially the reaction mixture was slightly yellow which gradually changed to orange red as the reaction proceeded. It was then allowed to stand overnight when succinimide floated at the top. It was filtered and the solvent was removed from the filtrate by distillation under reduced pressure. The viscous mass thus obtained turned into a definite solid under vacuum. It could not be crystallised and it melted at about 80°. Yield 0·65 g. (Found: Br, 14·9; $C_{25}H_{23}O_{11}$ Br requires Br, 13·8%). (+) Catechin gave the same yield of the bromo compound.

Cyanidin chloride

(*a*) The above bromo compound (0·25 g.) was refluxed with ethanol (50 c.c.) and concentrated hydrochloric acid (10 c.c.) for three hours. A deep red colour developed. Water was added and the insoluble phlobaphene was filtered off. The filtrate was extracted with isoamyl alcohol. By the addition of petroleum ether the cyanidin chloride was taken in 1% hydrochloric acid solution which was slowly concentrated at the ordinary temperature in the presence of potash when cyanidin chloride separated as small chocolate-coloured crystals (70 mg.). From the colour reactions, paper chromatography (circular Rf., 0·72) and absorption maximum at 545 mμ it was characterised as cyanidin chloride.

(*b*) By Lady Robinson's method[8] the yield of cyanidin picrate was 0·45 g. from 0·65 g. of the bromo compound.

(*c*) The suspension of the bromo compound (0·65 g.) in water (30 c.c.) containing crystallised sodium acetate (2·5 g.) was boiled for 10 minutes. The boiling was continued for another minute after the addition of powdered fused zinc chloride (3 g.). The sticky mass which gradually solidified on cooling was filtered. The aqueous filtrate gave no appreciable amount of anthocyanidin when treated separately. The solid was then heated with aqueous saturated picric acid (18 c.c.) for 8 minutes. Alcoholic hydrochloric acid (125 c.c.; 8%) was then added and the refluxing continued for 45

minutes. Water was added to the reaction mixture which was then extracted with isoamyl alcohol. The colouring matter was then transferred to 1% hydrochloric acid solution by the addition of petroleum ether. The acid solution, after washing thoroughly with benzene, was slowly concentrated at ordinary temperature in presence of potash when cyanidin chloride (250 mg.) separated out. It was characterised as in the previous case. (+) Catechin bromide gave a better yield (300 mg.).

SUMMARY

Cyanidin has been prepared in satisfactory yields from the acetates of (+) catechin and (−) epicatechin by monobromination with N.B.S. and subsequent treatment.

REFERENCES

1. Freudenberg, Fikentocher and Schmidt .. *Annalen*, 1925, **444**, 135.
2. Appel and Robinson .. *J.C.S.*, 1935, 426.
3. Robinson (Mrs.) .. *Ibid.*, 1937, 1157.

KINETICS OF ISOTHERMAL ANNEALING OF RADIATION DAMAGE IN SZILARD-CHALMERS REACTION WITH COBALT COMPLEXES

Part I. Tris-Acetylacetone Cobalt (III)—Section 1

By Amar Nath, K. S. Venkateswarlu and Jagdish Shankar

(*Atomic Energy Establishment, Trombay, Bombay*)

Received January 21, 1957

(Communicated by Dr. H. J. Bhabha, F.R.S., F.A.SC.)

Introduction

It has been observed earlier that the retention* of several neutron irradiated oxyanions[1-6] show an increase on subsequent heating. The kinetics of the process has been studied by heating samples of the irradiated compounds for known periods of time at fixed temperatures and an attempt made to analyse the data, but it was not found to obey any simple chemical rate law. Herr[13] investigated in some detail the thermal annealing of the neutron irradiated K_2ReCl_6 crystals. Zuber[7] showed that the data for tris-ethylene-diamine Co (III) nitrate admitted of graphical analysis to yield two specific first-order reaction rates associated with two different activation energies.

The present paper forms part of a general comprehensive study of the thermal and radiation annealing of several irradiated cobalt complexes, which is ultimately expected to give some insight into the nature of the damage centres resulting from Szilard-Chalmers effect and other extraneous radiations. It has been found that the retention reaches a maximum characteristic of the temperature of annealing. For each temperature studied thermal annealing has been shown to follow first-order kinetics. The results of two-stage and multistage experiments show that the thermal history has a profound influence on the annealing behaviour.

Experimental

Preparation of tris-acetylacetone cobalt (III).—It was prepared after Gach.[8] All the chemicals used were either G. R. or extra pure grades of E. Merck. M.P. 198° C. (*cf.* West[12] 196° C. uncorrected).

* Of the atoms undergoing a nuclear transformation, that fraction which remains in, or reverts to, its initial molecular condition is called 'retention'.

Analysis	Found	Calculated for $(C_5H_7O_2)_3Co$
Co	16·60	16·57%
C	50·56 50·64	50·6%
H	6·07 6·01	5·9%

Neutron irradiation.—Bulk quantities of the complex powder were irradiated in BEPO, Harwell, with a total integrated flux of the order of 2×10^{16} nvt. thermal neutrons and more than 10^6 roentgen of γ-radiation. It was stored at room temperature for about 2 years before the work reported here was commenced.

Heating and chemical separation.—Powder aliquots were drawn from the bulk irradiated sample and were maintained at specified temperatures for different periods of time in stoppered conical flasks in an electric air oven kept constant to within $\pm 0{\cdot}5°$ C. or in an oil-bath kept to within $\pm 0{\cdot}2°$ C. In the latter case, at the end of the heating period, the flask was chilled in cooled acetone to freeze the reaction.

Each aliquot was dissolved in about 15 ml. of benzene and the solution was transferred to a separating funnel. The flask was rinsed repeatedly with small amounts of benzene and the rinsings were transferred to the separating funnel. Eight to 10 ml. of an aqueous solution containing 3% EDTA (disodium salt) and 1% sodium-potassium tartrate and small amounts of cobalt sulphate (30–60 mg.) were added to the conical flask and then transferred to the separating funnel and struck with the benzene solution of the complex. The aqueous fraction was collected in a volumetric flask. The benzene fraction was struck successively with three aliquots of 8–10 c.c. 3% EDTA—1% tartrate solution, each time the solution being used first to rinse the conical flask to ensure its complete decontamination. The flask and the final fraction of the EDTA solution used for striking the complex were checked for the absence of activity using a probe monitor.

The aqueous extracts and the benzene fraction were both made up to the same volume with water and benzene respectively. Aliquots from these solutions were pipetted out in vials and the activity was measured in a well-type sodium iodide-thallium scintillation crystal assembly. In later work, the aqueous and the organic phases were made up to the mark in

standard volumetric flasks which had been previously matched with respect to a NaI (T l) crystal—fixed geometry set-up (20 ml. of a high counting Co^{60} aqueous solution taken in each flask and made up to the mark with water gave counts which agreed to within about 0·2%). The percentage retentions were calculated from the above measurements.

In a few tests, cobalt sulphate solution alone was used to extract the cobaltous activity from the benzene solution of the irradiated sample. It was observed that, although the benzene solution had to be struck a larger number of times, the final value of the retention was identical with that obtained by using the EDTA mixture for extraction. This indicated that the EDTA solution extracted only those species which exchanged readily with cobaltous ions.

It may be pointed out that the species that cannot be extracted by EDTA must be in the same chemical state as that of the parent complex (or perhaps some form very closely allied to it).

When an aliquot was dissolved in benzene, allowed to evaporate to dryness and then subjected to thermal treatment, no change in the value of retention occurred, showing that the metastable specie is destroyed by dissolution in a solvent.

Data and Observations

Single stage annealing.—Isothermal runs were made at 50°, 71°, 82·5°, 92°, 101·5°, 111°, 116·5° and 122·5° C. and the data is given in the following tables. It will be observed that the initial value of retention in Tables I–IV (*viz.*, 21·1%) is different from that in Tables V–VIII (*viz.*, 20·4%) due to the annealing which occurred during storage at room temperature.

Retention (R) *vs.* time (t) in hours has been plotted for Tables III–VIII in Fig. 1. It would be seen that, at each temperature R reaches a saturation value (R_∞) characteristic of the temperature of the isothermal run, after which even prolonged heating produces no change. The values of ($R_\infty - R$) are given in the last column of the tables and are plotted against 't' on the semi-log paper in Figs. 2 and 3. The plots are found to be perfectly linear, indicating that annealing is governed by first order kinetics. The time of half-reaction ($t_{\frac{1}{2}}$) has been determined from the semi-log plot for each temperature and its value and that of 'k', the specific reaction rate are recorded at the foot of each table.

Multistage annealing.—In order to study the effect of previous thermal treatment on annealing behaviour the following multistage heating experiments were undertaken.

TABLE I

Temperature 50 ± 1° C.

Time of heating days	Percentage Retention	$(R_\infty - R)$
0	21·1	5·7
1	22·7	4·1
2	23·6	3·2
3	24·7	2·1
6	25·85	0·95
10	26·2	0·6
14	26·5	0·3
21	26·8	
28	26·7 26·9	

R_∞: 26·8%; $t_{\frac{1}{2}}$: 55 h./00 m.; 'k': $0{\cdot}35 \times 10^{-5}$ sec.$^{-1}$

TABLE II

Temperature 71 ± 0·2° C.

Time of heating	Percentage Retention	$(R_\infty - R)$
Hrs. Min.		
0—00	21·1	8·5
4—00	22·8	6·8
8—00	24·1	5·5
18—00	26·1	3·5
30—00	27·6	2·0
40—00	28·5	1·1
57—00	29·2	0·4
72—00	29·4	0·2
96—00	29·6	
120—00	29·5	
144—00	29·6	
168—00	29·7	

R_∞: 29·6%; $t_{\frac{1}{2}}$: 13h./15 m.; 'k': $1{\cdot}45 \times 10^{-5}$ sec.$^{-1}$

TABLE III

Temperature 82·5 ± 0·5° C.

Time of heating	Percentage Retention	$(R_\infty - R)$
Hrs. Min.		
0—00	21·1	9·9
2—00	22·4	8·6
4—00	23·4	7·6
8—00	25·0	6·0
18—00	27·7	3·3
32—00	29·5	1·5
56—00	30·6	0·4
72—00	30·9	
87—00	31·0	
100—00	30·9	

R_∞: 31·0%; $t_{\frac{1}{2}}$: 11 h./37 m.; 'k': $1{\cdot}64\times10^{-5}$ sec.$^{-1}$

TABLE IV

Temperature 92·0 ± 0·2° C.

Time of heating	Percentage Retention	$(R_\infty - R)$
Hrs. Min.		
0—00	21·1	16·9
4—00	25·0	13·0
8—00	28·6	9·4
15—00	32·6	5·5
20—00	34·0	4·0
24—00	35·0	3·0
28—00	35·6	2·4
32—00	36·5	1·5
42—12	37·1	0·9
55—00	37·5	0·5
71—00	38·0	
87—00	38·1	
96—00	38·0	

R_∞: 38·0%; $t_{\frac{1}{2}}$: 9 h./48 m.; 'k': $1{\cdot}96\times10^{-5}$ sec.$^{-1}$

TABLE V

Temperature 101·5 ± 0·5° C.

Time of heating	Percentage Retention	$(R_\infty - R)$
Hrs. Min.		
0—00	20·4	32·2
1—30	24·7	27·9
3—00	28·3	24·3
5—30	33·3	19·3
9—30	38·2	14·4
14—00	43·8	8·8
15—00	44·5	8·1
16—00	45·2	7·4
17—00	45·8	6·8
21—00	48·0	4·6
26—00	50·0	2·6
34—00	51·1	1·5
55—00	52·3	
69—00	52·9	
72—00	52·5*	

R_∞: 52·6%; $t_{\frac{1}{2}}$: 7 h./36 m.; 'k': $2{\cdot}53 \times 10^{-5}$ sec.$^{-1}$

* Recent check value on the oil-bath.

TABLE VI

Temperature 111·0 ± 0·5° C.

Time of heating	Percentage Retention	$(R_\infty - R)$
Hrs. Min.		
0—00	20·4	35·4
1—00	25·8	30·0
2—00	28·3	27·5
3—00	31·1	24·7
5—00	36·9	18·9
7—00	40·4	15·4
9—00	43·8	12·0
11—00	45·5	10·3
15—36	50·5	5·3
22—30	53·0	2·8
33—00	55·1	0·7
57—00	55·9	
70—00	55·7	

R_∞: 55·8%; $t_{\frac{1}{2}}$: 5 h./42 m.; 'k': $3{\cdot}77 \times 10^{-5}$ sec.$^{-1}$

TABLE VII

Temperature 116·5 ± 0·5° C.

Time of heating	Percentage Retention	$(R_\infty - R)$
Hrs. Min.		
0—00	20·4	39·7
1—30	30·5	29·6
3—00	35·9	24·2
5—00	41·8	18·3
6—00	45·3	14·8
7—00	48·4	11·7
8—00	49·2	10·9
9—00	51·4	8·7
10—00	52·2	7·9
11—00	53·8	6·3
12—00	54·9	5·2
18—00	57·8	2·3
21—00	59·3	0·8
42—00	59·8	
56—00	60·5	
65—10	59·6	
80—00	60·3	

R_∞: 60·1%; $t_{\frac{1}{2}}$: 4 h./12 m.; 'k': $4{\cdot}58 \times 10^{-5}$ sec.$^{-1}$

TABLE VIII

Temperature 122·5 ± 0·5° C.

Time of heating	Percentage Retention	$(R_\infty - R)$
Hrs. Min.		
0—00	20·4	45·7
0—30	25·0	41·1
1—30	34·8	31·3
3—00	46·3	19·9
4—00	50·9	15·2
5—00	54·2	11·9
6—00	58·4	7·7
7—00	59·0	7·1
16—00	65·3	0·8
24—00	66·0	
54—00	66·2	

R_∞: 66·1%; $t_{\frac{1}{2}}$: 2h./36 m.; 'k': $7{\cdot}40 \times 10^{-5}$ sec.$^{-1}$

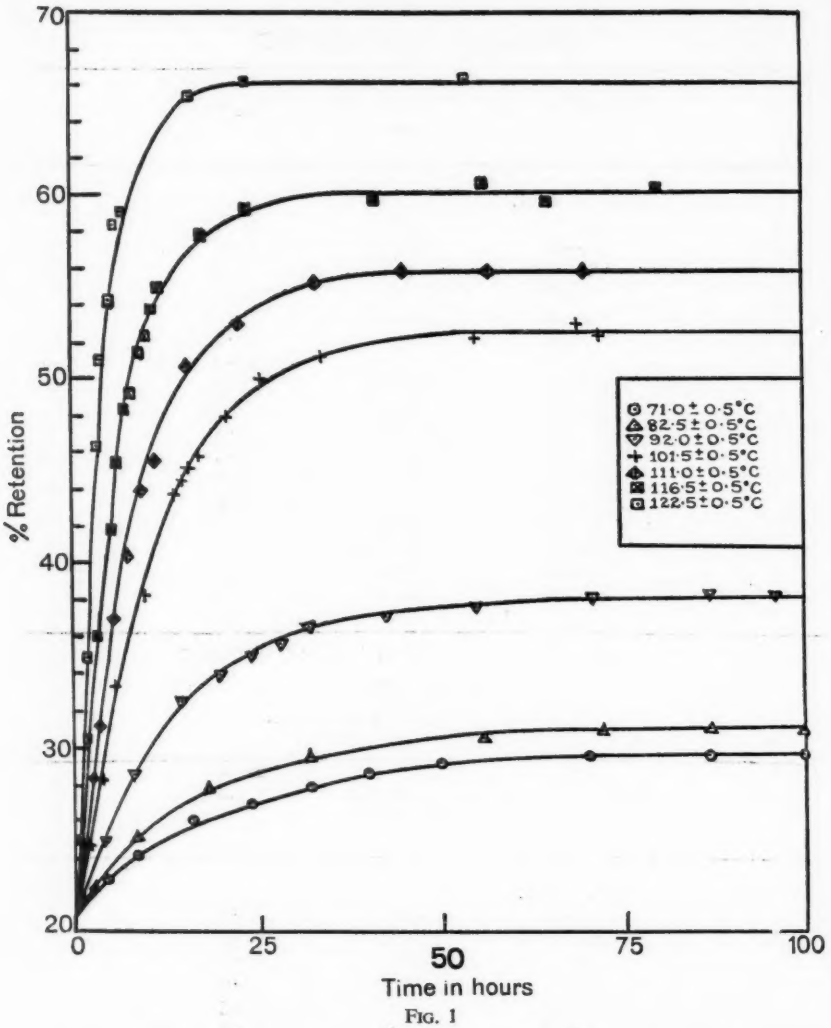

FIG. 1

An adequate portion from the irradiated bulk sample was heated at 82·5° C. for a period longer than that required to attain R_∞. Small aliquots were drawn from this heated sample and these along with the remainder were reheated at 92° C. The former were withdrawn at different periods to work out the kinetics, while the latter was heated to attain R_∞. The process was repeated through 101·5°, 116·5°, and 122·5° C ·

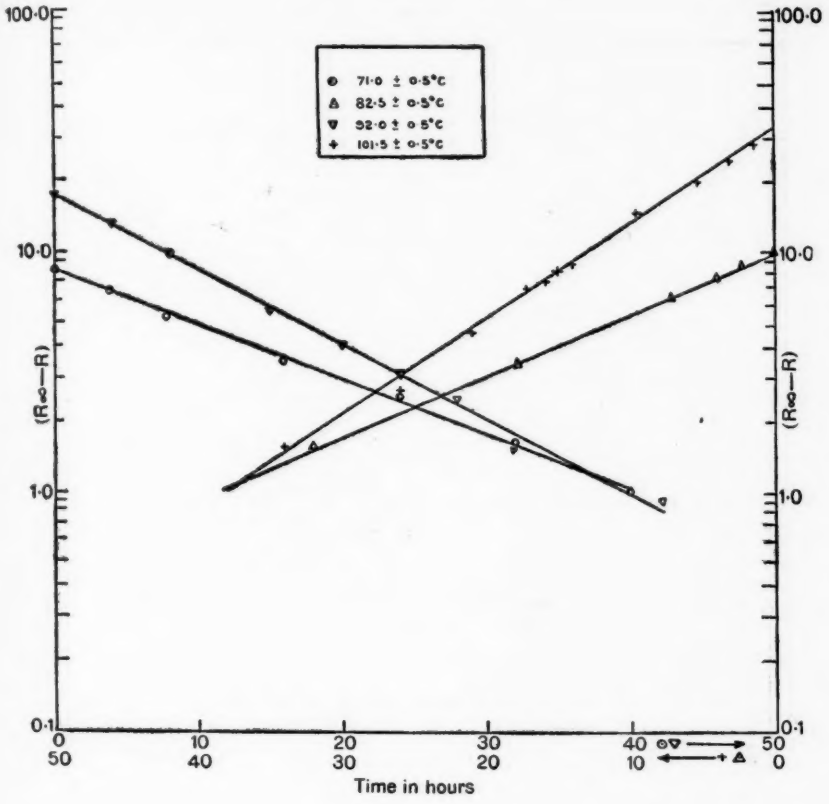

FIG. 2

Thus, the samples used for the run at 122·5° had previously been subjected to isothermal annealing to saturation values of retention successively at 82·5°, 92°, 101·5° and 116·5°. The data is given in Tables IX–XII and plotted in Fig. 4. The R_∞ values for multistage heating tests are summarized in Table XIII, in which, for the sake of comparison, R_∞ values for single stage annealing at the corresponding temperatures are also shown alongwith.

Value of R_∞ for multistage heating is lower than that for the single stage for the corresponding temperature. The rate constants also exhibit a marked decrease as compared to those for single stage annealing.

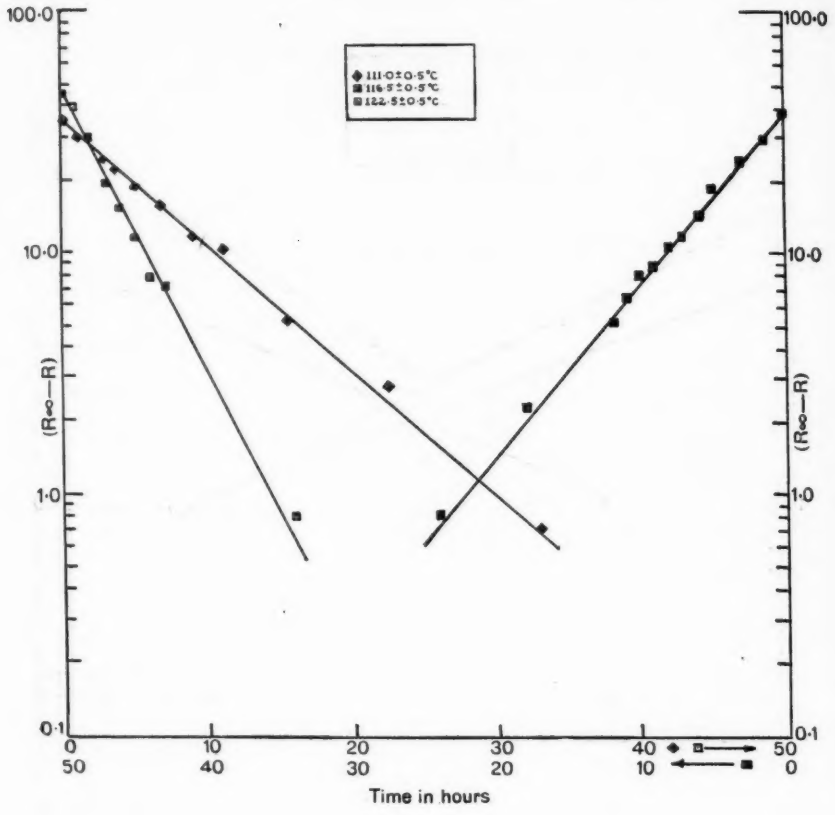

FIG. 3

Two stage-combination heating.—To gain further insight into the effect produced by the history of the heat treatment, the undermentioned investigations were carried out.

In one set, the initial treatment consisted of one step thermal annealing to R_∞ at a given temperature, and the final annealing at various higher temperatures. In Table XIV, the first column gives the temperature at which the final annealing was done, the second column the values of R_∞ at the corresponding temperature, with no previous heat treatment, columns 3–6 give the values of R_∞ obtained at temperature mentioned at the head of each column. The values of R_∞ for multistage annealing are given in the last column for the sake of comparison.

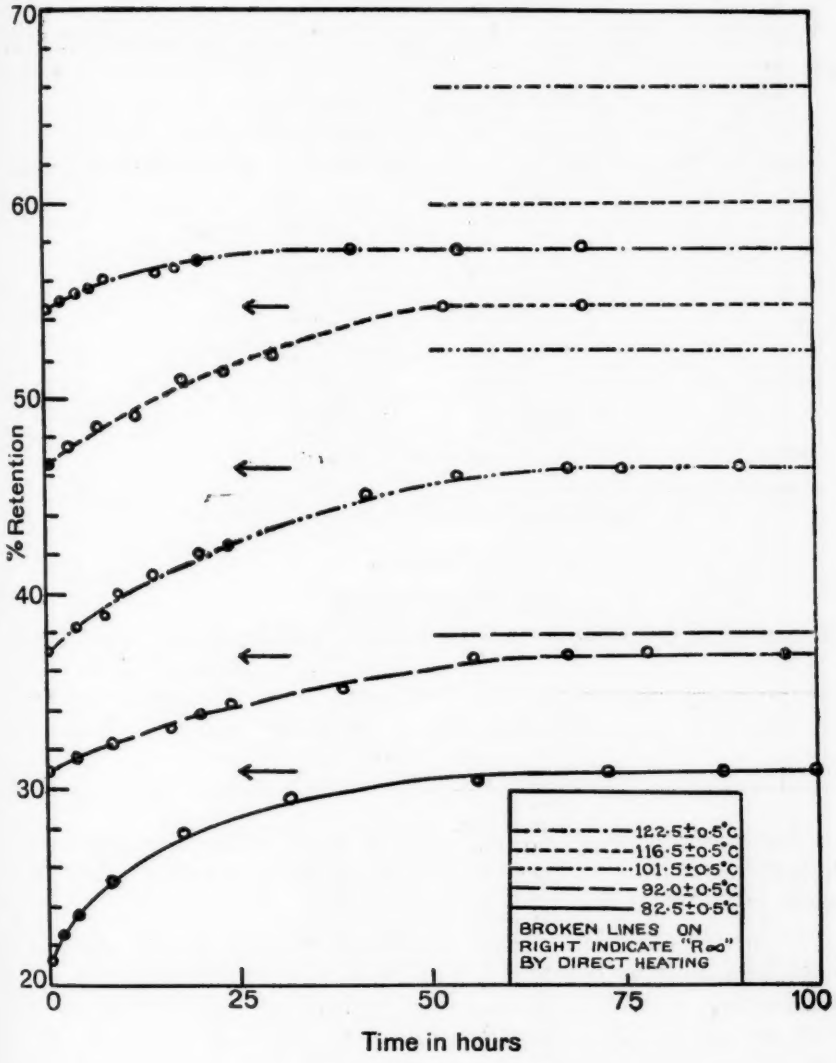
70
60
50
40
30
20
% Retention
0
25
50
75
100
Time in hours
122·5±0·5°C
116·5±0·5°C
101·5±0·5°C
92·0±0·5°C
82·5±0·5°C
BROKEN LINES ON RIGHT INDICATE "R∞" BY DIRECT HEATING

FIG. 4

TABLE IX

Multistage annealing

Run at 92·0 ± 0·2° C. Thermal history: 80 hrs. at 82·5° C.

Time of heating Hrs. Min.	Percentage Retention 'R'
0—00	31·0
4—00	31·6
8—00	32·3
16—00	33·2
20—00	33·8
24—00	34·3
39—00	35·3
56—00	36·7
68—00	36·9
78—00	37·1
96—00	37·0

R_{∞}: 37·0%; $t_{\frac{1}{2}}$: 22 h./31 m.; 'k' ; $0{\cdot}85 \times 10^{-5}$ sec.$^{-1}$

TABLE X

Multistage annealing

Run at 101·5 ± 0·2° C. Thermal history: 80 hrs. at 82·5° C. and then 78 hrs. at 92° C.

Time of heating Hrs. Min.	Percentage Retention 'R'
0—00	37·0
4—00	38·2
8—00	39·2
10—00	40·0
14—00	41·0
20—00	42·0
24—00	42·5
42—00	45·0
54—00	46·0
68—00	46·5
74—00	46·5
90—00	46·6

R_{∞}: 46·5%; $t_{\frac{1}{2}}$: 19 h./00 m.; 'k' = $1{\cdot}01 \times 10^{-5}$ sec.$^{-1}$

TABLE XI

Multistage annealing

Run at 116·5 ± 0·2° C. Thermal history: 80 hrs. at 82·5° C., 78 hrs. at 92° C. and then 68 hrs. at 101·5° C.

Time of heating Hrs. Min.	Percentage Retention 'R'
0—00	46·5
2—00	47·5
5—00	48·1
9—00	48·7
15—00	50·4
20—00	51·0
24—00	51·6
30—00	52·6
52—00	54·8
70—00	54·9

R_∞: 54·9%; $t_{\frac{1}{2}}$: 17 h./30 m.; 'k' ; $1 \cdot 10 \times 10^{-5}$ sec.$^{-1}$

TABLE XII

Multistage annealing

Run at 122·5 ± 0·2° C Thermal history: 80 hrs. at 82·5° C., 78 hours at 92° C. 68 hours at 101.5° C. and then 56 hours at 116.5° C.

Time of heating Hrs. Min.	Percentage Retention 'R'
0—00	54·9
2—00	55·1
4—00	55·5
6—00	55·7
8—00	56·0
15—00	56·5
17—00	56·7
20—00	57·0
40—00	57·8
54—00	57·9
70—00	58·0

R_∞: 57·9%; $t_{\frac{1}{2}}$: 13 h./02 m.; 'k' ; $1 \cdot 48 \times 10^{-5}$ sec.$^{-1}$

TABLE XIII

Summary of results of multistage heating tests

Temp. ° C.	R_∞		Rate constant (k) $\times 10^{-5}$ sec.$^{-1}$	
	Single stage	Multistage	Single stage	Multistage
82·5	31·0%	..	1·64	..
92·0	38·0%	37·0%	1·96	0·85
101·5	52·6%	46·5%	2·53	1·01
116·5	60·1%	54·9%	4·58	1·10
122·5	66·1%	57·9%	7·40	1·48

TABLE XIV

R_∞ is obtained by combination of two-stage heating experiments

Final heating temp. ° C.	Previous treatment					Value of multistage experiments
	None	82·5° C.	92·0° C.	101·5° C.	116·5° C.	
92·0	38·0*	37·0	..	..	..	..
101·5	52·5*	50·2	49·2	..	..	46·5
116·5	60·2*	58·8	57·7	56·0	..	54·9
122·5	66·2*	64·1	62·9	62·0	61·1	57·9

* R_∞ values redetermined for this set.

An essential feature of the above data for the temperatures studied, is that the higher the temperature of the initial thermal treatment,† the greater is the drop in the values of R_∞, as compared to its value for a single stage annealing at the higher temperature.

† With the reservation that if the difference between the temperature of the initial and final anneal is less than a certain value, the 'retention' would suffer only a slight or no change on undergoing the final treatment, *e.g.*, when the samples are heated *via* 118·6° C. and 120·5° C. to 122·5° C. the values of R_∞ 62·0% and 63·9% undergo no change. Similarly when heated *via* 99·5° C. to 101·5° C. the value of R_∞ remains practically constant (49·1%) while when heated *via* 97·5° C., R_∞ increases from 45% to 46% at 101·5° C. Thus within this narrow temperature range the difference in the value of R_∞ in the two stage and single stage heating may be very small.

In the second set of two-stage annealing tests, experiments were done, in the first stage of which samples were heated at different temperatures, for various periods, so as to attain nearly identical values of retention. They were then annealed to saturation values at (*a*) 101·5° C., and (*b*) 122·5° C. The results are presented in Table XV.

TABLE XV

Initial treatment			Final treatment			
			A: at 101·5 ± 0·2° C.		B: at 122·5 ± 0·2° C.	
Temp. ± 0·2° C.	Time of heating	Percentage retention	Time of heating	Percentage retention	Time of heating	Percentage retention
	Hrs. Min.		Hrs. Min.		Hrs. Min.	
101·5	15 – 48	45·1	72 – 00	52·4	30 – 00	64·65
111·0	9 – 54	45·0	72 – 00	51·3	30 – 00	64·3
116·5	5 – 48	45·2	72 – 00	51·0	30 – 00	64·0
122·5	2 – 54	45·2	72 – 00	50·8	30 – 00	66·0

The results indicate that the previous thermal history is reflected in the values of R_∞ for the final annealing, in spite of the fact that they had the same retention values at the end of the preliminary treatment.

In another set, aliquots were heated for varying periods of time at 116·5° C., and reheated to saturation anneal at a lower temperature, *viz.*, 101·5° C. The general trend of the change in retention is the same as observed in the other experiments in this series as shown in Table XVI.

It will be observed that as a result of heating at the higher temperature, when the retention acquires a value equal to or greater than R_∞ for the lower temperature (101·5° C.), it is not affected by the final thermal treatment. For example the value of R for 11 hours heating at 116·5° is 53·8 (Table XVI) and the same value has been obtained even after further heat treatment for 72 hours at the lower temperature 101·5° C.

DISCUSSION

The fact that the plot of log $(R_\infty - R)$ [*viz.*, log of the concentration of the metastable specie destined to anneal at a given temperature] *versus* time, gives a distinctly linear plot for isothermal annealing at each temperature studied, and also that, once R_∞ is attained, further heating at

TABLE XVI

Time of heating at 116·5 ± 0·2° C.	Saturation values obtained at 101·5 ± 0·2° C. after 72 hours heating	
0—20	51·9 52·1	52·0
0—40	51·65 51·54	51·6
1—00	51·2 51·2	51·2
7—00	50·4 50·6	50·5
9—54	52·5 52·5	52·5
11—00	53·7 53·9	53·8

that temperature does not affect the value of retention, go to show that the increase in R_∞ with temperature can hardly be accounted for by the existence of a wide 'spectra of activation energies' associated with the annealing of a variety of damage centres (*cf.* radiation damage in metal, graphite,[9, 10] etc.). The observation that heating at a higher temperature, after isothermal annealing at a lower temperature to infinity values (R_∞), results in further annealing eliminates the possibility of the existence of 'conventional' competing reactions,‡ which could have ordinarily accounted for the temperature dependence of R_∞. Hence, it appears that higher concentrations of the metastable specie undergoing annealing are made available with the increase of temperature by a 'thermally activated' intermediate process.

It was felt that it would be interesting to study the effect, if any, of prolonged heating at a lower temperature on the metastable specie destined to anneal at a higher temperature. Aliquots were, therefore, heated for varying periods of time after attainment of saturation anneal at 101·5° C.

‡ where once the reaction is completed, the fate of the reacting specie, at any temperature, is irreversibly determined by the juxtaposition of more than one reaction, and no further change is produced by changing the temperature.

and then reheated to maximum anneal at 122·5° C. The data are given in Table XVII. The decrease in the value of R_∞ (last column) is of a very small magnitude and is suggestive of very slight, if any, degradation or some other process incapacitating later thermal annealing of the specie. Also, in view of the above observations, the possibility of the existence of some type of a dynamic equilibrium after the saturation anneal is achieved at any given temperature, is discounted.

TABLE XVII

Preliminary heating at 101·5° *C. for various periods beyond attainment of* R_∞ *before annealing to infinity at* 122·5° *C.*

Initial treatment at 101·5 ± 0·2° C.		Final treatment at 122·5 ± 0·2° C.	
Time of heating	Percentage Retention (R_∞)	Time of heating	Percentage Retention (R_∞)
Hrs. Min.		Hrs. Min.	
65—00	(*a*) 52·6 (*b*) 52·8 (52·7)	30—00	62·0
120—00	(*a*) 52·7 (*b*) 52·8 (52·75)	,, ,,	(*a*) 61·8 (*b*) 61·9 (61·85)
170—00	(*a*) 52·5 (*b*) 52·6 (52·55)	,, ,,	(*a*) 61·5 (*b*) 61·7 (61·6)
214—00	(*a*) 52·5 (*b*) 52·6 (52·55)	,,	61·5

The plot of log '*k*' *versus* 1/T (Fig. 5) shows a marked curvature, which ordinarily could have been roughly accounted for by the existence of two or more annealing processes predominating at different temperatures, and associated with different values of activation energies. Since the plot of log $(R_\infty - R)$ *versus* '*t*' is strictly linear at all the temperatures studied, including the ones where the log *k* *versus* 1/T plot shows a large variation in the slope, it may be concluded that there is only a single annealing process which is exhibiting an apparent wide variation in activation energy and frequency factor, as shown in Table XVIII. This indicates that the annealing process is not a simple unimolecular reaction but is rather complex, perhaps involving several step

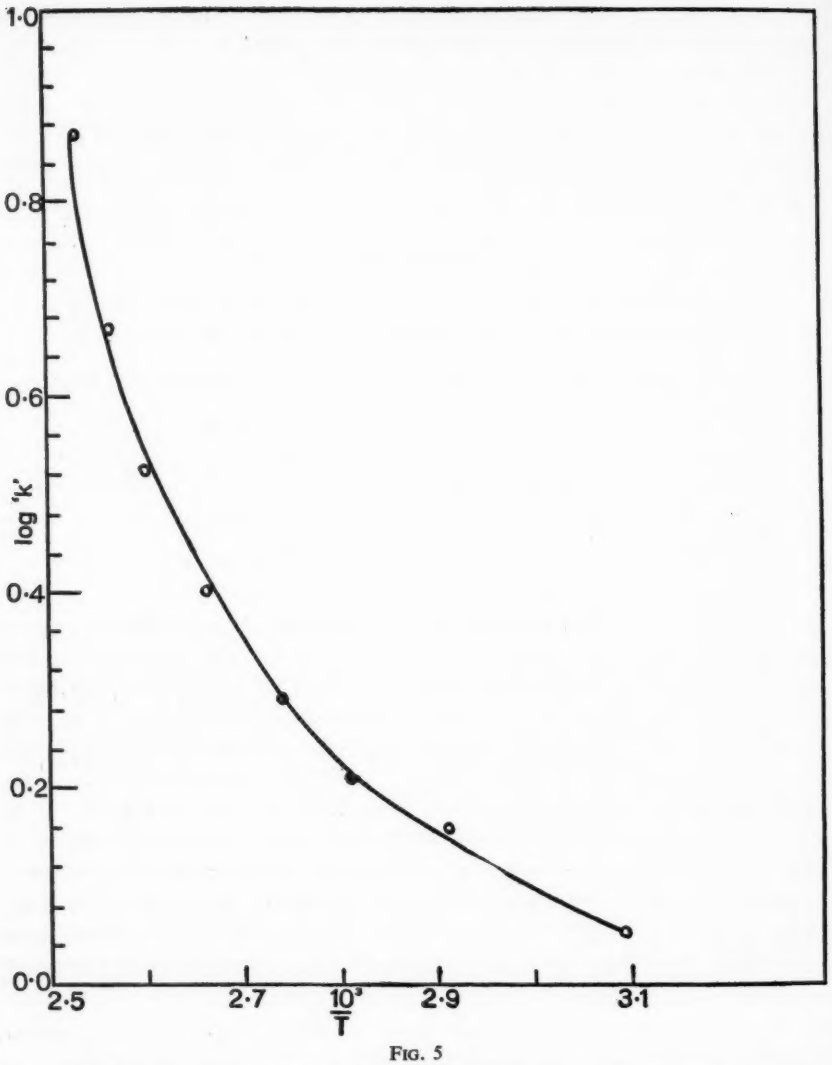

FIG. 5

The rate constant, 'k' and the saturation value of retention, R_∞ for any isothermal run are a function of the previous thermal history, as shown in the earlier sections. This can be explained by assuming the existence of competing reactions which, as has been stated, appear to be rather complex and involve more than one step in a fashion that they (reactions) mutually

influence each other. If the latter was not true, the value of 'k' would not have been affected by previous thermal treatment.

TABLE XVIII

Activation energies interpolated from Fig. (*log* k vs. $1/T$)

Temperature °C.	Activation energy E	Frequency factor A (calculated from $\ln k = \ln A - E/RT$)
50·0	2·12	..
82·5	3·06	$10^{-5.91}$
92·0	5·66	$10^{-4.81}$
101·5	8·03	$10^{-1.96}$
111·0	11·95	$10^{-0.13}$
116·5	18·54	10^{4}
122·5	35·25	$10^{13.4}$

Perhaps, it can be visualized that during an isothermal run the fate of the metastable specie is decided by two or more competing paths available for 'stabilization'. One of the processes is that of irreversible annealing to form the parent cobaltic specie (or some other specie closely allied to the parent which, however, does not appear probable). The other main process seems to consist of 'setting' or 'trapping'§ of the metastable specie with well-defined but variable depths—a physical process which inhibits, at the particular temperature, the annealing of the metastable specie directly or indirectly through an intermediate mechanism. But thermal activation at a higher temperature can result in a fraction of the metastable specie becoming available, directly or indirectly, for annealing. A third possible course can be the participation of the metastable specie in a process leading to irreversible degradation to the cobaltous state.

In the search for some tangible evidence for the above idea of competitive reactions, the following experiment was planned. If samples are heated for increasing periods of time at a fixed temperature and subsequently reheated to saturation value at a higher temperature, the trend followed by the decrease

§ This concept has been used by Lomer and Cottrell (*Phil. Mag.*, 1955, **46**, 711) in a different context and in a restricted sense. Here it is intended to have a wider significance.

in retention with longer periods of preliminary heating, could reflect the existence of competing reactions, as well as their numbers. Two sets of experiments were performed for 101·5° C. to 116·5° C., and 116·5° C. to 122·5° C. The data are given in Tables XIX and XX.

TABLE XIX

Time of heating at 101·5 ± 0·2° C.	Saturation values obtained at 116·5 ± 0·2° C. after 72 hrs. of heating	$(R_t' - R_\infty')$
Hrs. Min.		
0—00	60·1 (R_t' for $t = 0$)	4·0
0—30	59·0, 59·2 } 59·1	3·0
1—00	58·8, 58·6 } 58·7	2·6
1—30	58·35, 58·46 } 58·4	2·3
2—30	58·1, 57·9 } 58·0	1·9
4—00	57·6, 57·6 } 57·6	1·5
6—00	57·35, 57·44 } 57·4	1·3
8—00	57·1, 57·3 } 57·2	1·1
10—00	56·9, 57·1 } 57·0	0·9
16—00	56·5, 56·7 } 56·6	0·5
21—00	56·4 56·4	0·3
26—00	56·2, 56·2 } 56·2	0·1
72—00	56·0, 56·2 } 56·1	

TABLE XX

Time of heating at 116·5 ± 0·2° C.	Saturation values obtained at 122·5 ± 0·2° C. after 45 hrs. of heating	$(R_t' - R_\infty')$
Hrs. Min.		
0—00	66·1 (R_t' for $t = 0$)	4·9
0—24	64·5, 64·4 } 64·45	3·25
0—48	63·0, 63·3 } 63·15	1·95
1—12	62·75, 62·85 } 62·8	1·6
1—30	62·65, 62·5 } 62·57	1·37
2—00	62·4, 62·2 } 62·3	1·1
2—30	62·2, 62·1 } 62·15	0·95
3—00	62·1, 61·9 } 62·0	0·8
10—00	61·8, 61·7 } 61·75	0·55
22—00	61·5 61·5	0·3
45—00	61·2, 61·2 } 61·2	

The values for $R_t'-R_\infty'$ for the two sets (where R_t' is the value obtained from an aliquot heated for period 't' at the lower temperature, and reheated to saturation value at the selected higher temperature and R' is the value attained by an aliquot after preliminary heating to saturation anneal at the lower temperature and reheated to saturation value at the higher temperature) are plotted in Fig. 6. On analysis, the curves yield two linear plots indicating the existence of two first-order competitive reactions responsible for either removing the metastable specie from the site of the reaction or incapacitating

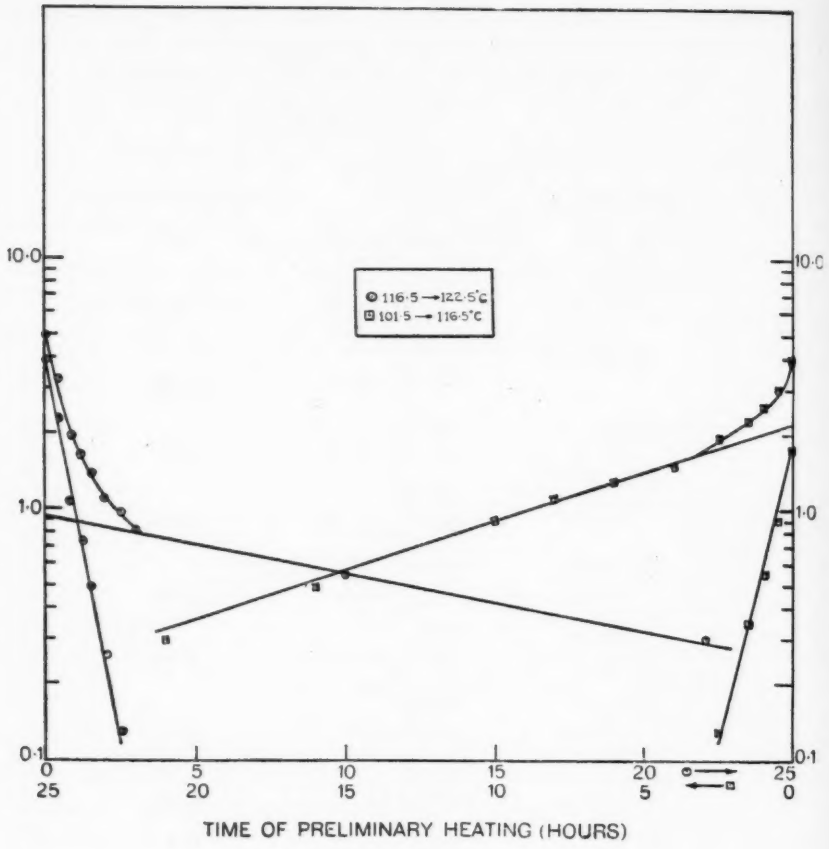

FIG. 6

it from annealing. In short, there are perhaps three competing processes operating, if only one is assumed for the annealing. As regards the nature of the damage centre undergoing annealing, some preliminary considerations come to the forefront. Can the thermal annealing be accounted for, by radical reactions in the 'brush-heap' of randomly fragmented molecules (as postulated by Willard and co-workers[11] for organics)? It is unlikely that this mechanism could be playing any significant role here for a variety of reasons. Firstly, it is rather difficult to conceive of such 'neat reconstitution' of the cobaltic chelate, from the debris (formed by random fragmentation of molecules). Secondly, such a process would place rather stringent demands on

the stability of the radicals concerned, especially at higher temperatures. Thirdly, barring the radicals which are in immediate neighbourhood, the reaction would be diffusion-controlled and hence obeying second-order kinetics, which is contrary to the present findings. The other possibility, which sounds more plausible, is the existence of 'configurational' and 'electronic' metastable states which are amenable to thermal and also irradiation annealing. Work on irradiation annealing will be published elsewhere.

Acknowledgements

We are particularly thankful to Mr. W. S. Eastwood of the Isotope Division, A.E.R.E., Harwell, for taking pains in arranging irradiation in BEPO under specified conditions. We express our appreciation of the assistance of Mr. S. Ramaswamy in the maintenance of the electronic equipment. Our gratitude is due to Prof. B. Peters and Dr. K. S. Singwi for the stimulating discussion.

Summary

Isothermal annealing has been found to follow first-order kinetics for the range of temperature studied. It has been found that the previous thermal history is reflected in the rate-constant (k) and the plot of log k *versus* 1/T exhibits a marked curvature. This has been explained as due to the fact that the annealing reaction leading to the parent specie is not a simple unimolecular one but is complex, involving several stages which in turn exercise mutual influence on other competing reactions preventing annealing.

During an isothermal anneal, the fate of the metastable specie is decided by three competitive reactions—one for annealing to the parent specie and the other two working in the reverse direction—the existence of which have been shown by graphical analysis of experimental data. One of the latter processes seem to be amenable to reversal in the sense that more metastable specie becomes available for anneal at a higher temperature after a run to infinity at a lower one. It seems that this process consists of 'setting' or 'trapping' of the metastable specie with variable depths—a physical process which inhibits at the particular temperature, the annealing of the metastable specie.

Considerable experimental work would be required to elucidate unambiguously the nature of the damage centre but the indications are that it is of a 'configurational' or 'electronic' nature, as it is amenable to both 'thermal' as well as 'radiation' annealing.

References

1. Green, J. H. and Maddock, A. G. *Nature*, 1949, **164**, 788.

2. Rieder, W., Broda, E. and Erber, J. — *Monatsh*, 1950, **81**, 657.
3. Cobble, J. W. and Boyd, G. E. — *J. Am. Chem. Soc.*, 1952, **74**, 1282.
4. Green, J. H., Harbottle and Maddock, A. G. — *Trans. Farad. Soc.*, 1953, **49**, 1413.
5. Maddock, A. G. and De Maine, M. M. — *Can. J. Chem.*, 1956, **34**, 275.
6. Aten, A. H. W. and Van Berkum, J. B. M. — *J. Am. Chem. Soc.*, 1950, **72**, 3273.
7. Zuber, A. V. .. *NYO*-6142 *BNL*, Columbia University, 1954.
8. Gach, F. .. *Monatsh*, 1900, **21**, 105.
9. Glen, J. W. .. *Adv. Phys.*, 1955, **4**, 403.
10. Burton, M. and Neubert, T. J. — *J. Ap. Phys.*, 1956, **27**, 557.
11. Willard, J. W. .. *Ann. Rev. Nu. Sci.*, 1953, **3**, 193
12. West, B. .. *J. Chem. Soc.*, 1952, 3115.
13. Herr, Wilfrid .. *Z. Elektrochemie*, 1952, **56**. 911.

STUDIES ON GROUNDNUT SHELLS

Part II. The Chemical Constitution of Groundnut Shell Hemicellulose A_1

By B. Radhakrishnamurthy and V. R. Srinivasan

(Department of Chemistry, Osmania University)

Received May 6, 1957

(Communicated by Prof. T. R. Seshadri, F.A.SC.)

As a number of agricultural residues have been utilised in industry after a proper appraisal of their chemical composition and physical properties, investigations on similar materials have been undertaken in these laboratories with the ultimate object of evolving suitable methods for their utilization. Groundnut shells have been chosen for the present investigation and their proximate analysis and the sugar make-up of the hemicellulosic fractions have been described elsewhere[1] by us. The chemical constitution of the first hemicellulosic fraction (A_1) forms the subject of this paper.

The hemicellulosic fractions which were extracted with cold 4% sodium hydroxide solution from powdered groundnut shells after a suitable pre-treatment, were resolved into six components by the usual methods. Hemicellulose A_1 which constitutes about 3% of the original material and 14% of the total alkali soluble part was found to contain pentosans (95·8%) and uronic acids (1·4%). Hydrolysis of the polysaccharide with dilute acid showed the presence of D-xylose (92%), an aldobiouronic acid (5·4%) and a small quantity of L-arabinose (0·4%), indicating that it is mainly composed of D-xylose residues. The mode of union of these sugar residues has been inferred from a study of the methylated hemicellulose A_1.

Methylation was carried out with sodium hydroxide and dimethyl sulphate and then with silver oxide and methyl iodide, till there was no increase in the methoxyl content. The methylated hemicellulose A_1 gave on hydrolysis with 2% methanolic hydrogen chloride and separation of the cleavage products on a cellulose column, tri- and di-O-methyl-D-xylose and a tetra-O-methyl-aldobiouronic acid in the molar ratio of 1 : 30 : 1. Traces of mono-O-methyl-D-xylose and D-xylose were also found among the cleavage products. Neither the methyl ethers of L-arabinose nor L-arabinose could be detected; so, it would appear that the L-arabinose obtained during the preliminary hydrolysis of the hemicellulose A_1 arose from an associated polysaccharide as an impurity.

The acidic fraction[2] on vigorous hydrolysis yielded D-glucuronic acid and D-xylose. Reduction of the methyl ester of the methyl aldobiouronoside

with lithium aluminium hydride by the method of Lythgoe and Trippet[3] gave a disaccharide which on hydrolysis yielded D-glucose and D-xylose confirming the observation that the aldobiouronic acid is composed of D-xylose and D-glucuronic acid. That the uronic acid moiety was linked through the C_2 position of the D-xylose residues was inferred from the identification of 3-O-methyl-D-xylose among the cleavage products of the tetra-O-methyl-aldobiouronic acid obtained from the methylated hemicellulose A_1. The tetra-O-methyl-aldobiouronic acid on complete methylation and subsequent hydrolysis gave rise to 3, 4-di-O-methyl-D-xylose, confirming the mode of union of D-glucuronic acid through the C_2 position of D-xylose.

Although the small quantities of mono-O-methyl-D-xylose and D-xylose formed duing the hydrolysis of the methylated polysaccharide could conceivably arise from demethylation[4] of 2, 3-di-O-methyl-D-xylose or incomplete methylation of the polysaccharide,[5] the possibility of their constitutional significance should not be overlooked at this stage. Experiments are under way towards further clarification.

Taking the results as a whole and the specific rotation[1] of the polysaccharide [$(\alpha)_D^{25}$, $-95{\cdot}6$] the following structure containing a linear chain of ca. 30, 1 : 4-linked β-D-xylopyranose units with D-glucuronic acid existing as a side chain through the C_2 position of one of the xylose residues, can be proposed for groundnut shell hemicellulose A_1.

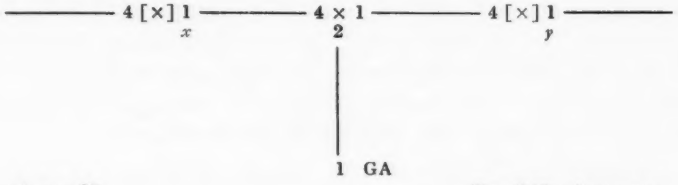

$x + y = 30$

X = β-D-xylopyranose
GA = D-glucuronic acid

This additional information concerning groundnut shell hemicellulose A_1 together with that already known about the hemicelluloses of esparto grass, wheat straw,[6] wheat flour[7], pear cell wall, etc., emphasises the view that in all these polysaccharides there is present a framework consisting of D-xylopyranose units. The properties of these hemicelluloses vary considerably which would seem to be due to the main structural framework of the xylopyranose units and to the extent of regularity of the branching. In the araboxylan from esparto grass, the side chain consists of L-arabofuranose units, while in the xylans obtained from wheat straw, pear cell wall, oat straw, etc., D-glucuronic acid or one of its methyl derivatives also forms the side

chain, branching being in all these cases through the C_3 position of one of the xylose residues. Although, there is concrete evidence in favour of C_3 branch points, the possibility that C_2 branch points also occur cannot be ruled out.[8] Branching through C_2 position has been found in the hemicelluloses of aspen wood,[9] beech wood,[10] Western hemlock[11] and the straw of flax.[12] The observations made in the case under discussion wherein also branching occurs through the C_2 position throws further weight on the possibility of C_2 branch points.

Experimental

Material.—Hemicellulose A_1 was prepared by acidifying the alkali extract of the powdered groundnut shells with acetic acid (*see* Part I for details of the preparation).[1]

Analysis.—The analysis of the groundnut shell hemicellulose A_1 was carried out by standard methods,[13] and the following results were observed: Ash 0·18%; Lignin 1·78%; Pentosans 95·80% and Uronic acids 1·44%.

Hydrolysis of the hemicellulose A_1 and the quantitative separation of the products of hydrolysis.—Hemicellulose A_1 (5 g.) was hydrolysed with 1% sulphuric acid (300 c.c.) at 50° C., till the optical rotation was constant. The reaction mixture was neutralised with barium carbonate, filtered and the residue was washed several times with hot water. The filtrate and the washings were added to excess of alcohol to precipitate the barium salt (B) of the acidic component, further experiments on which are described later.

The neutral solution obtained after removing the acidic component as the barium salt, was concentrated to a syrup under reduced pressure and fractionated on a cellulose column.[14] Two fractions identified as D-xylose (4·6 g.) and L-arabinose (0·02 g.) were obtained.

Methylation of hemicellulose A_1.—The hemicellulose (5 g.) was methylated six times with 40% sodium hydroxide solution and dimethyl sulphate in an atmosphere of nitrogen. The methylated product obtained thus, was further methylated with methyl iodide and silver oxide, till there was no change in methoxyl content. The pale yellow product (7·2 g.) which was extracted with chloroform had final OMe 36·4% and $(\alpha)_D^{24} - 48{\cdot}4$ (*c*, 0·84 in chloroform).

Hydrolysis of the methylated hemicellulose.—The methylated hemicellulose (3 g.) was hydrolysed with 2% methanolic hydrogen chloride (60 c.c.) for 12 hours (constant rotation). The solution was neutralised with silver carbonate, filtered and the filtrate concentrated under reduced pressure to a syrup. The syrup was treated with saturated barium hydroxide solution

(50 c.c.) to saponify the methyl ester of the acidic component. The excess of barium hydroxide was then neutralised with carbon dioxide and removed as barium carbonate. The resulting solution was concentrated to 15 c.c. under reduced pressure and passed through a column of Amberlite IR-120. The eluate was then concentrated and dried *in vacuo* to a syrup.

The syrup obtained thus was hydrolysed with N sulphuric acid to hydrolyse the methyl glycoside. The reaction mixture was neutralised with barium carbonate and filtered. The residue was thoroughly washed with hot water, the filtrate and the washings were combined, passed through Amberlite IR-120, concentrated to a syrup and dried *in vacuo*.

Separation of the cleavage products.—The syrup (2·2 g.) containing the methyl ethers of sugars as well as the acidic component was fractionated on a cellulose column using *n*-butanol-ethanol-water (4 : 1 : 5) as the developing solvent. Five fractions were first obtained and all of them were found to be neutral in reaction. For the isolation of the acidic component the column was eluted with water. The fractions were identified by their physical characteristics as well as by the preparation of derivatives. The identity and weights of the various fractions are given in Table I.

TABLE I

Cleavage products of the methylated hemicellulose A_1

Fraction	R_f value*	Identity	Weight in mg.	Moles
1	0·79	2, 3, 4-tri-O-methyl-D-xylose	62·14	1
2	0·63	2, 3-di-O-methyl-D-xylose	1020·0	30
3	0·63	2, 3-di-O-methyl-D-xylose	902·8	
4	0·31	3-O-methyl-D-xylose	13·92	(?)
5	0·12	D-xylose	12·74	(?)
6	..	Acidic component	100·68	1
			2112·28	

Total recovery 96%

* R_f values were determined on a sheet of filter-paper using the same developer.

Identification of the fractions

(*a*) *Fraction* 1 (2, 3, 4-*tri-O-methyl-D-xylose*):—The syrup on drying *in vacuo* gave a crystalline compound, m.p. 89° C., $(\alpha)_D^{25}$ + 22 (*c*, 0·5 in water. Found: OMe, 45·32. Calculated for $C_8H_{16}O_5$: OMe, 48·4%). The derived anilide[15] had m.p. 100° C. and $(\alpha)_D^{25}$ + 47 (*c*, 0·25 in ethyl alcohol),

(*b*) *Fractions* 2 *and* 3 (2, 3-*di-O-methyl-D-xylose*):—Fractions 2 and 3 were chromatographically identical and were combined. The combined syrup solidified after drying *in vacuo* for several days. The solid had m.p. 63° C. $(\alpha)_D^{23}$ + 68 (*c*, 1·0 in water). (Found: OMe, 34·23. Calculated for $C_7H_{14}O_5$ OMe, 34·8%). The anilide[16] prepared had m.p. 145° C. and $(\alpha)_D^{25}$ + 186 (*c*, 0·8 in ethyl acetate).

(*c*) *Fraction* 4 (3-*O-methyl-D-xylose*):—The solid obtained on drying the syrup *in vacuo*, had m.p. 101° C.,[17] $(\alpha)_D^{25}$ + 19 (*c*, 0·25 in water). Found: OMe, 18·4. Calculated for $C_6H_{12}O_5$, OMe, 18·9%.

(*d*) *Fraction* 5 (*D-xylose*):—This component had m.p. 152° C., $(\alpha)_D^{23}$ + 18 (*c*, 0·5 in water). Found: OMe, nil.

(*e*) *Fraction* 6 (*Acidic component*):—Described later.

Examination of the acidic component obtained during the hydrolysis of the hemicellulose A_1.—The barium salt (B) of the acidic component (0·37 g.) $(\alpha)_D^{25}$ + 69·6 (*c*, 0·5 in water) containing 18% of barium was dissolved in distilled water and de-ionised by passing through Amberlite IR-120. The clear eluate was concentrated under reduced pressure and dried *in vacuo*. The acid obtained (0·27 g.) had an equivalent weight 314 (Calculated for D-glucuronosyl-D-xylose 325).

Hydrolysis of the acid.—The methyl ester of the aldobiouronic acid was prepared by treating the acid (0·2 g.) with 2% methanolic hydrogen chloride (25 c.c.) for 8 hours. The resulting methyl ester was hydrolysed with 8% methanolic hydrogen chloride at 112–15° C. in a sealed tube for 8 hours. The solution was neutralised with silver carbonate, filtered and concentrated *in vacuo* to a syrup.

A small portion of the syrup obtained above was dissolved in N sulphuric acid and hydrolysed. The solution was neutralised with barium carbonate and filtered. The residue was washed with hot water. The filtrate and the washings were concentrated to 15 c.c., passed through a column of Amberlite IR-120 and concentrated to a syrup.

Paper chromatographic examination of the syrup revealed the presence of D-glucuronic acid and D-xylose.

The remaining larger portion of the syrup (0·15 g.) containing glycosides was dissolved in methanol (20 c.c.) and the solution was saturated with ammonia gas at 5° C. After allowing the reaction mixture to stand at room temperature for 18 hours a pale yellow solid separated out, which was identified as the amide of methyl-D-glucuronoside, m.p. 163° C. alone or admixed

with a pure specimen prepared from an authentic sample of D-glucuronic acid.

The mother liquor from which the amide of methyl-D-glucuronoside had been separated, was dissolved in water and 0·3 N barium hydroxide (30 c.c.) was added. The solution was heated on a water-bath at 80° C. to hydrolyse any remaining amide and a stream of carbon dioxide free air was bubbled through the solution during the hydrolysis to sweep out the ammonia generated. When ammonia was no longer evolved, the excess of barium hydroxide was neutralised with carbon dioxide and removed as barium carbonate. The neutral filtrate was evaporated to a syrup and hydrolysed with N sulphuric acid. The solution was neutralised with barium carbonate, filtered and the filtrate evaporated to dryness, when a solid was obtained which after recrystallisation from alcohol gave crystalline D-xylose, m.p. 152° C. alone or admixed with an authentic sample.

Reduction of the aldobiouronic acid with lithium aluminium hydride.—The aldobiouronic acid (10 mg.) was refluxed with 2% methanolic hydrogen chloride (30 c.c.) for 6 hours. The solution was neutralised with silver carbonate, filtered and the filtrate concentrated to a syrup *in vacuo*. The resulting syrup was dissolved in dry ether (30 c.c.) and lithium aluminium hydride (0·5 g. dissolved in 50 c.c. of dry ether) added during 3 hours to the refluxing solution. Excess of lithium aluminium hydride was destroyed by careful addition of water and the solution was acidified with 2 N sulphuric acid and hydrolysed for 12 hours at 115° C. in a sealed tube. The resulting solution was then neutralised with barium carbonate, filtered and the filtrate evaporated to dryness *in vacuo*.

Paper chromatographic examination of the product showed the presence of D-glucose and D-xylose.

Examination of the acidic component (*Fraction* 6) *obtained during the hydrolysis of the methylated hemicellulose* A_1.—The acidic component (20 mg.) obtained by eluting the cellulose column with water, after removal of the other products of hydrolysis of the methylated hemicellulose, was hydrolysed with 8% methanolic hydrogen chloride (20 c.c.) for 8 hours at 115° C. in a sealed tube. The solution was neutralised with silver carbonate and the resulting neutral solution was evaporated to a syrup. The syrup was dissolved in the minimum quantity of water and extracted twice with chloroform. The chloroform extract was treated with dry ammonia and the amide obtained was identified as the amide of methyl 2, 3, 4-tri-O-methyl-D-glucuronoside,[18] m.p. 185° C. $(\alpha)_D^{25}$ + 138 (*c*, 0·1 in water).

The aqueous layer from which the methyl ester of the methylated methyl glucuronoside had been extracted, was evaporated to a syrup, dissolved in N sulphuric acid and hydrolysed. On neutralisation with barium carbonate, followed by filtration, concentration to a syrup and drying *in vacuo*, it gave 3-O-methyl-D-xylose,[17] m.p. 89° C., $(\alpha)_D^{23} + 15$ (*c*, 0·5 in water). Found: OMe, 18·6. Calculated for $C_6H_{12}O_5$, OMe, 18·9%.

Complete methylation of Fraction 6.—Fraction 6 (60 mg.) was methylated with 30% sodium hydroxide and dimethyl sulphate in nitrogen atmosphere. There was no further change in the methoxyl content after the first methylation. The product obtained was thoroughly extracted with chloroform. Evaporation of the solvent under reduced pressure gave an yellow syrup which after purification by extraction with ether was identified as methyl 2-O-(2, 3, 4-tri-O-methyl-D-glucuronosyl)-3, 4-di-O-methyl-D-xyloside, $(\alpha)_D^{25} + 106$ (*c*, 0·5 in water). Found: OMe, 45. Calculated for $C_{17}H_{30}O_{11}$, OMe, 45·3%. Found: equivalent weight 410. Calculated for $C_{17}H_{30}O_{11}$, equivalent weight 425.

Hydrolysis of methyl 2-*O*-(2, 3, 4-*tri-O-methyl-D-glucuronosyl*)-3, 4-*di-O-methyl-D-xylose*.—The fully methylated aldobiouronic acid (50 mg.) obtained as above was hydrolysed with 8% methanolic hydrogen chloride (50 c.c.) in a sealed tube at 115° C. After the removal of hydrogen chloride, the acidic component was separated through its amide as in the previous case. The resulting neutral component which was obtained as a syrup was identified as 3, 4-di-O-methyl-D-xylose by the preparation of its lactone,[19] m.p. 66° C. $(\alpha)_D^{23} - 50 \rightarrow -23$ (*c*, 0·5 in water).

Summary

Groundnut shell hemicellulose A_1 has been shown to contain residues of D-xylose and D-glucuronic acid. The methylated polysaccharide gave on hydrolysis 2, 3, 4-tri-O-methyl-D-xylose, 2, 3-di-methyl-D-xylose and 2-O-(2, 3, 4-tri-O-methyl-D-glucuronosyl)-3-O-methyl-D-xylose in the molar ratio of 1 : 30 : 1. A structure is proposed for the hemicellulose which has a straight chain of ca. 30, 1 : 4-linked β-D-xylopyranose residues with D-glucuronic acid existing as a side chain through the C_2 position of one of the xylose residues.

References

1. Radhakrishnamurthy and Srinivasan — *J.S.I.R.*, 1957, **16 c**, 59.
2. ———— .. *Curr. Sci.*, 1957, **26**, 50.
3. Lythgoe and Trippet .. *J.C.S.*, 1950, 1983.

4. Chanda, Hirst, Jones and Percival — *Ibid.*, 1950, 1289.
5. ———— .. *J.C.S.*, 1951, 1240.
6. Adams .. *Canad. J. Chem.*, 1952, **30**, 698.
7. Perlin .. *Cereal Chem.*, 1951, **28**, 370, 382.
8. Hirst .. *J.C.S.*, 1955, 2974.
9. Jones and Wise .. *Ibid.*, 1952, 3389.
10. Aspinal, Hirst and Mahomed — *Ibid.*, 1954, 1734.
11. Dutton and Smith .. *J.A.C.S.*, 1956, **78**, 3744.
12. Geerdes and Smith .. *Ibid.*, 1955, **77**, 3569.
13. Doree .. *Methods of Cellulose Chemistry*, 1947 (Chapman & Ha. Ltd., 2nd Edition, Chapter XXII).
14. Hough, Jones and Wadman — *J.C.S.*, 1949, 2511.
15. Laidlaw and Percival — *Ibid.*, 1949, 1600.
16. Hampton, Haworth and Hirst — *Ibid.*, 1929, 1739.
17. Laidlaw and Percival .. *Ibid.*, 1950, 528.
18. Smith .. *Ibid.*, 1939, 1724.
19. James and Wise .. *Ibid.*, 1945, 739.

A MULTICHANNEL PULSE AMPLITUDE ANALYSER

By P. K. Iyengar, P. N. Rama Rao, G. Venkataraman
and
K. Usha
(*Atomic Energy Establishment, Trombay, Bombay-1*)

Received May 13, 1957
(Communicated by Prof. H. J. Bhabha, F.R.S., F.A.SC.)

The method of measuring the energy distribution of nuclear particles, consists in converting the particle energies to electrical pulses, in detectors like ionization chambers, proportional counters, scintillation counters, etc., and scanning the resulting pulse height distribution. A pulse amplitude analyser, single or multichannel is necessary for this purpose. A multichannel analyser is preferable as the scanning is done in a single step.

For satisfactory operation, a multichannel analyser should possess the following basic characteristics: (*a*) The greater the number of channels, the quicker and more precise will be the information obtained from the analyser, (*b*) The stability of the instrument should be such that it is stable to at least one channel width, over fairly long periods of time, (*c*) High speed of analysis is necessary for certain type of experiments such as the study of radiations from short-lived nuclei, (*d*) The circuits and other design features should be of the simplest type in order that servicing presents no difficulties.

Among the multichannel analysers, described in literature, the one which is most often used is of the Wilkinson[1] type. In this method of pulse height analysis, the input pulse produces a gate, whose width is proportional to the amplitude of the pulse. The gate opens an oscillator for the time of its duration, and produces a train of pulses, their number being thus proportional to the amplitude of the input pulse. The oscillator pulses are then counted in a decoding unit and a count is recorded in the appropriate channel.

A great advantage of using Wilkinson's method is that the stability of the instrument is mostly dependent on that of the pulse height to time converter unit and this unit can be made highly stable.

In the present work, many modifications have been introduced in the decoding units to make the instrument as simple as possible, without lowering its speed of analysis.

The number of channels of the analyser has been fixed to be 25 and the entire spectrum is scanned in 4 steps, making a total of 100 channels. Since

the selection of the 4 ranges is done by means of the number of oscillator pulses, and not by means of a discriminator bias adjustment, the uncertainty arising at the junction of two consecutive ranges is absent. Although, it would be preferable to have 100 channels in a single step, this would make the instrument too bulky, due to the increased number of recording stages.

This analyser can accept a maximum of 1000 pulses per second. It has not been made faster, as this requires more scaling capacity for individual recording units.

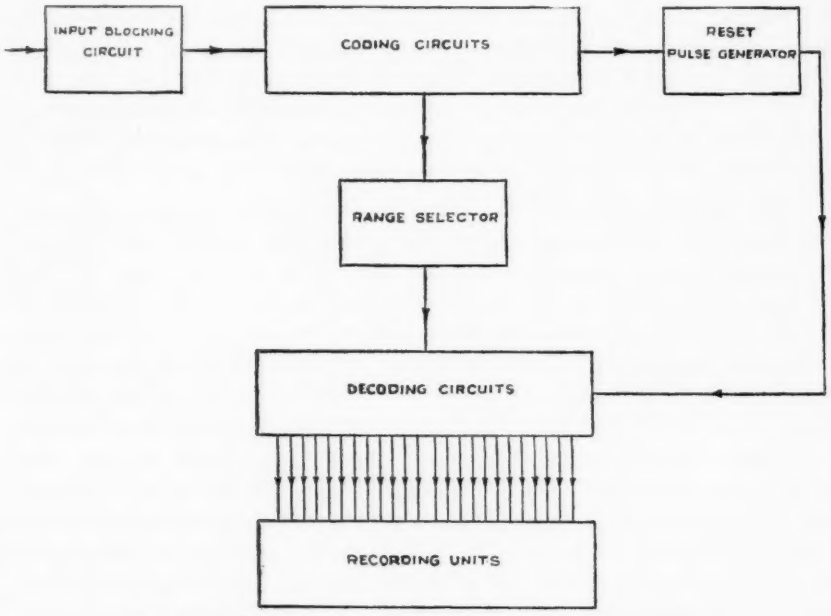

FIG. 1. Block Diagram. Multichannel Pulse Height Analyser.

CIRCUIT DESCRIPTION

The instrument is divided into different functional parts as shown in the block diagram Fig. 1. When a pulse is accepted by the instrument, the input blocking circuit, blocks all other pulses for a time until the accepted pulse is coded and recorded. Even though the time taken for a pulse to be coded and recorded depends on the amplitude of the pulse, for the sake of simplicity, the input is blocked for 1 millisecond. In the coding circuits the pulse amplitude is converted into a gate. The gate opens a blocking oscillator and produces a train of pulses for the time of its duration. The circuit

constants are so adjusted that a pulse amplitude of 100 volts produces 100 pulses from the blocking oscillator. In the range selector pulses of amplitude 1–25, 26–50, 51–75 and 76–100 are selected by a band-switch. The method of selection is explained later. Thus the range selector gives in its output a train of pulses whose number is anywhere between 0 and 25, depending on the pulse height. The decoding circuit essentially consists of 2 ring scalers in matrix form and of simple coincidence circuits forming the intersection points of the matrix. The reset pulse generator produces a pulse which is delayed by about 40 microseconds from the trailing edge of the gate pulse produced in the coding circuit. This pulse resets the ring scalers of the matrix. If a train of seven pulses had been sent to the decoding scalers, when the scalers are reset, we get an output from the coincidence circuit at position 7 in the matrix. This pulse is counted in the recording scaler of channel 7.

The input blocking circuit (Fig. 2) is similar to the one described by Wilkinson. Negative input pulses are fed to one grid of the double cathode

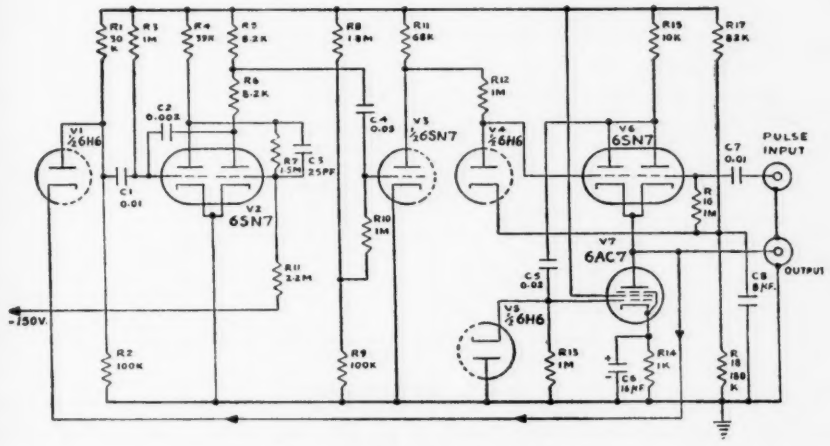

FIG. 2. Input Blocking Circuit.

follower V 6. The other grid is maintained at +40 volts by current passing in the tube V 3. The input pulse triggers the univibrator V 2 through the diode V 1. The gate pulse of the univibrator is about 1 millisecond wide. The negative gate cuts off the current in tube V 3 and raises the grid potential to 300 volts. This prevents the double cathode follower from passing any pulse during the 1 millisecond interval. The negative pulse from the cathode follower is inverted and fed to the pulse height to time convertor unit of the coding circuits.

Pulse height to time convertor circuit also is the same as that of Wilkinson with the only change that the values of charging condensor C and resistance R of the phantastron circuit are so adjusted that an input pulse of 100 volts amplitude produces a gate pulse at the output of about 800 microseconds duration.

The gated oscillator is shown in Fig. 3. The rectangular negative gate from the Wilkinson circuit is fed to the grid of tube V 2 which is normally conducting. Thus this tube is cut off and the blocking oscillator V 1

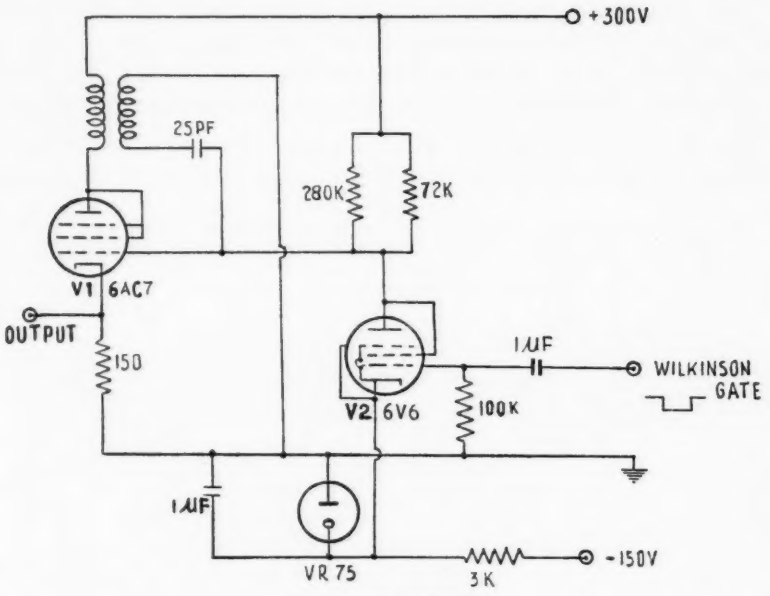

FIG. 3. Gated Oscillator.

produces oscillations for the duration of the gate pulse. The oscillator frequency is quite stable and is kept at about 150 kcs. Pulses are obtained at the cathode.

The time gate from the pulse height to time converter unit is differentiated and the pulse corresponding to its trailing edge is made to trigger a univibrator, which gives a gate pulse of 40 microseconds' duration. The positive pulse, corresponding to its trailing edge is used as the reset pulse.

A block diagram of the range selector is shown in Fig. 4. The pulses from the oscillator are fed to a scale of 25 consisting of two scales of 5 in cascade, so that output pulses are obtained for every 25. These pulses are again

fed to a ring of 4. The negative gate from the 1st tube of this ring lasts from 25 to the reset time or to 100. This gate is applied to a 6 A C 7 pentode coincidence A which selects oscillator pulses only from 0–25. For any pulse

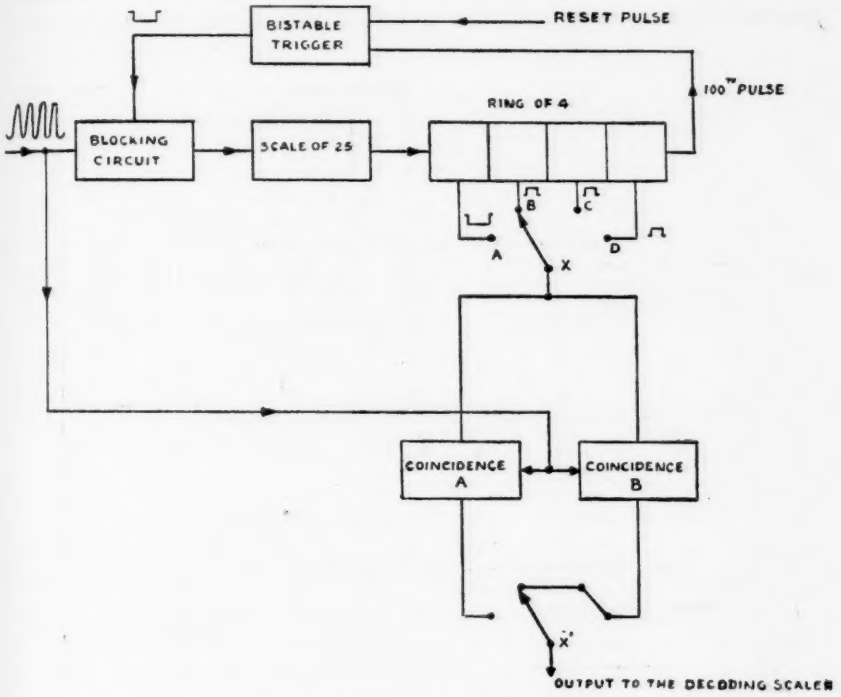

FIG. 4. Diagram of Range Selector

train of above 25, only 25 pulses are passed to the decoding unit if the band-switch is in postion 1. But nothing is recorded in the decoding unit as channel 25 is absent. If the number of pulses in the initial train is below 25, they will be passed on to the decoding unit. In the 2nd, 3rd and 4th tubes of the scale of 4, we get positive gates which last for the range 26–50, 51–75 and 76–100 respectively. These gate pulses are fed to another 6 A C 7 coincidence B and its output gives pulse trains of 25 or less depending on the position of the band-switch and whether the pulse train ends within that range or not. If the number of pulses in the pulse train is more than 100, spurious counts will be recorded in the lower channels; for instance, a pulse train of 108 will be recorded in the 8th channel. In order to avoid this, the input pulses to

the range selector are given through another diode blocking circuit, which cuts out the oscillator pulses above 100.

The decoding unit (Fig. 5) consists of 2 rings of 5 scalers in cascade. The ring scaler circuit is due to Gatti[2] (Fig. 6). In the normal conditions, the second half of the 1st tube and the 1st half of the other 4 tubes in each

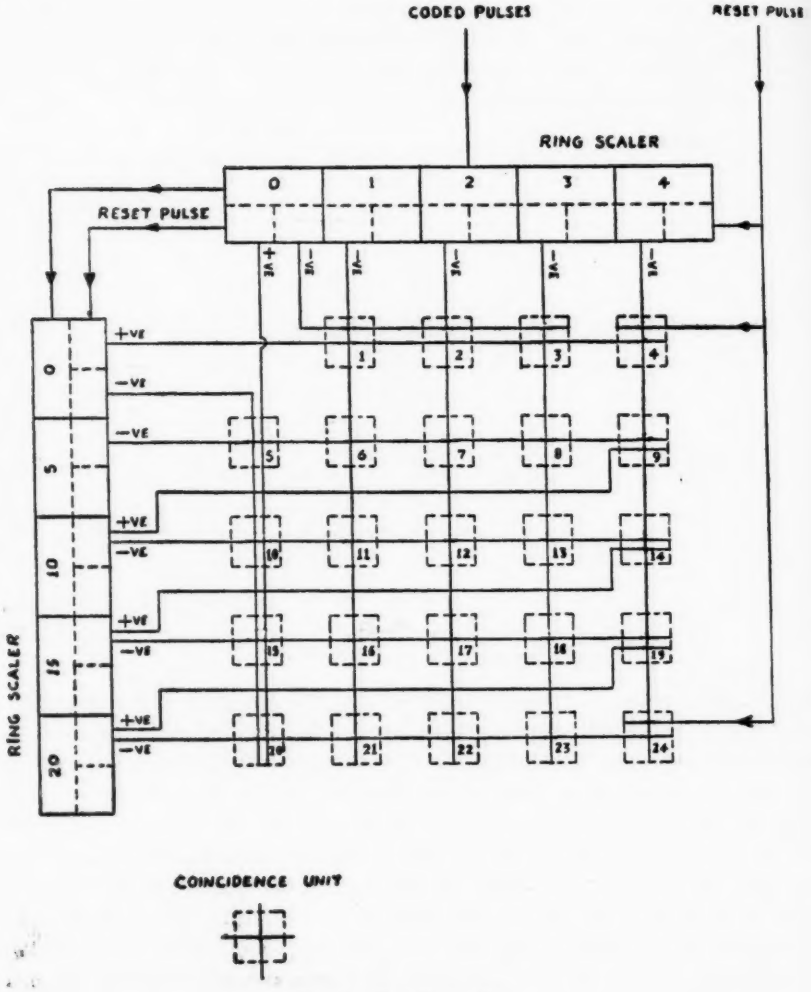

FIG. 5. Decoding unit.

ring are conducting. If a train of 17 pulses have passed through the scalers, then the 2nd tube of the first ring and 3rd tube of the 2nd ring will be left with their second halves conducting. If now the scalers are reset, we get negative pulses from the plates of the first halves as they flip over to their normal state. These negative pulses are taken through cathode followers to the coincidence circuits.

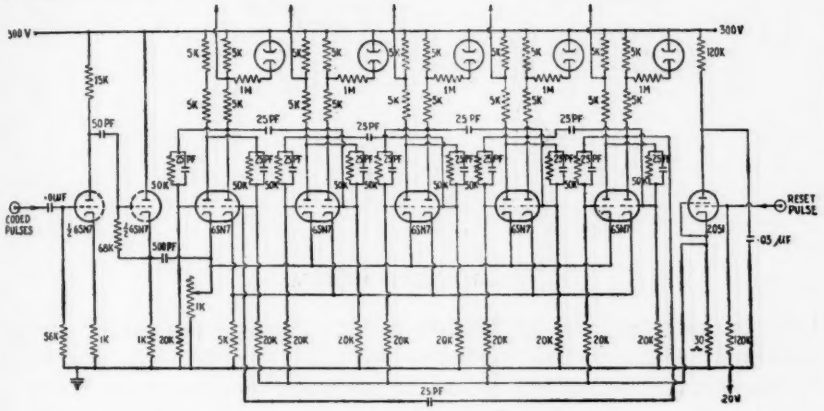

FIG. 6. Ring of Five scaler.

The resetting of all the ring scalers is done by a single pulse. The grid resistances of the second half of the 1st tube and the first half of all the other tubes, in each ring scaler are connected to ground through a common resistance of 30 ohms, which forms the cathode load of the thyratron 2051 (Fig. 6). The reset pulse fires the thyratron and the large positive pulse at its cathode, resets the ring scalers.

A simple double triode coincidence circuit (Fig. 7) gives a large negative pulse at the cathode. The ratio of the output pulse when there is coincidence to that when only one pulse is fed to the coincidence tube, is about 3. A negative voltage discriminator is biassed to accept only the coincidence pulse, and gives at its output a negative gate, which is fed to the dekatron in the recording unit.

Such simple coincidence does not suffice for all the points on the matrix, for while the pulse train is advancing, the scalers give output pulses and we may get a coincidence outputs at the points 4, 9, 14, 19 and 24. For instance, when the 10th pulse arrives the 4th tube of the 1st ring and the 2nd tube of the 2nd ring return to their normal state thus giving coincidence output which may be recorded in the 9th channel. In order to avoid this we feed

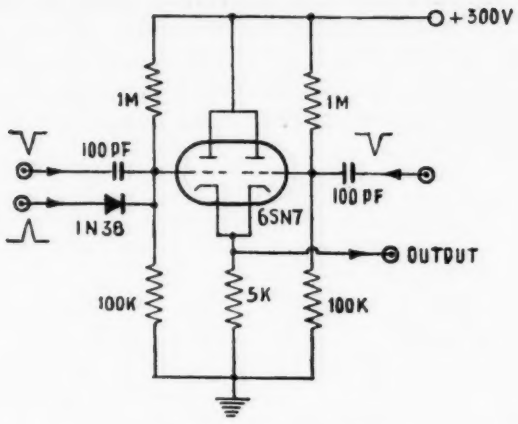

FIG. 7. Coincidence Unit.

in a positive pulse from the 3rd tube in the 2nd ring which cancels one of the negative pulses to the coincidence. At the points 1, 2, 3, 4, 5, 10, 15 and 20, the coincidences are established by the negative pulses from the same ring. As a result, *e.g.*, No. 2 will give coincidence, even when pulse trains of 7, 12, 17 or 22 have been fed and the scalers reset. To avoid this, we feed positive pulses from the 1st tube of the ring as indicated in Fig. 5. In the case of 4, it will require 2 positive pulses to cancel spurious counting since the arguments for 9, 14, 19 and 24 as well as 1, 2, 3, 5, 10 held here. One of the cancellation pulses is avoided by giving a negative pulse from the reset. These cancellations are done by just applying pulses through diodes to one of the grids of the coincidence tube and hence do not involve more tubes. A triple coincidence with the negative reset pulse as the third, eliminates spurious coincidences in the 24th channel. The 25th channel is absent, as it cannot be uniquely defined. Each channel has a recording unit consisting of a scale of 100 followed by a resettable call counter.

The scale of hundred consists of 2 dekatrons of the type GC 10 B in cascade. The output pulses from this scale of hundred is fed to another dekatron of the type GS 10 C. In this tube, each of its ten cathodes is brought out to separate terminals, such that positive gates appear successively at these terminals when the tube is counting. Each of these cathodes is directly connected to one of the terminals of a neon, the other terminals of all the neons being returned to a common negative bias. Thus for every 100th pulse, the neons light up successively giving a display of the counts in that channel and a visual indication of the spectrum in that range can thus be obtained.

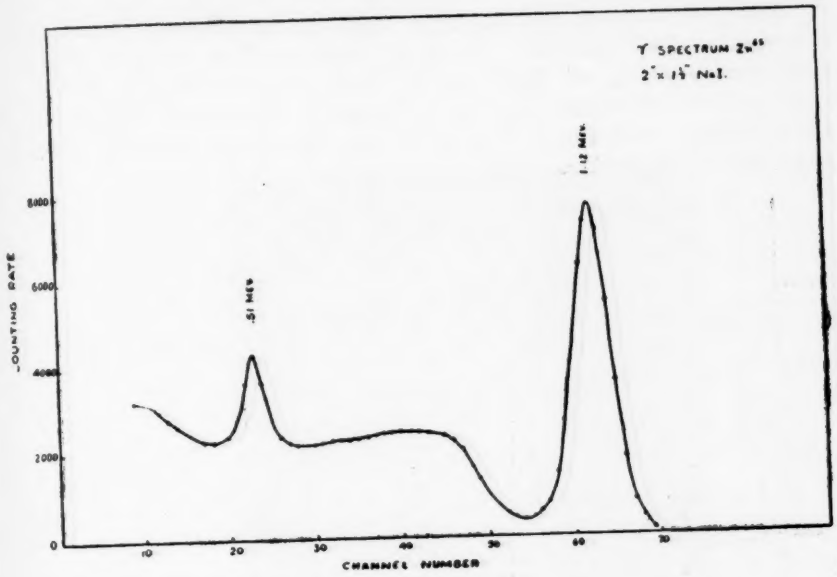
γ SPECTRUM Zn⁶⁵
2" x 1½" NaI.
1·12 MeV
·51 MeV
COUNTING RATE
8000
6000
4000
2000
0
10
20
30
40
50
60
70
CHANNEL NUMBER

FIG. 8

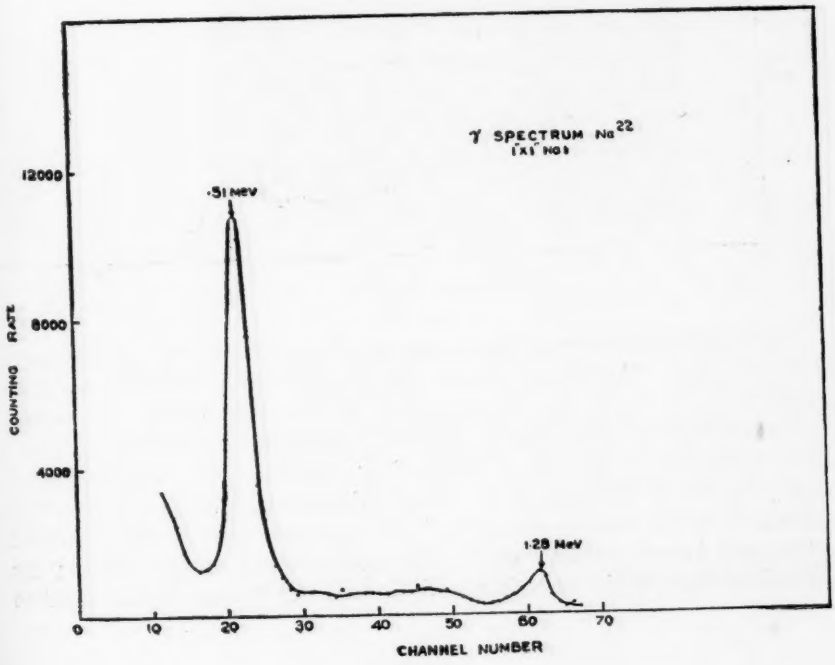
γ SPECTRUM Na²²
(1"x1" NaI)
·51 MeV
1·28 MeV
COUNTING RATE
12000
8000
4000
0
10
20
30
40
50
60
70
CHANNEL NUMBER

FIG. 9

The pulse analyser was tested by obtaining the spectra of the standard γ-ray sources, Zn^{65} and Na^{22}. These are shown in Figs. 8 and 9. Fig. 10 gives the γ-spectra of Mg^{27} and Al^{28} obtained by irradiating Al^{27} with neutrons from the reactor, Apsara at Trombay. The peaks at 0·84 Mev. and 1·01 Mev are due to Mg^{27} (half-life $\approx$ 9·5 min.), and that at 1·78 Mev. is due to Al^{28} (half-life $\approx$ 2·3 min.).

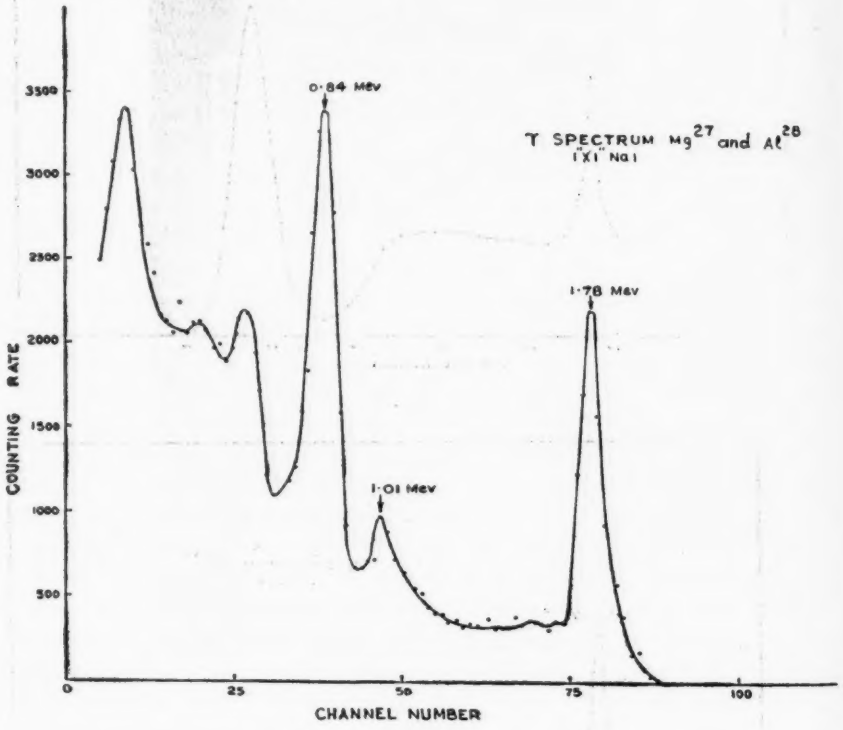

FIG. 10

It is also possible to use this instrument as a time analyser in experiments such as a time of flight spectrometer. A bistable trigger circuit can be made to give a gate pulse of the duration of the time interval between two pulses, one corresponding to the time at which the neutron in a time of flight spectrometer leaves the source (*e.g.*, a chopper) and the other, to the time when it is counted by the detector after a known flight path, the time of detection depending on the neutron energies. This pulse gates the oscillator instead of the gate from the pulse height to time converter unit in the analyser; the instrument then works as a time analyser with the channel widths equal to

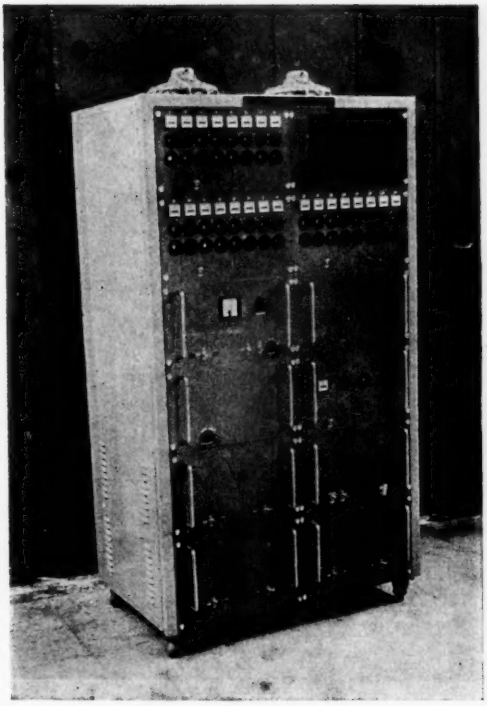

the period of the oscillator (about 8 microseconds). This system will only permit the recording of a single neutron for each burst; hence it can be used only in those cases, where low intensities are expected, as in the case of a chopper.

ACKNOWLEDGEMENTS

We thank Dr. R. Ramanna for helpful discussions. We also wish to thank Mr. Raote for his assistance.

REFERENCES

1. Wilkinson, D. H. .. *Proc. Cambridge Phyl. Sec.* 46, 1950, 508.
2. Gatti .. *Rev. Scientific Instruments*, 1953.

SLOWING DOWN AGE OF NEUTRONS FROM A Ra-α-Be SOURCE TO INDIUM RESONANCE IN ALUMINIUM LIGHT WATER MIXTURES

By V. P. Duggal and S. M. Puri
(*Atomic Energy Establishment, Trombay, Bombay*)

Received May 13, 1957
(Communicated by Prof. B. Peters, F.A.Sc.)

Introduction

Since water moderated reactors employ aluminium as an important structural material, it is necessary to know the mean square slowing down length, $\overline{r^2}$, for netrons in light water aluminium mixtures. This quantity has been experimentally measured by Roberts *et al.*[1] (hereafter referred to as I) for two aluminium water mixtures from a point fission source up to indium resonance (1·45 ev.). Williams *et al.*[2] (hereafter referred to as II) have made a comparison of the experimental value of $\overline{r^2}$ with different theoretical computations. The measured values of $\overline{r^2}$ differ progressively from the theoretical values, the difference increasing as the aluminium to water ratio is increased. The effects of inelastic scattering and anisotropy in elastic scattering in aluminium and oxygen were not taken into account in the theoretical formulæ employed in II.

Using a Ra-α-Be source, an experiment was performed to determine the value of Fermi age $\tau = 1/6\ \overline{r^2}$ up to indium resonance for pure water and four aluminium-water mixtures, the volume ratios being 1 : 1, 2 : 3, 1 : 2 and 1 : 4 for the four samples. Theoretical values of τ were also computed taking into account the effects of anisotropy in elastic scattering in oxygen and aluminium and inelastic scattering in aluminium.

Apparatus and Measurements

The experiment was performed in an aluminium tank of dimensions 3 ft. × 3 ft. × 4 ft. Aluminium plates 3 ft. × 4 ft. and 1/8 in. thick were stacked in the vertical position in the tank. The plates were separated by vertical aluminium spacers 1/8 in. 3/16 in. 1/4 in. and 1/2 in. thick to get the aluminium to water volume ratios of 1 : 1, 2 : 3, 1 : 2 and 1 : 4 respectively. The plates in the centre were cut to provide a gap of $4\frac{1}{2}$ in. × $5\frac{1}{2}$ in. cross-section running throughout the height of the tank. An aluminium frame with grooves at fixed positions for the detectors was placed in this gap. The source used was a 750 m.c., Ra-α-Be source which was placed at the top of this frame,

The indium foils used were 0·125 mm. thick and were wrapped in cadmium (0·4 mm. thick) boxes. The area of the foils was varied to keep the geometry correction small and at the same time to get a good counting rate. Up to a distance of 23 cm. from the source the foils used were 1 in. × 1 in. in area and afterwards 1·3 in. × 2·3 in.

At large distances from the source the foils were covered with copper boxes instead of cadmium boxes. The justification for this procedure rests on the work of Rush[3] who has shown that at large distances from the neutron source, a distribution measured with cadmium covered indium foils and a second one measured with aluminium covered foils were proportional within experimental error. Since the absorption in aluminium is very small, an uncovered indium foil would also measure a distribution proportional to

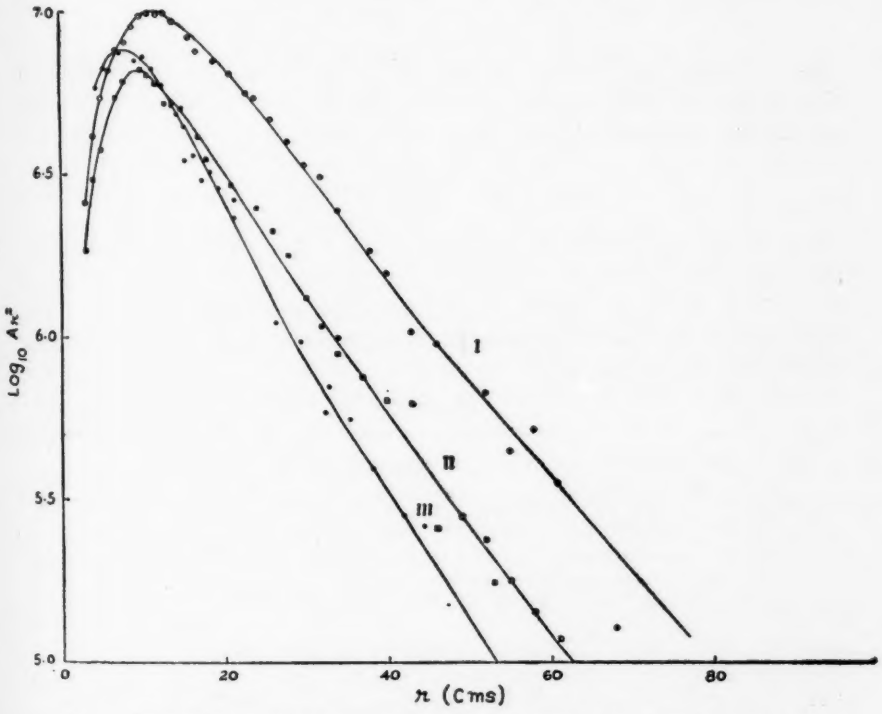

FIG. 1. Spatial Distribution of Indium Resonance neutrons in three media: Log. Ar^2 *vs.* r.

I .. Aluminium + Water (1 : 1).
II .. Aluminium + Water (1 : 2).
III .. Pure Water.

the one covered with cadmium. In our case copper covers were used to avoid contact with water.

The β activities of the foils were measured with two thin glass G.M. counters connected in parallel. The efficiency of G.M. counters was tested before each measurement with a standard uranium foil. The different indium foils were intercalibrated by irradiating them at a fixed distance from the neutron source and the activities obtained were normalised.

The saturation activity A of the indium foils was measured as a function of distance r from the Ra-α-Be source for all the ratios. The Fermi age τ was calculated from the relation;

$$\tau = \tfrac{1}{6}\overline{r^2} = \tfrac{1}{6}\frac{\int_0^\infty Ar^4 dr}{\int_0^\infty Ar^2 dr} \tag{1}$$

The integration was done graphically as far as it was possible to measure the neutron distribution experimentally. Beyond the measured points the curves were extrapolated assuming the neutron density to follow the relation

$$A(r) = \frac{\text{Const.}}{4\pi r^2}\, e^{-r/\lambda} \tag{2}$$

where λ is the experimental relaxation length. In each case the area under the extrapolated curve was less than 20% of the total area. Figure 1 shows a plot of log Ar^2 as a function of distance r for some volume ratios. The experimental values of relaxation length, extrapolated area and Fermi age τ for different ratios are given in Table I.

TABLE I

Al/H_2O	Relaxation length cm.	Experimental age $cm.^2$	Extrapolated area		Calculated value of age $cm.^2$
			$\int Ar^2\,dr$ %	$\int Ar^4\,dr$ %	
1	12·64	101·87±2·55	1·11	11·94	94·54
0·67	12·48	82·09±1·98	2·35	21·80	
0·50	12·27	80·34±3·41	0·81	11·45	76·61
0·25	11·40	69·14±1·67	1·02	12·53	
Pure water	10·52	54·11±2·14	1·82	18·03	59·59

Comparison with Theoretical Value

The value of age for various mixtures was calculated from the equation

$$\tau = \tfrac{1}{6}\overline{r^2} = \tfrac{1}{3}\left[\int_0^u \frac{l^2}{a\alpha}\,du + \int_0^u \frac{b}{2a}\,\frac{d}{du}\left(\frac{l^2}{a\alpha}\right)du + \int_0^u \frac{l\beta}{a\alpha}\,\frac{d}{du}\left(\frac{l}{a}\right)du - \left\{\frac{l^2}{a\alpha}\left(\frac{b}{a}+\frac{\beta}{\alpha}\right)\right\}_u\right] \quad (3)$$

derived by Marshak[4] for hydrogenous mixtures. Here u = lethargy = log E_0/E

$$a = \sum_j c_j\gamma'_{0j}(0); \qquad b = \sum_j c_j\gamma_{0j}''(0)$$

$$\alpha = \Sigma\, c_j\gamma_{1j}(0); \qquad \beta = \Sigma\, c_j\gamma_{1j}'(0)$$

The notations employed here are the same as in reference (4).

j is summed over various constituents, hydrogen, oxygen and aluminium of the mixtures.

Formula (3) has been used by Marshak to derive the Fermi age in water for various neutron energies under the assumptions

(*a*) Isotropic elastic scattering in the C.M. system.

(*b*) No inelastic scattering.

(*c*) No absorption.

The neutron spectrum from Ra-α-Be source extends up to about 11 Mev. with maxima at 4 and 6 Mev.[5] At these energies the above assumptions do not hold. To take account of anisotropy in elastic scattering and inelastic scattering, formula (3) was modified as follows:

The constant $\gamma_1(0)$ in the formula has the value 1–2 M/3 which is obtained in the case of isotropic scattering in the C.M. system. In place of this, the actual value of $(1 - \overline{\cos\,\theta})$ was used, where $\overline{\cos\,\theta}$ is evaluated from the differential scattering cross-section curve in the laboratory system. Experiments on the angular distribution of scattered neutrons have been performed[6] only at neutron energies 1·7 Mev., 2·5 Mev., 3·7 Mev., 4·1 Mev. and 7 Mev. in the case of aluminium and at 2·0 Mev., 2·5 Mev., 3·0 Mev., and 4·08 Mev. for oxygen. In the absence of any experimental data at higher energies, the value of $\overline{\cos\,\theta}$ was assumed to be the same as at 7 Mev. and 4·08 Mev. in the case of aluminium and oxygen respectively.

To take account of the inelastic scattering in aluminium the value of mean logarithmic energy decrement (ξ) was computed from a knowledge of the

energy spectrum of the inelastically scattered neutrons by aluminium. The value of ξ was weighted according to the proportions of σ_{elastic} and $\sigma_{\text{inelastic}}$, the elastic scattering cross-section and inelastic scattering cross-section respectively.

The energy of the inelastically scattered neutrons was evaluated from the energy levels of Al^{27} nucleus[7] up to 5 Mev. incident neutron energy. After 5 Mev. the spectrum of inelastically scattered neutrons was taken from the experimentally measured curve[9] at 14·8 Mev. energy. The energy spectrum thus obtained is in agreement with the theoretical formula derived by Weiskopff[8] using the continuous model which holds above 5 Mev. in the case of aluminium. The value of Fermi age τ was calculated for some volume ratios from various initial neutron energies ranging up to 11 Mev. Figure 2

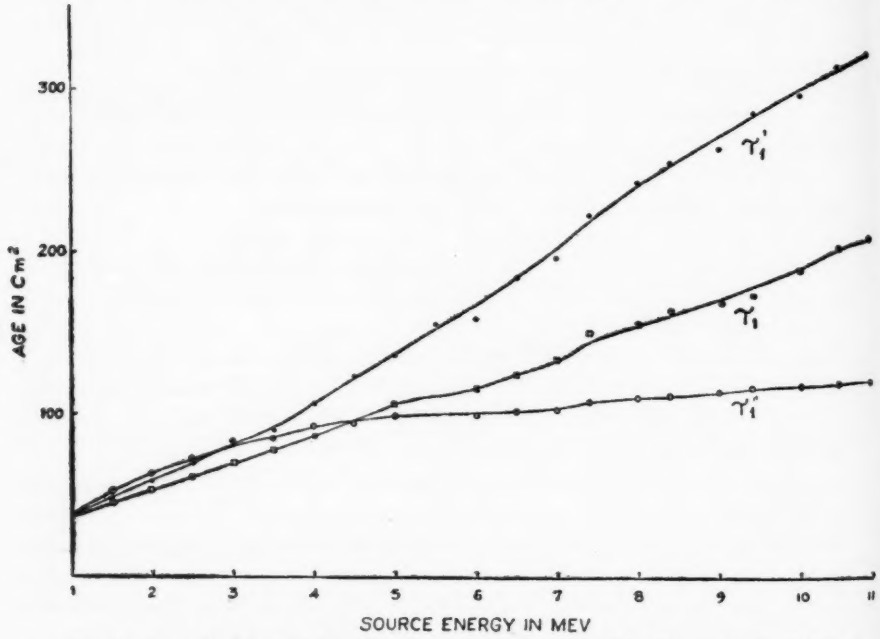

FIG. 2. Age of neutrons from various source energies to Indium Resonance (1·45 Mev.). Medium—Aluminium + Water (1 : 1).

τ_1 .. Incorrect theory.
τ_1' .. Theory corrected for anisotropy only.
τ_1'' .. Theory corrected for anisotropy and inelastic scattering.

shows the graph of age as a function of neutron energy for the volume ratio 1 : 1. Here τ_1 is the calculated age with the assumptions, (*a*) No anisotropy

in the C.M. system. (*b*) No inelastic scattering present. τ_1' is the curve obtained by taking into account the anisotropy of the elastic scattering and τ_1'' contains both the anisotropy and inelastic scattering.

The value of age τ averaged over Ra-α-Be and fission neutron spectra is plotted in Fig. 3 as a function of aluminium to water ratio together with

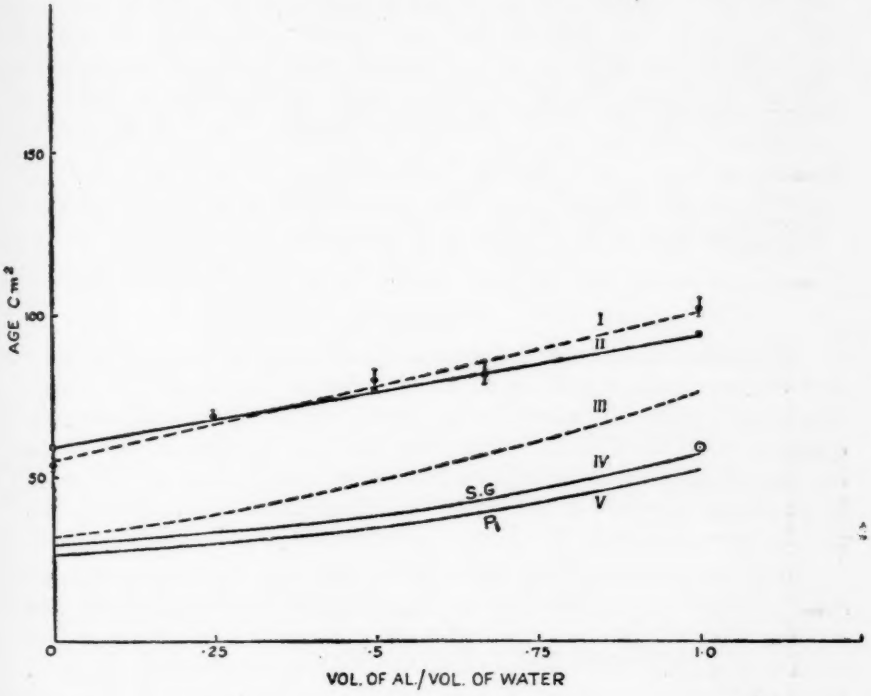

FIG. 3. Age as a function of aluminium water ratio.

I (Dashed line)	..	Experimental curve for Ra-α-Be source (Present experiment).
II (Solid line)	..	Calculated curve for Ra-α-Be source.
III (Dashed line)	..	Experimental curve of Roberts and Fitch (Fission Source).
IV & V (Solid line)	..	Theoretical curves for fission source.
. .. .		Calculated value with the theory corrected for anisotropy and inelastic scattering.

the experimental values. The calculated age averaged over Ra-α-Be spectrum is given in the last column in Table I for some volume ratios. The theoretical values under different assumptions for 1 : 1 volume ratio are given in Table II.

TABLE II

$Al/H_2O = 1$

Source	Marshak's formula			Experimental value cm.^{2}
	No correction cm.^{2}	With anisotropy cm.^{2}	With anisotropy and inelastic effects cm.^{2}	
Fission source	55·95	64·49	59·00	76·80 (I)
Ra-α-Be source (Present experiment)	102·46	150·05	94·54	101·87±2·55

DISCUSSION

The calculated value of τ averaged over Ra-α-Be spectrum agrees fairly well with our experimental results for the volume ratio 1 : 2. The experimental value lies above the theoretical value for the volume ratio 1 : 1, the difference being about 7·5%. This agreement is fairly good in view of the fact that the Ra-α-Be spectrum is not known accurately. Also the anisotropy in the angular distribution of elastically scattered neutrons at higher energies may be more than what has been assumed in our calculations.

From Fig. 2 it is clear that the calculated age gives a high value when the effect of anisotropic elastic scattering alone is considered in aluminium and oxygen. The average over the fission spectrum for the 1 : 1 volume ratio yields a value nearer to the experimental value, the difference being only 16%. When the inelastic scattering in aluminium is also considered, the value obtained (Table II) lies close to the value given by S.G. theory (II). This value is about 30% lower than the experimental value for volume ratio 1 : 1. This large discrepancy is probably due to the fact (pointed out by the experimenters themselves[1]), that the fission source in their experiments was only 10 cm. from the graphite of the thermal column. This would give higher values of age particularly for volume ratio 1 : 1 where the slightly degraded reflected neutrons from the graphite will alter the spatial distribution of neutrons considerably.

It is clear from the above results that the consideration of anisotropy in elastic scattering alone is not enough to explain the difference between the

experimental and theoretical values of age as pointed out in (II). The inelastic scattering effects also play an important role at higher neutron energies.

No account has been taken in our calculations of the absorption of neutrons at higher energies. This is particularly important in the case of oxygen where absorption cross-section is almost 20% of the total cross-section after about 6 Mev. The discrepancy observed between the theoretical value and experimental value in the case of pure water (Fig. 3) may be due to the fact that the absorption in oxygen has not been taken into account in the calculations. The contribution due to this effect will go on decreasing as the volume of aluminium increases. This will further improve the agreement between theory and experiment.

Acknowledgements

We wish to thank Messrs. J. N. Soni, V. Singh and M. L. Barde for help in the construction of aluminium-water assembly. We are also grateful to Dr. R. Ramanna for helpful criticisms.

References

1. Roberts, L. D., Hill, J. E. and Fitch, T. E. — *Jr. Appl. Phys.*, 1955, **26**, 1018.
2. Wilkins, J. E. Jr., Hellons, R. L. and Zweifel, P. F. — Paper presented in the International Conference on the peaceful uses of atomic engergy. *A./Conf. S./P/597.*
3. Rush, I. H. .. — *Phys. Rev.*, 1948, **73**, 271.
4. Marshak, R. E. .. — *Rev. of Mod. Phys.*, 1947, **19**, 185.
5. Teucher, M. .. — *Zeitschrift Fur Physik.*, 1949, **26**, 410.
6. .. — *Neutron Cross-Sections BNL* 325.

Baldinger, E., Huber, P. and Proctor, W. G. — *Helv. Phys. Acta*, 1952, **25**, 142.

Whitehead, W. D. and Snowdon, S. C. — *Phys. Rev.*, 1953, **92**, 114 and *Ibid.*, 1954, **94**, 1267.

.. Differential elastic scattering cross-section curve for aluminium at 7·0 Mev. has been privately communicated to us by S. C. Snowdon from unpublished work at Los Almos.

7. Browne, C. P., Zimmerman, S. F. and Buechner, W. W. — *Phys. Rev.*, 1954, **96**, 725.
8. Blatt, J. M. and Weisskopff, V. F. — *Theoretical Nuclear Physics* (John Wiley and Sons, Inc., New York), 1952.
9. O'Neill, G. K. .. — *Phys. Rev.*, 1954, **95**, 1235.

A PARADOXICAL CASE OF DIECKMANN CYCLISATION[1]

By D. K. Banerjee, F.A.Sc., J. Dutta and G. Bagavant

(Departments of Organic Chemistry, Indian Institute of Science, Bangalore, and Jadavpur University, Calcutta)

Received April 6, 1957

Perkin *et al.*[2] observed that the Dieckmann cyclisation of diethyl β-ethoxycarbonylpimelate (I) with sodium in benzene, followed by hydrolysis and decarboxylation, yielded 3-oxo*cyclo*hexanecarboxylic acid (III *a*), *via* β-keto-esters (II *a* and/or II *b*). Sen and Bagchi[3] proved that the Dieckmann product was mainly (II *a*). Ethyl 1-ethoxycarbonyl-2-oxo*cyclo*pentylacetate (IV) was isomerised by Chatterjee *et al.*[4] to ethyl 3-ethoxycarbonyl-2-oxo-*cyclo*pentylacetate (V), on treatment with an ethanolic solution of sodium ethoxide (1·1 mole). Following Openshaw and Robinson,[5] they suggested that the β-keto-ester (IV) underwent ring fission to form the triester (I) which cyclised to yield the diester (V).

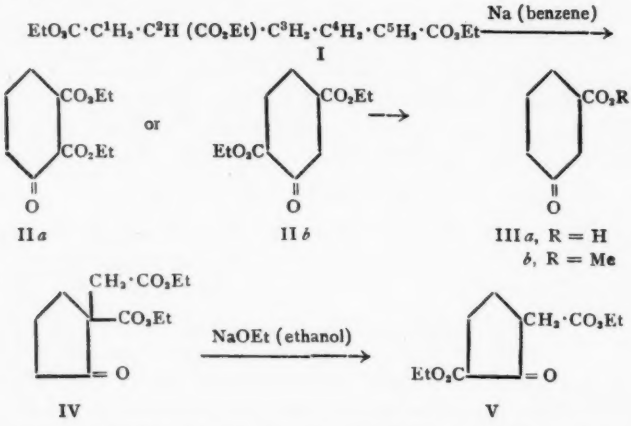

Chakravarti[1] explained the formation of (V) through an intra-molecular addition reaction of the mesomeric anion (VI *a* ⟷ VI *b*) which was formed by opening of the β-keto-ester (IV) with the ethoxyl ion. The proposed mechanism of ring closure is actually an interpretation of Nef's mechanism of the Claisen condensation[6] in terms of the electronic theory of valency, which, on the basis of Ingold's criticism of Nef's view,[7] is untenable. Further, the anion (VI *a*), in the presence of a large excess of ethanol, is likely to take

up initially a proton to form the triester (I), in which case, according to Chakravarti,[1] only the *cyclo*hexane-β-keto-ester (II *a*) should be formed. When the triester (I) was treated with ethanolic sodium ethoxide under Chatterjee's condition, the *cyclo*pentane-β-keto-ester (V) was formed as the major product.

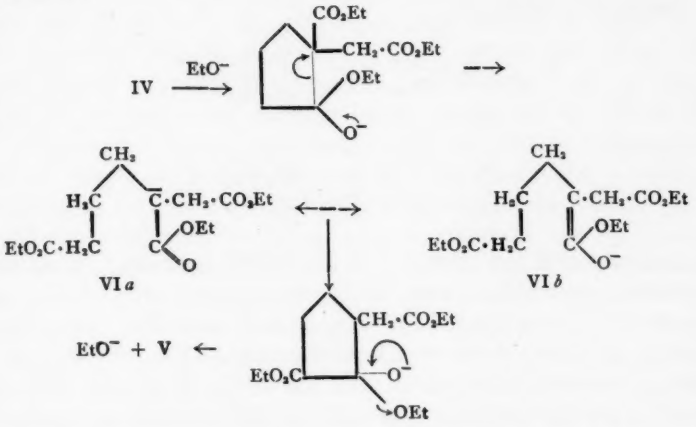

An explanation, not involving cleavage of the ring, is to assume ethyl-1-ethoxycarbonyl-2-oxo*cyclo*pentylacetate (IV) to undergo fission[8] in the presence of one molar quantity of sodium ethoxide in ethanol, yielding ethyl 2-oxo*cyclo*pentylacetate and diethyl carbonate which condense to yield (V). This, however, is unsatisfactory, as it involves an attack on the most hindered carbonyl group by the ethoxyl ion. Furthermore, β-keto-esters are formed in extremely poor yield during the condensation of ketones with diethylcarbonate in the presence of alcoholic sodium ethoxide.[9]

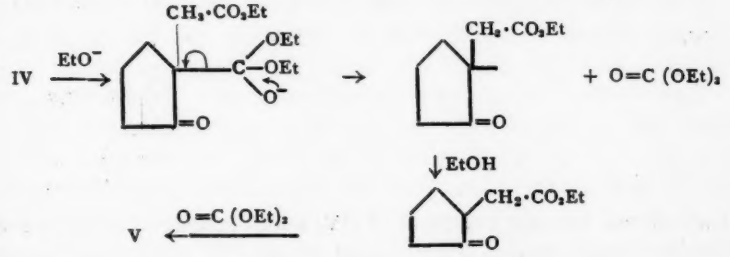

An alternative mechanism, which also dispenses with the formation of the anion (VI *a*), would be to assume the formation of a bicyclic (2 : 1 : 1-bi*cyclo*heptane) β-diketone intermediate (VII *a*) which opens up simulta-

neously with, or after, its formation to yield (V). But this also is not feasible as there is no *a priori* reason to assume its preferential formation to that of the more stable 2:1:2-bi*cyclo*octane derivative (VII *b*). It has been observed experimentally that ethyl 1-ethoxycarbonyl-2-oxo*cyclo*pentylacetate (IV), on treatment with sodium ethoxide in benzene, undergoes conversion to the *cyclo*hexane compound.

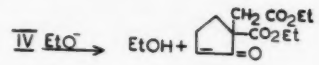

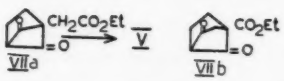

In order to find out whether the anion (VI *a*), resulting from an open chain system, would also yield the *cyclo*pentanone derivative (V), diethyl β-acetyl-β-ethoxycarbonylpimelate was treated according to Chatterjee's conditions. In this case, an attack of the ethoxyl ion on the carbonyl of the acetyl group was expected to yield the anion (VI *a*) and ethyl acetate. The reaction product had a strong smell of ethyl acetate and gave a deep colour with ferric chloride. The β-keto-ester fraction, on hydrolysis and decarboxylation, yielded a keto-acid identified as 2-oxo*cyclo*pentylacetic acid (VIII *a*), thus indicating that the anion (VI *a*) can yield the *cyclo*pentanone system (V) under the conditions employed.

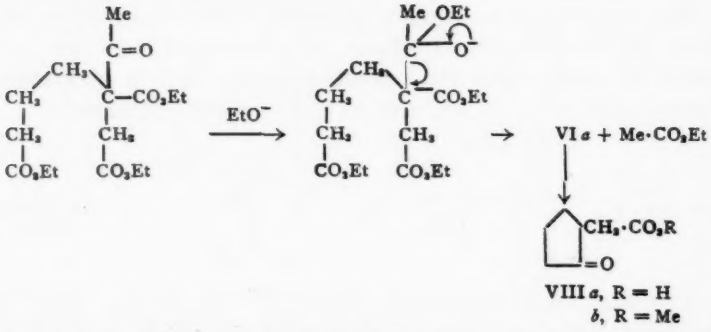

It was found that the treatment of (IV) with one-quarter mole of sodium ethoxide in ethanol produced the triester (I) in 75% yield, together with a small quantity of a β-keto-ester* which has been found to be mainly the

* We are indebted to Mr. P. Bagchi of the Association for the Cultivation of Science, Calcutta, for bringing to our notice the formation of a β-keto-ester in this reaction.

*cyclo*hexane derivative (II *a*). Treatment of the triester (I) with one or two moles of sodium ethoxide in benzene gave the *cyclo*hexane-β-keto-ester (II *a*) in good yield.

The aforementioned experimental facts suggest that the formation of the *cyclo*hexanone or the *cyclo*pentanone derivative depends on the amount of available ethoxyl ion. In benzene medium, as well as when one-quarter mole of sodium ethoxide in ethanol is used, due to the low concentration of ethoxyl ion, a proton is abstracted preferentially from the most acidic (C_1) of the methylene and methine groups, which, in the triester (I), is the one constituting a part of the succinic ester residue (*cf.* Chakravarti[1]), thus producing the anion (I *a*) which yields (II *a*) as the cyclised product. In the presence of an ethanolic solution of an excess of sodium ethoxide, the formation of a bianion (I *b*), even in traces, seems to explain satisfactorily the observed facts. In (I *b*) due to the presence of negative charges at C_1 and C_5, the carbonyl activity of the ethoxycarbonyl groups attached to these carbon atoms is reduced, leaving that of the ethoxycarbonyl group attached to the C_2-carbon atom strongest, so that the reaction of the C_2-ethoxycarbonyl with the C_5-anion furnishes the *cyclo*pentane-β-keto-ester (V). However, the existence of a highly energetic bianion of the type (I *b*) appears improbable.

$$\underset{I}{EtO_2C\cdot\bar{C}H\cdot CH(CO_2Et)\cdot CH_2\cdot CH_2\cdot CH_2\cdot CO_2Et} \rightarrow \underset{II\,a}{}$$

$$\underset{I\,a}{} \quad \updownarrow$$

$$\underset{I\,b}{EtO_2C\cdot\bar{C}H\cdot CH(CO_2Et)\cdot CH_2\cdot CH_2\cdot\bar{C}H\cdot CO_2Et} \rightarrow V$$

The cyclisation products in these experiments were characterised through the derivatives of the keto-acids (III *a* and VIII *a*) obtained by hydrolysis and decarboxylation of the β-keto-esters (II *a* and V). By this procedure identification of only the major product could be strictly claimed. The purity of the keto-esters (III *b* and VIII *b*) was therefore investigated by infra-red spectra and authentic samples of (III *b* and VIII *b*) required for this purpose were prepared; the former by the addition of hydrogen cyanide to *cyclo*hexen-3-one followed by treatment of the resulting keto-nitrile with methanolic hydrogen chloride, and the latter by the method of Linstead and Meade.[10]

The infra-red spectra revealed that none of the samples was absolutely pure. The intensity distribution in a spectral line being Gaussian, the observed intensity due to overlap of the two lines at 1740 $cm.^{-1}$ (*cyclo*pentanone carbonyl) and at 1720 $cm.^{-1}$ (*cyclo*hexanone carbonyl) could be

uniquely resolved into the two respective Gaussian curves. On this basis percentage compositions of the mixtures were calculated.

The spectra of samples obtained from the triester (I) and the keto-diester (IV), by treatment according to Chatterjee's conditions, were found to be identical, indicating the presence of *ca.* 90% of methyl 2-oxo*cyclo*pentyl-acetate (VIII *b*). This indicates the possibility of the triester (I) being an intermediate (*vide antea*) in the transformation of (IV) to the isomerised β-keto-ester (V).

The spectra of samples, obtained from (I) by treatment according to Perkin's[2] conditions and with sodium ethoxide in benzene, and from the diester (IV) by treatment with one-quarter mole of sodium ethoxide in ethanol, showed that these consisted mainly of methyl 3-oxo*cyclo*hexane-carboxylate (III *b*); the first two samples were very similar and contained *ca.* 80% of (III *b*).

Recent kinetic studies[11, 12] indicated agreement with the accepted mechanism[7] of Dieckmann cyclisation being composed of four stages (1–4). Reed and Thornley[11] showed that the reaction, in an ethanolic solution of an excess of sodium ethoxide, was reversible and unimolecular, and that the

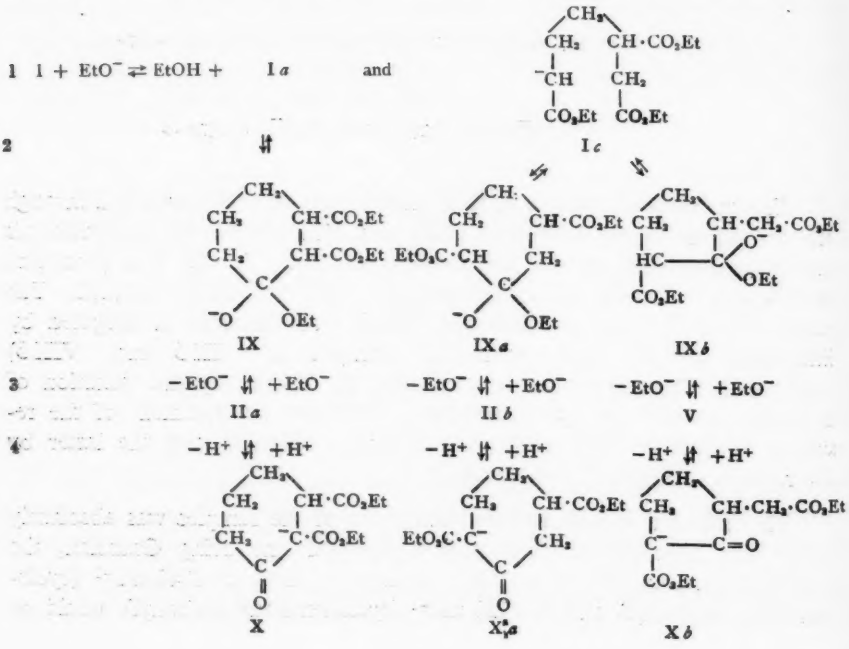

second step was rate-determining.[12] The English workers also showed that this reaction, in a solvent of low dielectric constant and a high concentration of sodium ethoxide, was bimolecular and that the first step was rate-determining. They also provided some evidence for the existence of steric retardation.

Various courses, which the Dieckmann cyclisation of the triester (I) can follow, have been indicated in the chart, and these involve two reactive methylene groups at C_1 and C_5 in (I). The particular case where the anion (VI *a*) is formed by removal of the proton from the C_2-carbon atom has not been considered, because the third step in this case should give rise to a β-keto-ester without an enolisable hydrogen, thus rendering its isolation from the equilibrium mixture impossible.[13] Although, for reasons mentioned before, the carbanion (I *a*) is expected to be formed predominantly, yet the formation of a small quantity of the carbanion (I *c*) along with the former is always possible. The results obtained under different conditions of Dieckmann reaction in the present case may be interpreted on the basis of these considerations and the findings of the aforementioned kinetic studies.[11, 12]

A. *Treatment of Diethyl β-Ethoxycarbonylpimelate* (*I*) *with Sodium* (*Two Moles*) *or Sodium Ethoxide* (*One or Two Moles*) *in Benzene*.—Under these conditions the reaction is bimolecular[11] and the triester (I) should yield predominantly the anion (I *a*) and traces of the anion (I *c*) (*vide antea*). As the second step is faster than the first (the rate-determining step[11]), conversion of the anion (I *a*) to the cyclised anion (IX) will be faster than its formation, and thus it will be continuously removed. This coupled with the low solubility of the sodium salt[12] of (X) in benzene make the Dieckmann reaction yield (II *a*) as the major product. Small quantities of β-keto-esters (II *b* and V) should also be produced from the anion (I *c*).

B. *Treatment of* (*I*) *or Ethyl* 1-*Ethoxycarbonyl*-2-*oxo*cyclo*pentylacetate* (IV) *with Sodium Ethoxide* (1·1 *Mole*) *in Ethanol*.—In this case the reaction is unimolecular,[11] and the second step is rate-determining[11, 12] and therefore slower than the first, thus resulting in the accumulation of the anions (I *a* and I *c*). All steps are reversible, and the presence of a large quantity of ethanol facilitates the formation of the neutral ester (I) from the anions, so that the transformation of the anions (IX and IX *a*) to the *cyclo*pentane-β-keto-ester (V) is possible through the following sequences:

$$\text{IX} \rightarrow \text{I}a \rightarrow \text{I} \rightarrow \text{I}c \rightarrow \text{IX}b \rightarrow \text{V} \qquad (1)$$

$$\text{IX}a \rightarrow \text{I}c \rightarrow \text{IX}b \rightarrow \text{V} \qquad (2)$$

Reed and Thornley[11] found that an α-alkyl substituent causes steric retardation in the ring fission. In the β-keto-esters (II *a*, II *b* and V), α-substi-

tuents to the keto group are most bulky in (V), thus creating maximum hindrance in the approach of the ethoxyl ion and making the third step comparatively more irreversible in this case than in others.

The loss of a proton, in the fourth step, from the β-keto-esters (II *a*, II *b*, and V) changes the co-ordination number of the involved carbon atoms from four to three. Such a change is aided in and opposed by five-membered and six-membered ring systems respectively,[14, 15] resulting in the *cyclo*-pentane derivative being comparatively more acidic and hence existing predominantly in the equilibrium mixture.

Brown *et al.*[14] have shown that exocyclic and endocyclic double bonds are preferred by five-membered and six-membered ring systems respectively. The canonical structure of the enolate ion (synion S), formed in the last step, suggests that the mesomeric anion should possess considerable exocyclic double bond character,† and thus be more stable in the case of the *cyclo*-pentanone anion (X *b*).

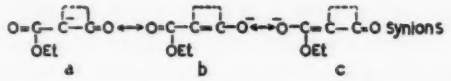

XI

† Russel,[15] in explaining the higher enolisation of *cyclo*-hexanone compounds compared to *cyclo*pentanone derivatives pointed out that in the equilibrium mixture (*vide infra*) the form *c'* would be subordinate when R is OEt, since diethyl malonate does not enolise appreciably (Gero, *J. Org. Chem.*, 1954, **19**, 1961).

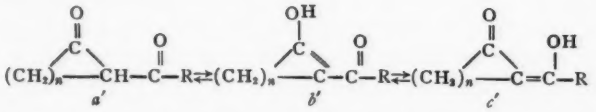

Bender and Figueras (*J. Amer. Chem. Soc.*, 1953, **75**, 6304) have shown in the infra-red study of the "enolate ion" that in β-keto-ester and β-diketone systems the ester and ketonic carbonyl bands practically vanish to give "enolate ion" band(s). The infra-red study of diethyl malonate anion establishes that it is best represented by (XI) in contrast to the structure of diethyl malonate, so that the contribution of the form (*c*) in the (synion S) should be considerable.

Thus due to the greater acidity and higher stability of the *cyclo*pentanone system, and the comparative irreversibility of the third step in the formation of (V), the triester yields the *cyclo*pentane-β-keto-ester (V), as the major product, under Chatterjee's conditions.

It is now proposed that the keto-diester (IV), under these conditions, first yields the anion (VI *a*)[1] which, in the presence of a large amount of ethanol, takes up a proton to form the triester (I), finally to yield (V) as the major product.

The aforementioned arguments were conclusively proved by treating ethyl 2-oxo*cyclo*hexane-1 : 2-dicarboxylate (II *a*)[2] under Chatterjee's conditions and obtaining thereof ethyl 3-ethoxycarbonyl-2-oxo*cyclo*pentylacetate (V), which on hydrolysis, decarboxylation, and subsequent esterification yielded a sample of methyl 2-oxo*cyclo*pentylacetate (VIII *b*) having an infra-red spectrum identical with those of the products obtained from (I) or (IV) by a similar procedure.

C. *Treatment of (I) with One-Quarter Mole of Sodium Ethoxide in Ethanol.*—In this case, in the β-keto-ester fraction, the *cyclo*hexane-β-keto-ester (II *a*) was predominantly formed, but the infra-red spectrum showed that the *cyclo*pentane-β-keto-ester (V) was present in comparatively larger quantity than when (I) was treated with sodium ethoxide in benzene (*vide antea*). According to the equilibrium nature of the reaction, however, the β-keto-ester (V) ought to have been formed preponderantly also in this case. It was therefore concluded that sufficient time had not been allowed for attainment of the equilibrium of the reaction mixture in the presence of low concentration of ethoxyl ion, and this was confirmed when the reaction mixture was heated for a prolonged period to yield (V) as the major product in the β-keto-ester fraction. This observation is not in agreement with the bianion theory.

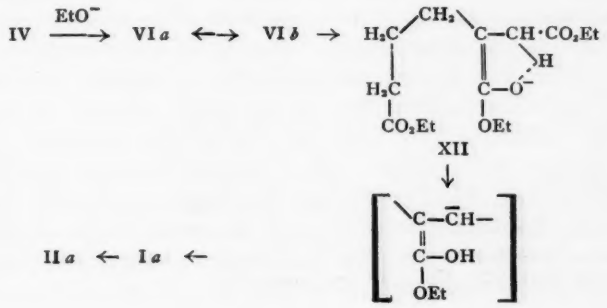

D. *Treatment of* (*IV*) *with Sodium Ethoxide in Benzene.*—The formation of the *cyclo*hexane system in this case may be assumed to proceed through the mesomeric anion (VI *a* ⟷ VI *b*),[1] followed by conversion to the anion (I *a*) *via* the hydrogen-bonded intermediate (XII).

EXPERIMENTAL

Ethyl 1-*Ethoxycarbonyl*-2-*oxo*cyclo*pentylacetate* (*IV*).—This was prepared by the method of Chatterjee *et al.*[4] The treatment of the sodio-derivative of ethyl 2-oxo*cyclo*pentanecarboxylate, formed by the Dieckmann cyclisation of diethyl adipate, *in situ* with ethyl chloroacetate under refluxing conditions yields mainly diethyl β-ethoxycarbonylpimelate, b.p. 153–158°/0·8 mm., n_D^{28} 1·4390, together with a small quantity of a β-keto-ester fraction, b.p. 118–123°/1 mm.

2-*Oxo*cyclo*pentylacetic Acid* (VIII *a*).—This was obtained adopting the procedure of Linstead and Meade,[10] m.p. 52° (lit.[10], m.p. 53°), semicarbazone m.p. 198° (lit.[4], m.p. 198°). The 2:4-*dinitrophenylhydrazone* was prepared by the perchloric acid method[16] and crystallised from dilute acetic acid, m.p. 215–216° (decomp.) (Found: N, 17·44. $C_{13}H_{14}O_6N_4$ requires N, 17·39%). The *methyl ester* (VIII *b*) was prepared using methanol and sulphuric acid, b.p. 94–96°/0·8 mm. (Found: C, 61·42; H, 7·81. $C_8H_{12}O_3$ requires C, 61·54; H, 7·69%).

When the β-keto-ester (purified through alkali extraction) obtained from ethyl 1-ethoxycarbonyl-2-oxo*cyclo*pentylacetate (IV) by the procedure of Chatterjee *et al.*[4] was hydrolysed, decarboxylated, and subsequently esterified with methanol and sulphuric acid, a sample containing about 90% of methyl 2-oxo*cyclo*pentylacetate (VIII *b*) (*vide* Fig. 3) was obtained.

3-*Cyano*cyclo*hexanone.*—To a stirred and cooled (ice and salt) solution of *cyclo*hexen-3-one[17] (9·6 g.) and glacial acetic acid (6 ml.) in rectified spirit (80 ml.) was added an aqueous solution of potassium cyanide (13 g. in 38 ml.) in course of 35 min., and it was allowed to stand overnight at 0°. After the addition of brine (150 ml.), the nitrile was thoroughly extracted with ether. The combined ethereal extract was washed with brine and dried (Na_2SO_4). The residue, after removal of the solvent, was fractionated to yield the *nitrile* (5·4 g.), b.p. 149–150°/17 mm. (Found: N, 11·11. C_7H_9ON requires N, 11·38%). The *semicarbazone* was crystallised from rectified spirit, m.p. 177–178° (Found: N, 31·15. $C_8H_{12}ON_4$ requires N, 31·11%). The 2:4-*dinitrophenylhydrazone*, prepared by the perchloric acid method, was crystallised from ethyl acetate-alcohol, m.p. 205° (Found: N, 23·12. $C_{13}H_{13}O_4N_5$ requires N, 23·12%).

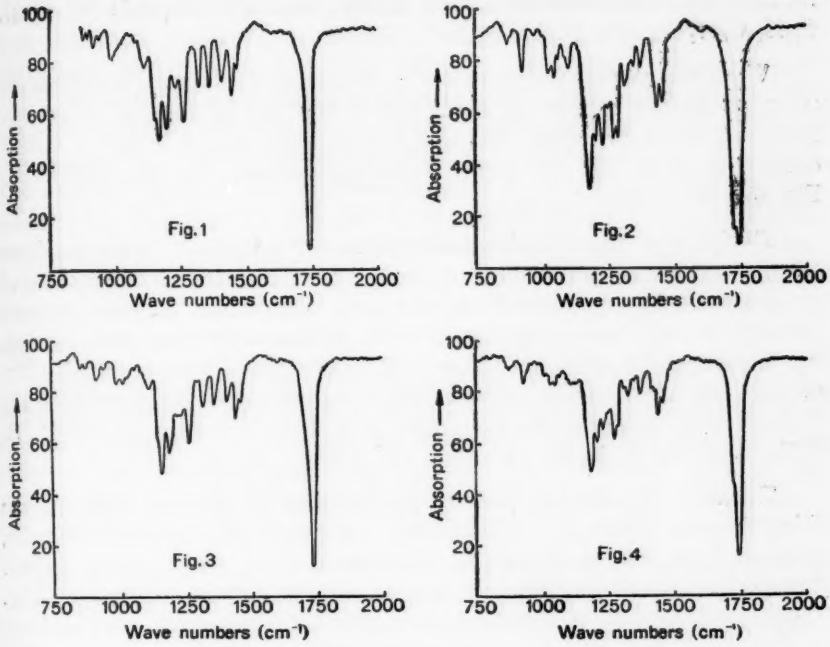

FIG. 1. Methyl 2-oxo*cyclo*pentylacetate.

FIG. 2. Methyl 3-oxo*cyclo*hexanecarboxylate.

FIG. 3. Keto-ester obtained under Chatterjee's conditions from Ethyl 1-ethoxycarbonyl-2-oxo*cyclo*pentylacetate.

FIG. 4. Keto-ester obtained under Perkin's conditions from Diethyl β-ethoxycarbonylpimelate.

Methyl 3-*Oxo*cyclo*hexanecarboxylate* (*III* b).—To a cooled (ice and salt) solution of the aforementioned nitrile (2·7 g.) in dry methanol (10 ml.) was added anhydrous methanol (35 ml.) saturated with dry hydrogen chloride at 0°. After allowing it to stand for 2 hr. in the freezing mixture and overnight in a refrigerator, the mixture was refluxed for 10 hr. After removal of a part of the methanol, brine was added to the cooled mixture, and it was worked up in the usual manner to yield *methyl* 3-*oxo*cyclo*hexanecarboxylate* (III *b*) (1·02 g.), b.p. 121–123°/16 mm., n_D^{24} 1·4590 (Found: C, 61·2; H, 7·7. $C_8H_{12}O_3$ requires C, 61·5; H, 7·69%). The *semicarbazone* was crystallised from aqueous methanol, m.p. 168° (Found: N, 19·33; $C_9H_5O_3N_3$ requires N, 19·72%). 3-Oxo*cyclo*hexanecarboxylic acid was prepared by hydrolysis of the ester with 6 N-hydrochloric acid. The 2:4-*dinitrophenylhydrazone* of this acid, obtained by the perchloric acid

method, was crystallised from ethyl acetate, m.p. 202° (Found: N, 17·27. $C_{13}H_{14}O_6N_4$ requires N, 17·39%).

When the β-keto-ester obtained from diethyl β-ethoxycarbonylpimelate (I) by the method of Dobson, Ferns and Perkin[2] was hydrolysed, decarboxylated, and subsequently esterified with methanol and sulphuric acid, a sample containing about 80% of methyl 3-oxo*cyclo*hexanecarboxylate (III *b*) (*vide* Fig. 4) was obtained.

Diethyl β-Acetyl-β-ethoxycarbonylpimelate.—Diethyl α-acetyladipate (13 g.) was added dropwise to a cooled (ice) and stirred suspension of potassium (2·2 g.) in toluene (50 ml.), and the mixture allowed to stand overnight at the room temperature. The potassio-derivative, thus formed, was heated under reflux for 12 hr. with ethyl bromoacetate (10 g.). The product, on fractionation, yielded diethyl β-acetyl-β-ethoxycarbonylpimelate (8·6 g.) as a colourless oil, b.p. 165–170°/1 mm. (Found: C, 58·4; H, 8·33. Calc. for $C_{16}H_{26}O_7$: C, 58·2; H, 7·94%).

Treatment of Diethyl β-Acetyl-β-ethoxycarbonylpimelate with Sodium Ethoxide under Chatterjee's[4] *Conditions.*—To a solution of sodium ethoxide, prepared from sodium (0·4 g.) in dry ethanol (7 ml.), was added diethyl β-acetyl-β-ethoxycarbonylpimelate (6·1 g.), and the mixture refluxed for 8 hr. The reaction product, which had a strong smell of ethyl acetate, was acidified to Congo red with iced hydrochloric acid and extracted with ether. The extract was washed with brine, sodium hydrogen carbonate solution, and water successively, and distilled to yield a colourless liquid (1·73 g.), b.p. 132–137°/1 mm., which gave a deep colour with alcoholic ferric chloride. This was refluxed for 24 hr. with a mixture of acetic acid (5·3 ml.), hydrochloric acid (2·2 ml.), and water (1·5 ml.). The reaction mixture was distilled to give a solid, m.p. 50–53°. The semicarbazone and 2:4-dinitrophenylhydrazone melted at 196° and 215–217° respectively; mixed melting points with authentic semicarbazone and 2:4-dinitrophenylhydrazone of 2-oxo*cyclo*pentylacetic acid respectively were not depressed.

Treatment of (*a*) *Diethyl β-Ethoxycarbonylpimelate* (*I*) *and* (*b*) *Diethyl* 3-*Oxo*cyclo*hexane*-1:2-*dicarboxylate* (II *a*)[2] *with Alcoholic Sodium Ethoxide under Chatterjee's Conditions.*—The β-keto-esters (purified through alkali extraction), obtained from these experiments, were hydrolysed, decarboxylated, and esterified with methanol and sulphuric acid, when samples of keto-esters having infra-red spectra identical with Fig. 3 were obtained.

Treatment of Ethyl 1-*Ethoxycarbonyl*-2-*oxo*cyclo*pentylacetate* (*IV*) *with One-Quarter Mole of Sodium Ethoxide in Ethanol.*—(*a*) To a solution of

sodium ethoxide, from sodium (1·4 g., 0·06 mole) and ethanol (11·1 g., 0·24 mole), was added the diester (IV) (59·0 g., 0·24 mole), and the mixture was heated for 3 hr. on a steam-bath. The crude product (65·8 g.), obtained after acidification and extraction with ether, gave a deep purple colour with alcoholic ferric chloride. It was dissolved in ether, and the β-keto-ester was removed by repeated extraction with cold, 5% aqueous sodium hydroxide. The ethereal solution, on distillation, yielded diethyl β-ethoxycarbonylpimelate (I) (52·8 g.), b.p. 158–160°/1 mm., which gave a faint colour with ferric chloride. To obtain the pure triester (I), this was hydrolysed, and esterified with ethanol-sulphuric acid, and then the product could be easily fractionated from the considerably lower boiling keto-monoesters (III R = Et; and VIII R = Et).

The alkaline extract was acidified with ice and hydrochloric acid and thoroughly extracted with ether. The ether extract, after being washed with sodium hydrogen carbonate solution and water, was dried, and then distilled to give a colourless oil (4·8 g.), b.p. 125–135°/1 mm. A redistilled portion b.p. 125–127°/0·8 mm. was analysed (Found: C, 59·51; H, 7·32. Calc. for $C_{12}H_{18}O_5$: C, 59·51, H, 7·44%).

The aforementioned β-keto-ester was hydrolysed and decarboxylated by the usual procedure. The crude 2: 4-dinitrophenylhydrazone, m.p. 170–195°, of the resulting product, after two crystallisations from ethyl acetate-light petroleum (40–60°), melted at 202°; the mixed melting point with the 2: 4-dinitrophenylhydrazone of 3-oxo*cyclo*hexanecarboxylic acid remained undepressed, whereas with the 2: 4-dinitrophenylhydrazone of 2-oxo*cyclo*pentylacetic acid the mixed m.p. was depressed (180–187°).

The above acid was converted to its methyl ester by the methanol-sulphuric acid method, the infra-red spectrum of which showed that it was a mixture of methyl 3-oxo*cyclo*hexanecarboxylate and methyl 2-oxo*cyclo*pentylacetate, with the former predominating.

(*b*) A similar experiment using sodium (0·14 g.), ethanol (1·12 g.) and the diester (IV) (6·1 g.) was performed, except that the heating was continued for five days, when the triester (I) (2·9 g.) along with a keto-acid (0·1 g.) were obtained. The 2: 4-dinitrophenylhydrazone of the latter was crystallised from dilute acetic acid, m.p. 213–215°. The m.p. remained undepressed with the 2: 4-dinitrophenylhydrazone of 2-oxo*cyclo*pentylacetic acid, but was depressed with that of 3-oxo*cyclo*hexanecarboxylic acid.

Treatment of Diethyl β-Ethoxycarbonylpimelate (I) with Sodium Ethoxide in Benzene.—To dry sodium ethoxide, from sodium (0·6 g.), was added the triester (I) (7·2 g.) in dry benzene (20 ml.), and refluxed for 6 hr. The

β-keto-ester (3·1 g.), b.p. 120–130°/0·8 mm., isolated in the usual manner, was hydrolysed and decarboxylated with hydrochloric acid to yield a keto-acid, and this was identified as 3-oxo*cyclo*hexanecarboxylic acid by m.p. and mixed m.p. of the 2:4-dinitrophenylhydrazone.

Essentially the same experiment was repeated using two moles of sodium ethoxide. The methyl ester of the keto-monoacid was isolated in the usual way. The infra-red spectrum was identical with Fig. 4.

Reaction of Ethyl 1-*Ethoxycarbonyl*-2-*oxo*cyclo*pentylacetate* (*IV*) *with Sodium Ethoxide in Benzene*.—To dry sodium ethoxide, from sodium (1 g.), under dry benzene (8 ml.) was added the diester (IV) (9·5 g.), and heated for 8 hr. in an oil-bath at 130–140°. On working up in the usual manner, a product (6·7 g.) was collected at 125–127°/0·8 mm. This gives a deep purple colour with alcoholic ferric chloride. The product was dissolved in ether, and the β-keto-ester extracted with ice cold 5% alkali, and the alkaline extract acidified and worked up to yield a β-keto-ester (4·6 g.), b.p. 125–127°/0·8 mm. (Found: C, 60·07; H, 7·45%).

The β-keto-ester (3 g.) was hydrolysed by refluxing with hydrochloric acid (15%, 35 ml.), and the keto-monoacid (1·3 g.), thus obtained, was distilled at 110–120° (bath)/1 mm. The m.p. (202°) and mixed m.p. (201–202°) of its 2:4-dinitrophenylhydrazone showed it to be 3-oxo*cyclo*hexanecarboxylic acid.

SUMMARY

The isomerisation of ethyl 1-ethoxycarbonyl-2-oxo*cyclo*pentylacetate to ethyl 3-ethoxycarbonyl-2-oxo*cyclo*pentylacetate has been shown to proceed *via* diethyl β-ethoxycarbonylpimelate. The mechanism proposed by Chakravarti[1] is untenable. A mechanism based on the equilibrium nature of the reaction has been formulated to explain the formation of ethyl 3-oxo*cyclo*hexane-1:2-dicarboxylate or ethyl 3-ethoxycarbonyl-2-oxo*cyclo*pentylacetate, as the major product, from diethyl β-ethoxycarbonylpimelate under different experimental conditions of Dieckmann cyclisation. Other mechanisms have also been discussed.

ACKNOWLEDGEMENTS

We thank the National Physical Laboratory, New Delhi, the Wisconsin Laboratories, U.S.A., Dr. W. Zehden of Hilger & Co., and Dr. S. Ramaseshan, Department of Physics, Indian Institute of Science, Bangalore, for helping us with the infra-red study. We also thank Messrs. B. R. Seetharamiah and D. P. Bose for the microanalyses. One of us (G. B.) is grateful to the Nagpur University for a stipend.

REFERENCES

1. Chakravarti .. *J.C.S.*, 1953, 1315.
2. Dobson, Ferns and Perkin *Ibid.*, 1909, 2010.
3. Sen and Bagchi .. *Science and Culture*, 1953, **19**, 312.
4. Chatterjee, Das and Barpujari *J. Indian Chem. Soc.*, 1940, **17**, 161.
5. Openshaw and Robinson .. *J.C.S.*, 1937, 941.
6. Nef .. *Annalen*, 1897, **298**, 202.
7. Ingold .. *Structure and Mechanism in Organic Chemistry*, Cornell University Press, Ithaca, N.Y., 1953 p. 791.
8. Johnson, Peterson and Gutsche *J. Amer. Chem. Soc.*, 1947, **69**, 2942.
9. Wallingford, Homeyer and Jones *Ibid.*, 1941, **63**, 2252.
10. Linstead and Meade .. *J.C.S.*, 1934, 940.
11. Reed and Thornley .. *Ibid.*, 1954, 2148.
12. Fry and Carrick .. *J. Amer. Chem. Soc.*, 1955, **77**, 4381.
13. Alexander, E. R. .. *Principles of Ionic Organic Reactions*, John Wiley & Sons, Inc., New York, 1950, p. 186.
14. Brown, Brewster and Schechter *J. Amer. Chem. Soc.*, 1954, **76**, 467.
15. Russel .. *Chem. and Ind.*, 1956, **17**, 326.
16. Neuberg Grauer and Pisha *Anal. Chim. Acta*, 1952, **7**, 238.
17. Wanzlick, Gollmer and Milz *Ber.*, 1955, **88**, 72.

672–57. Printed at The Bangalore Press, Bangalore City, by C. Vasudeva Rao, Superintendent, and Published by The Indian Academy of Sciences, Bangalore.

NOTICE TO AUTHORS

Scientific papers intended for publication in the *Proceedings of the Indian Academy of Sciences* can be accepted only when they are communicated by a Fellow of the Academy whose duty shall be to satisfy himself that such communications are fit to be read at the Meeting of the Academy and published in its *Proceedings*.

Papers should not ordinarily exceed fifty pages of foolscap. MSS. should be either typewritten or written in legible hand on one side of the paper. All papers should be carefully revised by the authors and should be absolutely in final form for printing. Position for text-figures should be indicated. Each paper shall conclude with a critical summary not exceeding 350 words.

Drawings, diagrams or other illustrations should be made on larger scale (preferably) twice the size than the ones in which they are intended to appear. They should be done in Indian ink on bristol board with lettering in pencil. Scale of magnification of camera lucida tracings should be indicated by the side of drawings. In certain special cases arrangements will also be made for monochrome lithographic and other colour plates. Reduction of illustrations desired should be indicated in pencil. Appropriate legends should accompany all drawings. Names of authors are to be marked in pencil on the left-hand corner of drawing sheets. Photomicrographs should be securely mounted with colourless paste.

All tables, quotations and footnotes which will be set hereafter (beginning from Vol. I, No. 2) in types smaller than the text, should be typewritten on separate sheets and placed with the text in proper sequence. Footnotes should be numbered in Arabic numerals.

References to literature in the text should be given, whenever possible, in chronological order, only the names of authors and years of publication, in brackets, being given. They should be cited in full after the summary, the authors' names following in alphabetical order. Thus,

Name or Names of author; Name of Journal (abbreviation) with a single underline; Year of publication; Number of Volume with a double underline, and lastly page. The following would be a useful illustration:—

Bergmann and Stather . . . . . Z. Physiol. Chem., 1926, 152, 189.

Two copies of slip-proof and wherever possible, a page proof for final revision will be sent to authors. All corrections are best made on the slip-proof which should be transmitted to the Office of the Academy. All proof corrections involve heavy expenses which would be negligible if the papers are carefully revised by the authors before submission.

Fifty free reprints including plates and with cover will be supplied for each paper. Additional copies can be supplied at cost on previous intimation.

Blocks appearing in the *Proceedings* will be available for purchase by their respective authors. Orders for the same should be sent along with the corrected proofs and in any case not later than one month after the date of publication of the paper. The price charged would be 25% of the actual cost of the blocks *plus* freight and despatching charges. If the blocks are reproduced in other journals or publications, due acknowledgment should be made in them to the *Proceedings*.

The original drawings and plates of blocks appearing in the *Proceedings* will be returned to such of the authors as may require them provided the cost of despatching such originals is borne by them.

CONTENTS

PAGE

Generalised Theory of Interference and Its Applications. Part IV. Interference Figures in Absorbing Biaxial Crystals . . . S. Pancharatnam 1

Synthetic Experiments in the Benzopyrone Series. Part LXV. Synthesis of α-Methyl Karanjin and Related Compounds . . . . . S. S. Chibber, A. K. Ganguli, S. K. Mukerjee and T. R. Seshadri 19

A Convenient Method of Preparation of Cyanidin Chloride from (+) Catechin and (−) Epicatechin . . . . . A. K. Ganguli, T. R. Seshadri and P. Subramanian 25

Kinetics of Isothermal Annealing of Radiation Damage in Szilard-Chalmers Reaction with Cobalt Complexes. Part I. Tris-Acetylacetone Cobalt (III)—Section 1 . . . . . Amar Nath, K. S. Venkateswarlu and Jagdish Shankar 29

Studies on Groundnut Shells. Part II. The Chemical Constitution of Groundnut Shell Hemicellulose A_1 . . . . . B. Radhakrishnamurthy and V. R. Srinivasan 53

A Multichannel Pulse Amplitude Analyser . . . . . P. K. Iyengar, P. N. Rama Rao, G. Venkataraman and K. Usha 61

Slowing Down Age of Neutrons from a Ra-α-Be Source to Indium Resonance in Aluminium Light Water Mixtures . . . V. P. Duggal and S. M. Puri 72

A Paradoxical Case of Dieckmann Cyclisation . . . . . D. K. Banerjee, J. Dutta and G. Bagavant 80